SYNTHESIS AND CHARACTERIZATION OF HYDROXYAPATITE FROM WASTE MATERIALS

NOR ADZLIANA BINTI SAJAHAN

FACULTY OF ENGINEERING
UNIVERSITY OF MALAYA
KUALA LUMPUR

2017

SYNTHESIS AND CHARACTERIZATION OF HYDROXYAPATITE FROM WASTE MATERIALS

NOR ADZLIANA BINTI SAJAHAN

**DISSERTATION SUBMITTED IN FULFILMENT OF
THE REQUIREMENTS FOR THE DEGREE OF MASTER
OF ENGINEERING SCIENCE**

**FACULTY OF ENGINEERING
UNIVERSITY OF MALAYA
KUALA LUMPUR**

2017

UNIVERSITY OF MALAYA

ORIGINAL LITERARY WORK DECLARATION

Name of Candidate: (I.C/Passport No:)

Registration/Matric No:

Name of Degree:

Title of Project Paper/Research Report/Dissertation/Thesis (“this Work”):

Field of Study:

I do solemnly and sincerely declare that:

(1) I am the sole author/writer of this Work;
(2) This Work is original;
(3) Any use of any work in which copyright exists was done by way of fair dealing and for permitted purposes and any excerpt or extract from, or reference to or reproduction of any copyright work has been disclosed expressly and sufficiently and the title of the Work and its authorship have been acknowledged in this Work;
(4) I do not have any actual knowledge nor do I ought reasonably to know that the making of this work constitutes an infringement of any copyright work;
(5) I hereby assign all and every rights in the copyright to this Work to the University of Malaya (“UM”), who henceforth shall be owner of the copyright in this Work and that any reproduction or use in any form or by any means whatsoever is prohibited without the written consent of UM having been first had and obtained;
(6) I am fully aware that if in the course of making this Work I have infringed any copyright whether intentionally or otherwise, I may be subject to legal action or any other action as may be determined by UM.

Candidate’s Signature Date:

Subscribed and solemnly declared before,

Witness’s Signature Date:

Name:

Designation:

ABSTRACT

Due to resemblance of mineral components of bones and human hard tissue, hydroxyapatite, HA with chemical formula $Ca_{10}(PO_4)_6(OH)_2$ has been widely used in medical field especially as bone replacement. All the waste materials such as chicken eggshells (CHA), duck eggshells (DHA) and cockle shells (SHA) are mainly composed of calcium carbonate, $CaCO_3$. In this study, HA was fabricated from $CaCO_3$ of the waste materials and diammonium hydrogen solution via microwave irradiation technique. Under the effect of microwave irradiation for 15 min, HA was produced directly in the solution and involved in crystallographic transformation. X-ray diffraction, XRD pattern revealed that no impurities other than HA was produced and the peaks were complement with standard HA (JCPDS file- 00-024-0033). All HA characteristics were evident in Fourier Transform Infra-Red, FTIR spectrum such as chemical groups of PO_4^{3-}, OH^- and a weak spectra of CO_3^{2-}. As microwave power increased from 550W to 900W, Field Emission Scanning Electron Microscopy, FESEM micrographs showed a transition of HA particles shape from needle-like to mixture of needle-like and spherical to spherical shape. Energy Dispersive X-ray, EDX results showed that non-stoichiometric HA was produced for all samples except for SHA900 where the Ca/P ratio is 1.66 under microwave irradiation of 900W. CHA and DHA samples showed an abundance of Ca with a decreasing Ca/P ratio while Ca/P ratio of SHA increased as the microwave power increased (550-900W). Compression test showed a decreasing trend in compressive strength as the microwave power increased for all types of samples. CHA550 has the highest value of compressive strength (71.61 MPa) under the irradiation of 550W. In conclusion, the production of HA powder is reproducible, fast and environmentally friendly. The optimum microwave power to fabricate non-stoichiometric HA was 550W and 700W.

ABSTRAK

Hidroksiapatit dengan formula kimia $Ca_{10}(PO_4)_6(OH)_2$ telah digunakan secara meluas di dalam bidang perubatan terutamanya sebagai pengganti tulang kerana mempunyai persamaan dari segi komponen tulang mineral dan tisu keras manusia. Kandungan utama semua bahan buangan (cengkerang telur ayam, cengkerang telur itik dan cengkarang kerang) terdiri daripada kalsium karbonat. Dalam kajian ini, hidroksiapatit telah dihasilkan daripada kalsium karbonat bahan-bahan buangan dan diammonia hydrogen fosfat melalui kaedah sinaran gelombang mikro. Di bawah kesan pemanasan gelombang mikro selama 15 minit, hidroksiapatit telah dihasilkan secara langsung dalam cecair dan terlibat dalam transformasi kristal. Corak belauan sinar-x, XRD menunjukkan tiada bendasing selain daripada hidroksiapatit telah dihasilkan dan semua corak adalah setanding dengan standard hydroksiapatit (JCPDS file- 00-024-0033). Semua ciri-ciri hydroksiapatit telah ditunjukkan dalam spektrum fourier transform infra-merah, FTIR seperti kumpulan ion PO_4^{3-}, OH^- dan spektra lemah oleh ion CO_3^{2-}dikesan. Apabila kuasa gelombang mikro meningkat dari 550W kepada 900W, mikrograf imbasan electron, FESEM menunjukkan peralihan bentuk zarah hidroksiapatit dari bentuk seperti jarum kepada campuran bentuk jarum dan sfera kepada bentuk sfera. Keputusan data serakan tenaga sinar-X, EDX menunjukkan bahawa hidroksiapatit yang dihasilkan oleh semuasampel adalah bukan stoikiometrik kecuali SHA900 di mana nisbah Ca/P adalah 1.66 di bawah kuasa gelombang mikro. Sampel- sampel CHA dan DHA menunjukkan lebihan kalsium dengan penurunan nisbah Ca/P apabila kuasa gelombang mikro semakin tinggi (550-900 W). Ujian kekuatan mampatan menunjukkan kekuatan mampatan menurun apabila kuasa gelombang sinaran meningkat untuk semua jenis sampel. CHA550 mempunyai kekuatan mampatan (71.61 MPa) yang paling tinggi pada kuasa gelombang micro 550 W jika dibandingkan dengan yang lain. Kesimpulannya, penghasilan serbuk hidroksiapatit boleh diulang-ulang, cepat dan mesra alam. Didapati, gelombang kuasa 550 W dan 700 W adalah kuasa gelombang mikro yang optimum untuk menghasilkan bukan stoikiometrik HA.

ACKNOWLEDGEMENTS

First and foremost, I am grateful to Allah the almighty for the gifts and blessing of my life and for the health that was necessary to complete this thesis.

Next, I would like to express my sincere gratitude to my supervisor, Associate Professor Dr. Wan Mohd Azhar bin Wan Ibrahim for his guidance throughout my thesis and for sharing his vast knowledge, skills and information on this project. Not to mention his constructive comments and assistance in writing reports. Without his help, this thesis would not have been completed or written.

I would also like to express my deepest gratitude to my family for their endless support and encouragement with love, time and financial especially to my parents, Mr. Sajahan Mohamed and Mrs. Jalilah Zainal Abidin. With them, I'm all inspired and have the strength to finish this thesis.

I would also like to offer my appreciation to all technicians for assisting in characterization and testing of the samples for XRD, FTIR, SEM, EDX and UTM machine. Without them, I would not have any results for my report. Not to forget, a highly appreciation to all my friends and people who help me directly or indirectly during my work.

Last but not least, I notice that this research would not has been possible without the financial support from Postgraduate Researh Grant (PPP), University of Malaya, project number PV012-2012A, hence my deepest gratitude to this agency.

TABLE OF CONTENTS

LIST OF FIGURES

LIST OF TABLES

LIST OF SYMBOLS AND ABBREVIATIONS

$(NH_4)_2HPO_4$	:	Diammonium hydrogen phosphate
3Y-TZP	:	Yttrium cation-doped tetragonal zirconia polycrystals
Ca	:	Calcium
$Ca(H_2P0_4)_2.H_20$	:	Monocalcium phosphate monohydrate
$Ca(NO_3)_2.4H_2O$	:	Calcium Nitrate Tetrahydrate
$Ca(OH)_2$	:	Calcium hydroxide
Ca/P	:	Calcium to phosphate ratio
$Ca_{10}[PO_4]_6[OH]_2$	:	Calcium hydroxyapatite
$CaCO_3$	:	Calcium carbonate
CaO	:	Calcium oxide
$CaPO_4$	:	Calcium phosphate
CES	:	Chicken Eggshells
CF/PEEK	:	Fluorocarbon/ polyether ether ketone
CF/PMMA	:	Fluorocarbon/poly(methyl methacrylate)
CF/PS	:	Fluorocarbon/ Polystyrene
CO_3^{-2}	:	Carbonate ion
Co-Cr-Mo	:	Cobalt-Chromium-Molybdenum
Co-Ni-Cr-Mo	:	Cobalt-Nickel-Chromium-Molybdenum
CS	:	Cockle shells
CTAB	:	cetyltrimethylammonium bromide
DES	:	Duck Eggshells
EDX	:	Energy Dispersive X-Ray Spectroscopy
F^-	:	Fluoride ion
FDA	:	Food and Drug Administration

FTIR : Fourier Transform Infrared

GF/PMMA : Glass fiber/poly(methyl methacrylate

H_2O : Distilled water

HA : Hydroxyapatite

HA-CS : HA- chitosan

HCl : Hydrocholric acid

HPO_4^{2-} : Hydrogen phosphate

KF/PMMA : Polyvinylidene fluoride resin/poly(methyl methacrylate)

KH_2PO_4 : Potassium dihydrogenphosphate

Na^+ : Natrium ion

NH_3 : Ammoniu solution

nHA : Nano-hydroxyapatite

OH^- : Hydroxyde

P : Phosphorus

PCL : Polycaprolactone

PEEK : Polyether ether ketone

PGA : Polyglycolic acid

PLLA : Poly-L-lactic acid

SCS : Citric acid solution combustion

SEM : Scanning Electron Microscopy

TCP : Tricalcium phosphate

TEM : Transmission Electron Microscope

Ti/Ti : Titanium/titanium

UHMWPE : Ultra-high molecular weight polyethylene

UTM : Universal Testing Machine

XRD	X-ray Diffraction

CHAPTER 1: INTRODUCTION

1.1 Introduction

Over the last few decades, biomaterials have progressively developing into better performance in clinical application. It is used as treatment of injuries or disease due to trauma, accident or illnesses to improve the quality of life of the patients. A high demand worldwide has made biomaterials one of the most crucial necessities in life. Biomaterials that are used in clinical applications including metals, bioceramics, polymers and composites.

Due to good mechanical properties, metallic biomaterials such as stainless steel, titanium, Ti and its alloy and cobalt alloys are used in load-bearing systems such as hip and knee prostheses and for the fixation of internal and external bone fractures . The main components of total knee replacement consist of femur, tibia (tibial tray and tibial insert) and patella or kneecap. The femoral component and tibial tray are made of Ti alloys, stainless steel or Co-Cr-Mo while the tibial insert and the kneecap are made of plastics such as ultra-high molecular weight polyethylene, UHMWPE or cross-linked polyethylene, PE. Currently, Co-Ni-Cr-Mo alloy has been developed to be used as stems in hip and knee replacements due to their high resistance to fatigue and corrosion resistance as well as good wear resistance (Nasab & Hassan, 2010). In the design of hip replacement device, the femoral stem is normally made of Ti and its alloys while the acetabular cup is usually made of UHMWPE (Nasab & Hassan, 2010). Figure 1.1 illustrates the artificial hip joint where the femoral head and cup are design in such a way that they can function as normal hip movement and these components position are secured using the stem (Liu, Chu & Ding, 2004).

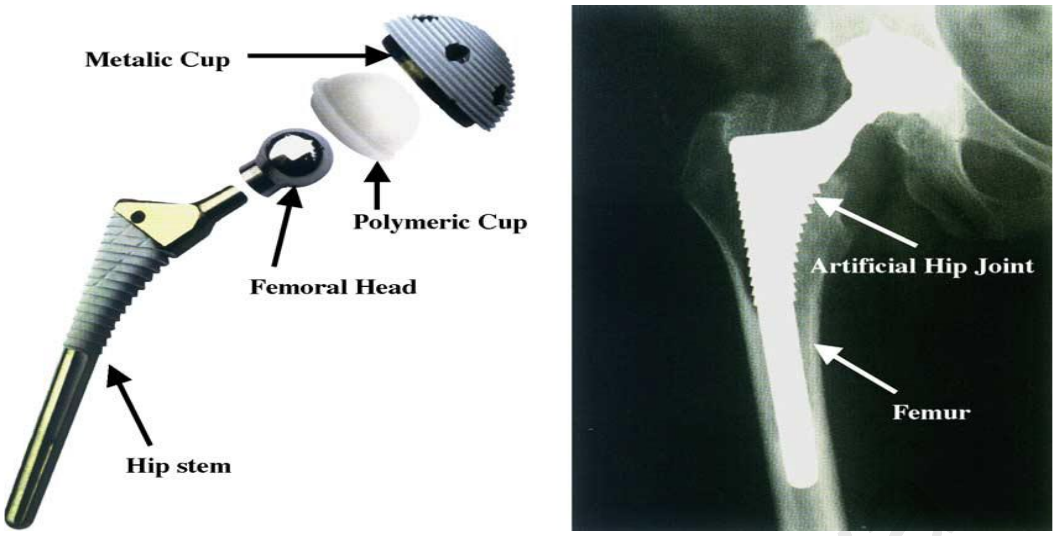

Figure 1.1: Schematic diagram of artificial hip joint (Liu et al., 2004)

Another application of metals is in osteosynthesis such as internal and external bone fracture fixation. Through osteosynthesis, a bone fracture can be treated by surgical means where the main components used are screws, plates, nails and pins, in different design to fulfill the implant requirements (Rodríguez-González, 2009). The most common metals used in osteosynthesis are Ti and its alloy as well as stainless steel 316L. Stainless steel is well known for excellent fabrication properties, accepted biocompatibility and great strength. It is also easy availability and lower cost (Nasab & Hassan, 2010). Figure 1.2 shows the common implants for osteosynthesis.

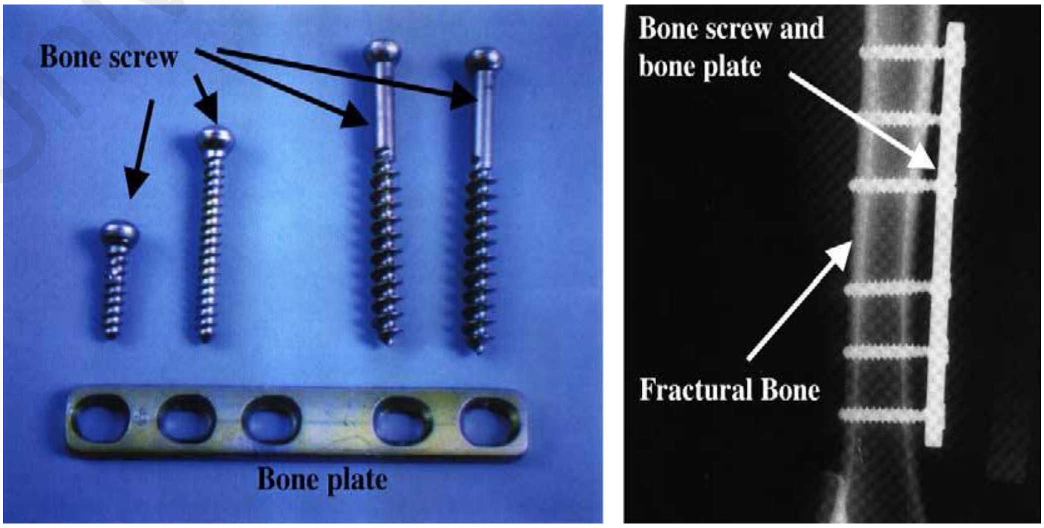

Figure 1.2: Bone screw and bone plate used in fractural bone (Liu et al., 2004)

Another application of Ti and its alloy is in cardiac and cardiovascular application due to its excellent mechanical properties such as relatively low modulus, good fatigue strength, formability, machinability, corrosion resistance, and biocompatibility (Liu et al., 2004). In dental field, Ti and its alloy has been used as dental implants. The fusion between the implants and bone is done according to “osseointegration” concept. Figure 1.3 illustrates a screw-shaped devices and cylinders of dental implant.

Figure 1.3: Schematic diagram of the screw-shaped artificial tooth (Liu et al., 2004)

In clinical application especially orthopedics devices, most of the polymers used are biodegradable and bioabsorbables because they are able to transfer stress over time to the damaged tissues as it heals and eliminates a second surgery to remove the implants (Tian, Tang, Zhuang, Chen & Jing, 2012). Apart from that, they are friendly environmental, hence, use as disposable medical devices such as syringes, injection pipes, surgical gloves, pads and etc. UHMWPE, acrylic bone cements and thermoplastic polyether ether ketone, PEEK are the common polymers used in joint replacement (Navarro, Michiardi, Castano & Planell, 2008). Biodegradable poly-L-lactide, PLLA is used as coatings on stents or fully stents due its ability to control drug release and excellent mechanical performance preventing the stents to deform or fracture (Tian et al., 2012). Development of polymers has advanced the drug delivery technology that optimizes the administration of drugs by controlling the release of therapeutic agents in constant doses (Raizada, Bandari & Kumar, 2010).

Polyesters composed of homopolymers or copolymers of glycolide and lactide are the most common biodegradable devices used along with copolymers of trimethylene caronate, e-caprolactone and polydioxanone. In orthopaedic applications, polyglycolide, PGA is used as orthopedic fixation devices such as pins, rods, screws, tacks and ligaments as well as wound closure (sutures, staples) due to high tensile strength and low elongation and high modulus compared to amorphous polymers (Middleton & Tipton, 2000). These orthopedic fixation devices are also can be made of PLLA, PGA and other biodegradable polymers (Liu et al., 2004). Tissue engineering offers significant approach of restoring, maintaining, or enhancing formation of tissues or organ function combining cells, biomaterials and microenvironmental factors. Biodegradable polymers are used as scaffold because of their properties is similar to extracellular matrix and able to provide mechanical stability, enhance cell attachment and growth, and have appropriate rate of degradation allowing the load to be transferred to the new tissue (Raizada et al., 2010). Extensive research has been investigated about synthetic biopolymers such as PLLA, polycaprolactone, PCL, PGA and poly[d,l-(lactide-co-glycolide)] due to good biocompatibilty and mechanical properties (Tian et al., 2012).

Bioceramics can be classified as bioinert (alumina, zirconia), resorbable (tricalcium phosphate, TCP), bioactive (hydroxyapatite, HA, bioactive glasses and glass-ceramics) (Hench, 1991). It is widely used in hard-tissue replacements. For example, HA and bioactive glass enhance the bonding between bone tissues and those materials because they will create a bone-like apatite layer on their surface after implantation. It also prevents the unnecessary formation of fibrous tissue around the implants. Due to its resorbable property, TCP is also used in non-load bearing application such as in some repairs of the jaw or head (Hench, 1991).

Besides HA, high-density, high-purity alumina is the most common ceramics material used clinically especially in load-bearing orthopedics application (hip prostheses, knee prostheses, bone screws), ossicular bone substitutes, corneal replacements, segmental bone replacements, and blade and screw as well as dental implants (alveolar ridge augmentation, maxillofacial reconstruction) due to its excellent corrosion resistance, good biocompatibility, high wear resistance and high strength. It also allows cementless fixation of prostheses by forming a very thin capsule (Hench, 1991). In Europe, alumina non-cemented cups and femoral ball which is fitted to metallic stem are used in the hip replacement.

In dental applications, zirconia-based ceramics has received a considerable attention due to its excellent mechanical properties compared to other dental ceramics which allows the realization of posterior fixed partial dentures and reduce the core thickness. Even so, there are only three used extensively i.e yttrium cation-doped tetragonal zirconia polycrystals (3Y-TZP), magnesium cation-doped partially stabilized zirconia (Mg-PSZ) and zirconia-toughened alumina (ZTA). 3Y-TZP is used to fabricate dental crowns and fixed partial dentures (Denry & Kelly, 2008).

Even though these biomaterials are extensively used in biomedical applications, many of them have certain drawbacks that limit their usage in those applications. For example, many metals are low biocompatible, low corrosion resistance, too high stiffness compared to tissue, high density, and cause allergic tissue reactions. Shortcomings of ceramics include brittleness, low fracture strength, difficult to fabricate, poor mechanical properties and high density (Ramakrishna, 2000). While polymers are too flexible, has poor mechanical and may absorb liquids and swell. Composite provides alternative to improve these limitation by reinforcing one material to another matrix material.

Carbon fibre / polyether ether ketone, CF/PEEK and carbon fibre / polystyrene, CF/PS composites have been developed as plates and screws replacing stainless steel to stabilize the substitution of body and spine. It is proven to be biocompatible, high strength, fatigue resistance and biological inertness without causing any adverse effect (Tian et al., 2012). Currently, carbon fibre/polymethyl methacrylate, CF/PMMA, Kevlar fibers/polymethyl methacrylate, KF/PMMA, UHMWPE/PMMA and glass fiber, GF/PMMA composites are used as bridges and dentures since the current gold bridges are highly-cost and time consuming.

1.2 Problem Statement

Fabrication of HA can be done through several methods such as sol-gel technique, precipitation route, hydrothermal method, mechanochemical and solid-state reaction, etc. However, most of these methods produce fairly inferior crystallinity and thermal stability (Pratihar, Garg, Mehra and Bhattacharyya, 2005). Sol- gel method requires high cost of raw materials (Kothapalli, Wei, Vasiliev & Shaw, 2004) and long aging time (Ben-Arfa, Salvado, Ferreira & Pullar, 2017). Bakan, Lacin & Sarac (2013) found that aging time is crucial in synthesis of HA using sol-gel method as shorter aging time contribute to secondary phase of β-TCP along with HA. A pure HA was produced at aging time of 48 hours compared to aging time of 12 and 24 hours which β-TCP occurred. Despite of the occurrence of the secondary phase in the synthesis, the obtained size of all the products were in nano sizes with needle-like morphology.

On the other hand, precipitation is considered as complicated process since many parameters such as pH, temperature of solution, aging time, reagent’s concentration, stirring technique and speed need to be prepared carefully. Angelescu, Ungureanu &

Anghelina (2011) have studied some factors that affect the HA synthesis by precipitation technique such as stirring speed, acid addition rate, aging time of precipitates. The experimental conditions are tabulated in Table 1.1.

Table 1.1: Experimental conditions for precipitation of HA

Experiment	Concentration (mol/l)	Temperature (^oC)	Addition rate (ml/min)	Stirring speed (rpm)	Aging time (h)
E1	2	75	1	1000	48
E2			10	1000	48
E3			1	300	2
E4			10	300	2

They found that a slower addition rate, faster stirring speed and longer aging time (E1) was important to produce a pure HA phase. Sample E2 and E3 showed the presence of calcium oxide, CaO while β-TCP and CaO were presence in sample E4. The crystallite size of all samples were slightly different with E4 has the lowest crystallite size followed by E1, E3, and E2. These factors can be explained as following:

a) a high rate of addition of acid causing the pH environment to decrease drastically thus incomplete the dissociation process of phosphoric acid. This condition unable HA to be well-precipitated without $PO_4{}^{3-}$ ions.

b) a low stirring speed leads to a decrease in pH solution and formation of soluble precipitated as it leads to heterogeneous reaction environment thus increases the local concentration of $PO_4{}^{3-}$ ions.

c) as the HA precipitate aging, it undergoes dissolution and recrystallization process causing the crystals to grow further and eliminate the smallest crystals. Therefore, the longer the aging time, the bigger crystallite size is formed.

Major drawback of hydrothermal method is several heat-treatment steps are involved (Avecedo-Davilla, Lopez-Cueves, Gutierrez, Rendon-Angeles, and Mendez-Nonell,

2007) and it requires relatively high temperature in the procedure (Kothapalli et al., 2004). Hui, Meena, Singh, Agarawal and Prakash (2010) have synthesis HA from chicken eggshells by hydrothermal technique. This study involved 3 stages of heat-treatment (0-450 ^{o}C, 450-600 ^{o}C and 600-900 ^{o}C) with soaking time in between the stages. However, calcium oxide and and calcium hydroxide were produced along with HA. Agglomerates of irregular oval shape and spherical shape with micron size was observed.

Microwave-irradiation technique has been developed to overcome this problem (Arami et al., 2009). It has been reported that this technique is simple, shorter synthesis time, fast reaction due to heating throughout the volume and efficient energy transformation, produce high purity and narrow particle distribution of HA powder (Siddharthan, Seshadri & Kumar, 2006; Kalita & Verma, 2010). Fabrication of HA from biowaste materials provide a low cost method compared to other techniques using high purity and expensive starting materials. With the aid of ethylenediaminetetraacetic acid, EDTA, Kumar et al. (2017) have synthesized non-stoichiometric (Ca/P of 1.79) HA from mussel shells as calcium source using microwave irradiation at power of 700W for 15 mins. At pH 13, they found that the morphology of obtained HA was flower-like architecture which consisted flakes with 100-200 nm width and 2-5 μm length. They claimed that this technique is facile and rapid with single step involved in synthesizing HA.

Shavandi, Bekhit, Ali and Sun (2015) have successfully synthesize nano HA from mussel shells using microwave heating at power of 1100 kW with pH of 13. The synthesis was aid with EDTA and the heating was carried out until the mixture was dried. No secondary phases were found when the dried HA was further heated at 650 ^{o}C for 1 hr. They found that the heated HA has bigger size compared to dried HA but still in nano range size with spherical and rod-like shape respectively.

By manipulating the pH value of the mixture of calcium and phosphate solution, Liu, Li, Wang, Zhu and Yan (2004) succeeded in synthesizing 3D HA with different shapes with the aid of EDTA. The synthesis was carried out using microwave irradiation with a reflux system at power of 700 W for 30 mins. At pH 9, 11 and 13, the morphologies of HA were nanorods, bowknot-like and flower-like structure respectively.

1.3 Scope of Research

This study attempted to produce HA from waste materials such as chicken egg shells, duck eggshells and cockle shells as a calcium source due to vast availability and low cost of obtaining these materials. This study involved microwave-assisted wet chemical technique where the effect of different microwave power was investigated by means of X-ray Diffraction, (XRD), Fourier Transform Infrared (FTIR), Field Emission Scanning Electron Microscopy (FESEM) and Energy Dispersive X-Ray Spectroscopy (EDX) to obtain information on powder phase purity crystallinity, functional groups, morphology and etc. Compression strength test of the synthesized HA was conducted to investigate the mechanical property for biomedical applications.

1.4 Aim and Objectives

The main aim of this study is to synthesize and characterize HA powder from chicken eggshells, duck eggshells and cockle shells for biomedical applications. The synthesis is conducted using microwave irradiation technique which is considered as a new approach in fabrication of HA powder. The specific objectives of this study is listed below:

i. To determine the effect of different microwave oven power on the characteristics of obtained HA powder
ii. To characterize the properties of HA powder produced using XRD, FTIR, SEM and EDX.
iii. To study mechanical properties of as-prepared HA for biomedical applications.

1.5 Outline of the Research Methodology

A well-planned structure of the study can be realized with the following steps:

i. Background study on HA which relates the latest finding to the previous findings including its properties, application, synthesis methods and etc.

ii. Experimental design and planning on synthesizing HA, characterization method and compression test. The sequence of HA synthesis and characterization are shown in Figure 1.4.

iii. Performing experiment to fabricate HA from waste materials, which includes:

   a. Preparation of raw materials i.e. cleaning, drying and grinding of waste materials

   b. Preparation of stock reactant solutions

   c. Synthesis of HA powder

iv. Characterization of HA obtained using XRD, FTIR, SEM and EDX.

v. Conducting compression test for biomedical application.

vi. Analysis of the results obtained.

vii. Report writing and documentation.

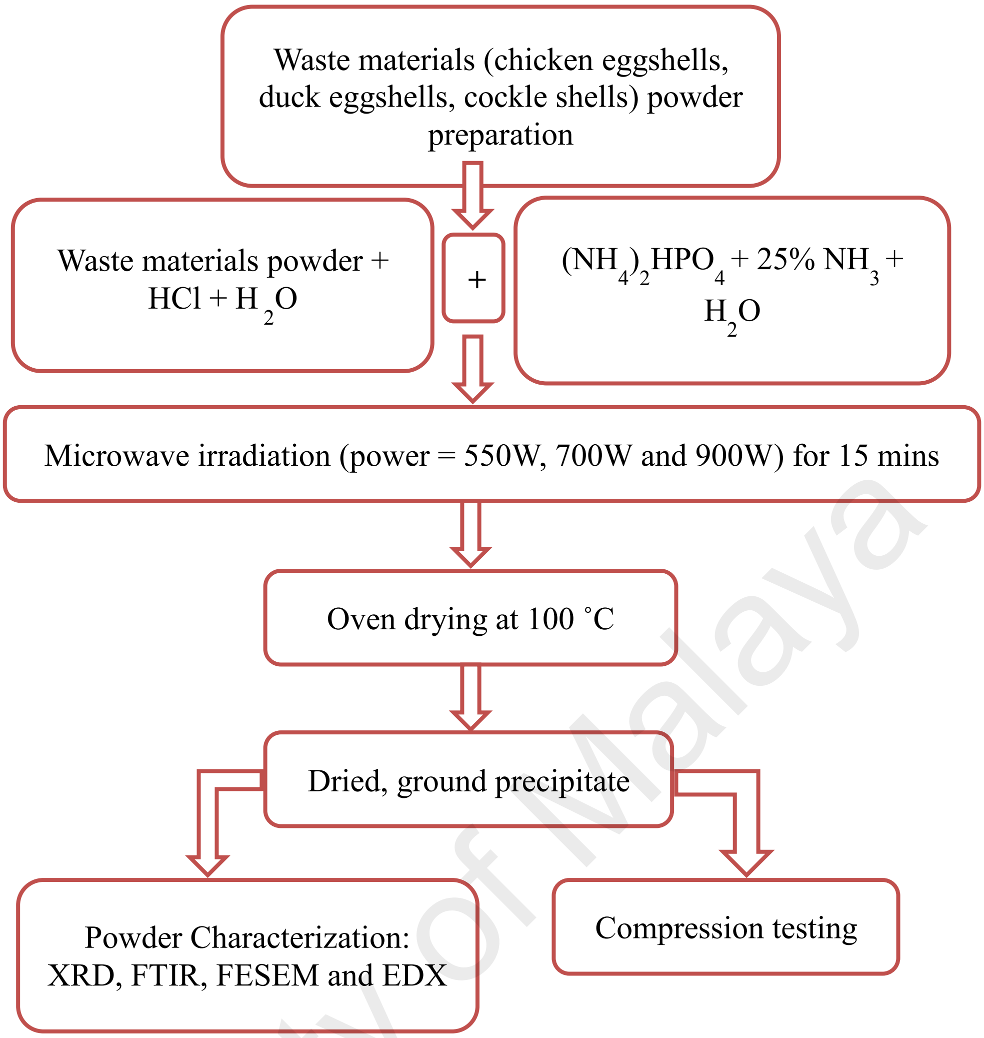

Figure 1.4: Flow chart of synthesis of HA via microwave-assisted wet chemical method

1.6 Research Organization of Study

This thesis can be divided into five chapters including introduction, literature review, methodology, results and discussion, and conclusion and suggestion. These are the brief descriptions of chapters mentioned:

CHAPTER 1: This chapter presents the introduction. It mainly describes about the biomaterials in clinical application, problem statement, scope of research, aim and objectives and the outline of research methodology

CHAPTER 2: This chapter focuses on HA including its properties, composition and application as well as other techniques to synthesize HA such as sol gel, precipitation, hydrothermal and sol gel, citric acid solution combustion and microwave method as well as waste materials that are used.

CHAPTER 3: This chapter explains in details the procedure on how to synthesize HA starting from the materials and equipment used to preparation of calcium carbonate, $CaCO_3$ from waste materials, until the reaction of $CaCO_3$ with phosphate precursor via microwave irradiation with different microwave power. The compaction of HA powder for compression test is also included. The formation of HA powder is characterized using XRD, FTIR, FESEM and EDX.

CHAPTER 4: All results obtained are organized in this chapter. Mostly, they are in form of graphs and images obtained from the characterization of XRD, FTIR, FESEM and EDX as well as result of compressive strength test. Phase identification of the samples is verified from XRD while the composition of the samples at corresponding wavenumber can be obtained from FTIR. From FESEM, the crystal morphology can be analyzed. Calcium to phosphate ratio can be determined from EDX. Compressive strength of the powder formed can be seen from data and graphs obtained using Universal Testing Machine (UTM).

CHAPTER 5: The overall conclusion on synthesis of HA is drawn in this chapter including the recommendations or suggestions pertaining to this study. This suggestion is to improve the method or results of this study so that the upcoming study can be more successful and organize.

CHAPTER 2: LITERATURE REVIEW

HA is a type of bioceramics which belongs to family of calcium phosphate. There is a mutual relationship between HA and human hard tissue as hard tissue consist of mineral apatite as well as in enamel and dentin of teeth. Hence, HA is widely used for bone replacement due to its similarity to the chemical composition and structural morphology to the natural bone. It is crucial to investigate the physical, chemical and mechanical properties of hard tissue because the alternative and development of synthetic bone can be achieved. In addition, various technique has been developed to prepare HA for obtaining the most suitable properties close to natural bone. Many sources of materials have also been employed to fabricate HA whether chemical synthesis of materials or natural/ waste materials.

2.1 Bioceramics

Ceramics have been used decades ago in pottery making. However, its use has been evolved in fabrication of ceramics and their composites in medical applications with high technology materials due to high compatibility property with human bodies. Ceramics involve in repair and reconstruction of diseased and damaged part of musculo-skeletal system is termed as bioceramics (Dasgupta, Singh, Adak & Purohit, 2004). Bioceramics function as materials to ease pain and restore function to diseased and damaged part of the body. It may be bioinert, bioresorbable or bioactive and its categories can be seen in Table 2.1 and Figure 2.1.

Table 2.1: Example of bioceramics including their applications and properties

Categories	Example	Usage	Remarks
Non-absorbable or relatively bioinert ceramics	Calcium. Aluminates. Dense HA. Zirconia ceramics porous. Aluminium Oxides	As bone plates and screws. As femoral heads. As drug delivery device. As middle ear ossicles.	Maintain their physical and mechanical properties while in the host. They resist corrosion and wear.
Biodegradable or resorbable ceramics	Calcium Phosphate ($CaPO_4$). Coralline. Tricalcium Phosphate. Aluminium-Calcium Phosphate.	As drug delivery devices. For repairing bone damage due to disease or trauma. For filling space vacated by bone screws. Donor bone.	It degrades upon implantation in the host. The resorbed material is replaced by endogenous tissues. Rate of degradation varies from material to material.
Bioactive or surface reactive ceramics	Bioglass and ceravital. Dense and nonporous glasses HA.	For coating of metal prosthesis in reconstruction of dental defects. As bone plates and screws in replacing subperiosteal teeth.	Upon implantation of the host, surface reactive ceramics form strong bonds with adjacent tissue.

(Park and Bronzino, 2002)

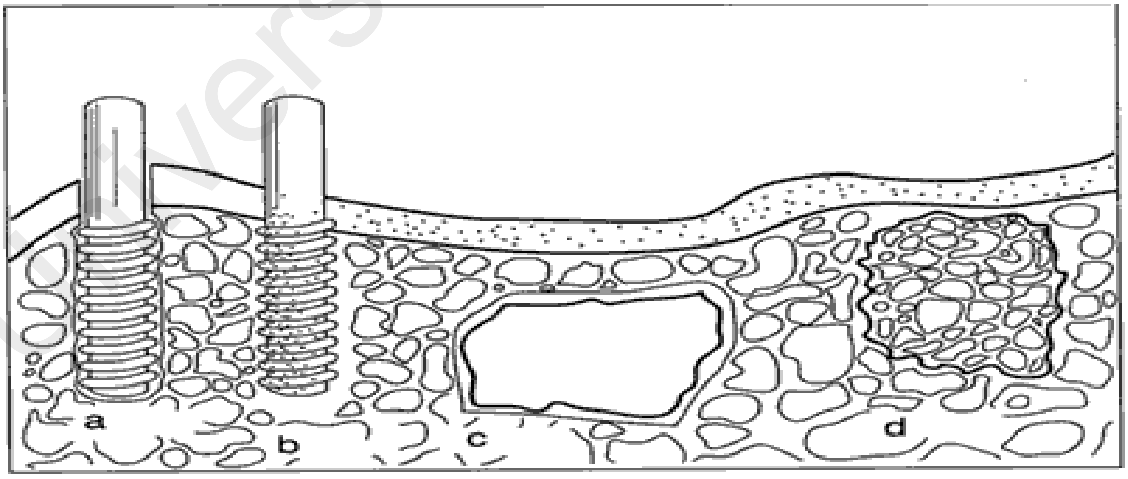

Figure 2.1: Classification of bioceramics according to their bioactivity; (a) bioinert (alumina dental implant), (b) bioactive, HA coating on metallic dental implant, (c) surface active, bioglass or A-W glass, (d) bioresorbable TCP implant (Lewis, Choi, Chou & Ben-Nissan, 2007)

Due to their relative inertness to the body fluid, high compressive strength and aesthetically, they are used in dentistry as dental crown. They are also used as reinforcing components of composite implants materials and for tensile loading applications such as artificial tendons and ligaments because of their high specific strength as fibers and they are biocompatible with human body. In order to implant bioceramics in human body, the bioceramics must be non-toxic, non-carcinogenic, non-allergic, non-inflammatory, biocompatible and biofunctional for its lifetime in the host (Park & Bronzino, 2002).

2.2 Relationship between Hydroxyapatite and Hard Tissue

Hard tissue is one of the crucial components of our body that support the body. It was found that nano-HA is an important mineral component of bone, enamel and dentin of teeth (Wojnar, 2010). Natural bone is a type of nanocomposite containing organic (30%) and inorganic compounds consisting of apatite crytals (70%) in a form of needle or rod materials with length of 25-50nm (Nejati, Mirzadeh & Zandi, 2008; Zhou & Lee, 2011). Although, bone apatite comprises of nanocomposite apatite, the mineral component of bone is usually referred to HA or carbonated HA (Wojnar, 2010). HA has received a considerable attention for bone substitute due the resemblance of mineral component, chemical composition and structural morphology to the natural bone (Nejati et al., 2008). Generally, HA can make up 65% of the weight of bone tissue that provides stability, hardness and function to bone, teeth and tendons (Adak, Chatthopadhyay & Purohit, 2011; Petit, 1999).

The most importance difference between the pure synthetic HA and bone mineral is the presence of carbonate, small amount of sodium, magnesium and other trace elements (Prabakaran, Balamurugan & Rajeswari, 2005) while dental apatite consists of fluoride ion substitute (Jaffe & Scott, 1996). From Raman spectra obtained, the HA in enamel shows presence of OH modes for hydroxyl within the apatite structure but not in bone apatite which is also not contained high concentration of OH groups that is significant component in HA ceramics . Another distinct property between those is presence of protonated phosphate ions in bone mineral.

However, it is difficult to determine the actual chemical composition of bone due to lack of very accurate chemical analytic techniques to measure it. For instance (Rey, Combes, Drouet & Glimcher, 2009) (a) amount of $HPO_4{}^{2-}$ and OH^- ions in one apatite cannot be measured by this technique, (b) mineral component of bone contains various trace elements that replacing other bone elements and its crystals and (c) different concentrations of mineral ions on the surface of hydrated surface layer of both bone crystals and synthetic apatite crystals Hydroxyapatite

2.2.1 Historical Background of Hydroxyapatite

Apatite is known as a family of crystals with the formula $M_{10}(PO_4)_6X_2$ where is M usually calcium, R is usually phosphorus, and X is hydroxide or a halogen such as fluorine or chlorine (Ben-Nissan, 2014). Werner (1788, as cited in Jaffe & Scott, 1996) found the relationship between this apatite and bone mineral and the similarity between the apatite and the constituent of bone was confirmed through the progress and use of XRD. From the XRD pattern, the composition of bone mineral can be seen as a complex structure that consist of different types of hydrated calcium phosphates especially calcium hydroxyapatite ($Ca_{10}[PO_4]_6[OH]_2$) (Jaffe & Scott, 1996).

The earliest application of calcium phosphates materials in human were used as bone substitute or bone graft (Al-Sanabani, Madfa, & Al-Sanabani (2013). Albee and Morrison (1920, as cited in Petit, 1999) have used triple calcium phosphate to treat radius bone defect in rabbits. They found that it accelerated the formation of new radius bone compared to the one without triple calcium phosphate treatment. It is proven from the studies conducted that the industrial synthesis of this powder has no toxicity effect and produced a powder with high purity which led to usage in surgery to promote bone formation (Petit, 1999). Since then, the advancement of this ceramic has raised much attention to biomedical applications and this material was named bioceramics (Dorozhkin, 2010).

In the early 1970's, calcium phosphates began to use in dental application (Eliaz & Metoki, 2017). Later on, it is demonstrated the success use of calcium phosphate bioceramics composed of HA in dental field and in bone substitution. Patients with HA grafts have to undergo clinical, radiography and computer-assisted densitometry evaluation and examine regularly for at least seven years (Jaffe & Scott, 1996).

With regard to the use of HA coatings, the earliest of such coatings are the maxillofacial surgeons. They used it in hostile environment because of the acid pH of the saliva (Petit, 1999). Furlong and Osborn (1985, as cited in Petit, 1999) were the earliest implanted HA-coated hip prosthesis in humans. The HA-coated hip implant has 200 μm thickness with 40 MPa bonding strength. Afterwards, the HA-coated implants began to grow as the experimental study on animals showed no toxicity effect and many studies on qualities and technological aspects were conducted.

Over the few past decades, various studies have been conducted in order to enhance the biocompatibility and mechanical strength of the implant materials. After a series of biological evaluation through numerous in vivo and in vitro tests, these bioceramics have been accepted in biomedical applications (Thamaraiselvi & Rajeswari, 2004). Recently, HA-based bioceramics has been revolutionizing the biomedical area especially in bone replacement and tissue engineering (Balázsi, Wéber, Kövér, Horváth & Németh, 2007). It is also found its use in industrial fields such as catalysis, ion exchange and sensor (Jingbing, Kunwei, Hao, Mankang, Hui, 2004).

2.2.2 Composition and structure of Hydroxyapatite

The word “apatite” can be applied to any group of compounds with a general formula of $M_{10}(XO_4)_6Z_2$, where M^{2+} is a metal and species XO_4^{3-} and Z^- are anions. The elements or radicals M, X and Z are important in naming each of apatite. According to this term, HA possesses molecular structure of apatite where M is calcium (Ca^{2+}), X is phosphorus (P^{5+}) and Z is the hydroxyl radical (OH) (Rivera-Muñoz, 2011).

This stoichiometric HA has the chemical formula of $Ca_{10}(PO_4)_6(OH)_2$ and Ca/P ratio of 1.67 consisting weight of 39% of calcium (Ca), 18.5% phosphorus (P) and 3.38% of OH. Its hexagonal structure with a $P6_3/m$ space group and cell dimensions of a=b=9.418 Å y c=6.884 Å has a hexagonal rotational symmetry and reflection plane (Rivera-Muñoz, 2011). The crystalline structure of HA is shown in Figure 2.2.

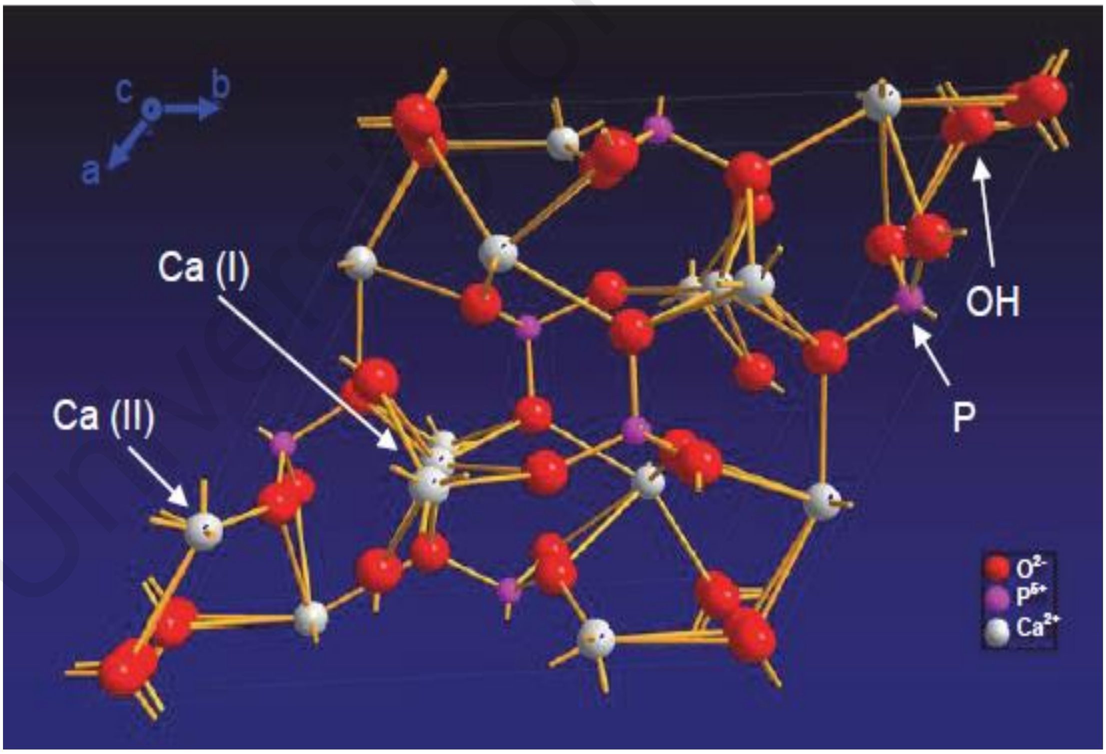

Figure 2.2: Unit cell of HA (Rivera-Muñoz, 2011)

The HA unit cell is occupied by tetrahedral arrangement of phosphate ion (PO_4^{3-}). Two of oxygen atoms are aligned both in the c axis and the horizontal plane. Phosphates are divided into two layers in the unit cell and form two types of channels along the c axis, assigned by A and B. Type A channel constitute of oxygen atoms of phosphate group and calcium ions namely calcium ions type II [Ca (II)]. It has two equilateral triangles rotated 60˚ relatively to each other, at at the heights of 1/4 and 3/4, respectively. The B type channel constitutes by calcium ions type I [Ca (I)]. Each cell consists of two channels with two calcium ions at heights 0 and1/2. In pure HA, OH radicals occupies at the centers of the channels type A with alternating orientations (Rivera-Muñoz, 2011).

2.2.3 Properties of Hydroxyapatite

To date, the development of materials are not limited in industrial field but in clinical applications especially the use of HA ceramics as bone substitute in order to replace or repair seriously damaged tissue and restore its function due to trauma, diseases and accidents. These foreign materials have been used widely as implants inside or outside the human body. In order to be able to be use in clinical applications such as dental implants, bone repair and augmentation or orthopedic implants, etc, the materials should possess or fulfill certain requirement. HA ceramic is an excellent choice of materials due to its reliable properties.

2.2.3.1 Biological properties

HA is an excellent choice for bone repair due to its high biocompatibility property and stability under in vivo conditions (Kalita & Verma, 2010). It has the ability to elicit specific response of the host and not bring any adverse effect in the body which enables the interaction between the materials and bone tissue in both directions (Vijayalakshmi & Rajeswari, 2006). Non-biocompatible or toxic materials will cause the death of surrounding tissue. A biocompatible material that has no reaction with tissue and stable for indefinite of time is term as inert (Rivera-Muñoz, 2011). HA is also bioactive ceramics. It means that it dissolves slightly while enhancing the formation of surface layer of bone resulting in the formation of strong bond to the bone (Vijayalakshmi & Rajeswari, 2006).

This property provides a good stability of materials that are subjected to mechanical loading. The difference between bioactive and bioresorbable bioceramics may be due to structural factor (Dorozhkin, 2010). Tahriri, Solati-Hashjin & Eslami (2008) has studied the bioactivity of HA by controlling its crystallite size and composition. The bioactivity evaluation was done in a stimulated body fluid media at 37 ˚C. It showed that the HA produced possess high bioactivity as more calcium ions were released from the HA crystals.

Another important property of HA is osteoconductivity properties. This property is essential to induced bone ingrowth on the surface. Woodard et al. (2007) have conducted a study on pigs to evaluate the osteoconductivity of HA bone scaffold with multi-scale porosity. Recombinant human bone morphogenetic protein-2 (rhBMP-2) was incorporated to encourage bone ingrowth. Microporous scaffold demonstrated higher osteoconductivity compared to macroporous scaffold as it has larger surface area. Microporosity is crucial to improves one growth for protein adsorption, increasing ionic solubility in the microenvironment and providing attachment points for osteoblast. Apart from that, HA ceramics is non-toxicity, show no inflammatory or pyrogenetic response. Purity, properties and morphology of the HA powder plays a vital role in its application (Hui et al., 2010).

2.2.3.2 Mechanical properties

It is preferably that bone substitute can resist the mechanical loading before being replaced by mature bone. However, human body presents a wet and both chemically and biologically active while exert quite large force concentrations and the variance. Thus, the implantable bioceramics must be able to uphold the aggressive environment of the body (Dorozhkin, 2010). Despite of its excellent bioactivity and biocompatibility, HA ceramics possess low mechanical properties and restrict its use in load bearing applications such as orthopedic implants (Sasikumar & Vijayaraghavan, 2006).

Mechanical properties are largely depended on crystallinity, grain size, grain boundaries, porosity and composition (Dorozhkin, 2010). It is very sensitive to slow crack growth. HA has fracture toughness of <1.2 MPa.m$^{1/2}$ compared to human bone which is 2-12 MPa.m$^{1/2}$ (Prakasam et al., 2015). As the grain size/porosity decreases, the fracture toughness increases (Rice, 1996). In wet environment, the Weibull modulus is in range of 5-12 meaning that HA act as a brittle ceramics (Vasconcelos, 2012).

Dense HA ceramics has bending, compressive and tensile strengths of 38–250 MPa, 120–900 MPa and 38–300 MPa, respectively (Orlovskii, Komlev & Barinov, 2002). Similarly, porous HA ceramics are in the range of 2–11 MPa, 2–100 MPa and 3 MPa, respectively (Prakasam et al, 2015). The differences are due to both structural variations such as an influence of remaining microporosity, grain sizes, presence of impurities, etc and manufacturing processes, as well as caused by a statistical nature of the strength distribution (Kaur, 2017). It is found that as Ca/P ratio increases (maximum value 1.67), the strength is also increase. Conversely, it decreases when Ca/P > 1.67. High porosity also affects the strength of HA ceramics. The porous HA ceramics are less fatigue resistant compared to dense ones (Dorozhkin, 2010).

Young's modulus of dense HA ceramics is quite similar to natural tissue which is 35–120 GPa and (a) dental enamel: 74 GPa, (b) dentine: 21 GPa and (c) compact bone: 18–22 GPa), respectively while human bones is 300 MPa. In bending, the Young's modulus is found to be between 44 and 88 GPa (Dorozhkin, 2010).

2.2.4 Clinical application of Hydroxyapatite

HA has been used as coating for total hip implant due to failure of fixation of cementless total hip arthroplasty to the femoral component. HA coating done on animal showed that it helped in converting fibrous tissue to surrounded loaded bone implant and healed the gap between the implant and bone. Vedantam & Ruddlesdin (1996) have conducted a work on HA-coated total hip implant on 45 patients. Titanium alloy (Ti-6AI-14V) was coated with a plasma-sprayed 200gm layer of HA ceramics. The result showed that the successful outcome was obtained in 89% while 7.4% need revision surgery due to component loosening and infection, 1.85% for aseptic loosening of femoral component and 3.7% aseptic loosening of the acetabular component.

HA can be in forms of powders, porous blocks or beads to fill bone defects or void where a large portion of bone have had to be removed or when bone augmentations are needed (Yoruc & Koca, 2009). This can be found in bone cancers and maxillofacial reconstructions or dental applications respectively. The bone filler will provide a scaffold and encourage the rapid filling of the void by forming the bone, thus serves as an alternative to bone grafts (Martinetti, Dolcini & Mangano, 2005). If there is no usage of bone filler, it would also become part of the bone structure and will reduce healing times compared to the situation (Czernuszka, 2001).

HA is also known for its unfavorable mechanical properties. It also has been used as thin film coatings on metallic alloys. Among all of the studied metallic alloys, titanium based alloys have shown the most suitable potential for thin film coatings (Heness & Ben-

Nissan, 2004). Such coatings are applied by plasma spraying method (Gross, 2002). Titanium is chosen as it possesses good mechanical strength and fatigue resistance under load bearing conditions. They are also lightweight with high strength to weight ratios (Heness & Ben-Nissan, 2004). HA is also applied to metallic implants especially in Ti/Ti alloys and stainless steels to alter the surface properties because it is thermally unstable compound and decomposing at temperature from about 800-1200^{o}C depending on its stoichiometry (Petit, 1999).

HA is currently used in liquid chromatography, as a stationary phase for protein, nuclei acid and virus isolation and purification (Dasgupta et al., 2004; Sung, Lee & Yang, 2004), production of biocompatible ceramics and coatings, drug delivery, heavy metal immobilization in water treatments and soil remediation.

2.2.5 Diverse Structure of Nano-hydroxyapatite

Typically, natural hard tissues consist of non-stoichiometric HA crystals with various ions substitute such as CO_3^{-2}, Na^+, F^- and other ions in a collagen fiber matrix. These apatite crystals is in nanometer-sized taking form of needle-like or plate-like particles of approximately 5-20 nm width by 60 nm length (Ferraz, Monteiro & Manuel, 2004). Hence, nano-HA is said to be suitable used as bone substitute and regeneration (Sadat-Shojai, Khorasani, Dinpanah-Khoshdargi & Jamshidi, 2013). Nanostructures i.e morphology, stoichiometry, crystallographic structure and phase purity provide significant characteristics of HA particles such as strength, toxicity to cells, osseointegrativity and bioresorbability (Sadat-Shojai et al., 2013). Nevertheless, it seems that one is greatly interested in the morphology and dimension of particles when producing the nano- or micropowder HA. Nano-structured HA has better biocompatibility and bioactivity due to its high surface area and ultrafine structure (Bilton, Brown & Milne, 2010). Also, nano-particles with complex shapes improve the mechanical properties of HA and sintering kinetics which may avoid microcracks resulting from high-temperature sintering (Lin, Wu, & Chang, 2014; Sadat-Shojai et al., 2013). Hence, many have investigated the way to develop methods to synthesize nano-HA, nHA with various geometric shapes and sizes as these closely related to HA characteristics as well as its application. This can be done by controlling the processing parameters and various synthetic routes. The shapes can be in form of rod-like, needle-like, spherical, flower-like and even irregular.

Bakan et al. (2013) have successfully produced nano-needle like HA using alcohol based sol-gel technique. This was done at room temperature using $Ca(NO_3)_2.4H_2O$ and $(NH4)_2H_2PO_4$ as calcium and phosphorous precursors respectively without the use of catalyst. As the aging time increased (12 hours, 24 hours and 48 hours), it was found that less β-TCP was formed along with HA. The as-dried average particle size was smaller than the sintered powder as sintering process caused the structure to shrink and bend as well as the growth of the crystal size. By using simple wet chemical route, Chandrasekar, Sagadevan & Dakshnamoorthy (2013) have fabricated stoichiometric nHA with $Ca(NO_3)_2.4H_2O$ and $(NH4)_2H_2PO_4$ as starting materials. The aging time took 24 hours for the precipitate to fully form. The spherical particles were found to be highly agglomerated with diameter of 60 to 70 nm.

Different nanostructures of HA particles may enhance the cell biomaterial interaction upon implantation in different parts of bone in human as HA crystals exhibit diverse nanostructures in different part of human hard tissues (Mishra, Rai, Asthana, Parkash & Kumar, 2014). Moreover, the particles sizes and shapes are important in biological responses (Lin et al., 2014). Kalia et al. (2014) have found that the round nHA with lower aspect ratio compared to rice-like nHA has greater osteogenic effect that may enhances the new bone formation. Recently, nHA has been used in toothpastes, mouthwashes, etc as it is potentially remineralize artificial carious lesions (Huang, Gao & Yu, 2009). Moreover, nano-size enamel and bone may inhibit the demineralization process (Sadat-Shojai et al, 2013). In addition, it could control protein and cell-matrix interaction, enhance osteoblast activity by decreasing apoptotic cell death and long-term functionality (Ferraz et al., 2004). Webster, Ergun, Doremus, Siegel & Bizios (2000) found that the osteoblast proliferation on nanophase HA increased significantly compared to conventional HA during the cell culture. Nano-sphere and nano-rod HA crystals are suitable to be used as hip implant coating, for cell targeting, gene transfecting and silencing (Abidi & Murtaza, 2014; Lin et al., 2014). Even though nanophase HA has become a great interest in medical application, the preparation of HA with specific characteristics still need to be explored. It is important to control the geometry, size and size distribution, crystallinity, stoichiometry and degree of particle agglomeration as the biological response and mechanical properties of HA are very depended on its structural characteristics (Sadat-Shojai et al., 2013).

2.3 Synthesis of Hydroxyapatite Powder

2.3.1 Precipitation Wet Chemical Method

Precipitation is one of the most common used techniques to synthesize HA. It is also known as wet precipitation or chemical precipitation or aqueous precipitation. It involves a chemical reaction between calcium and phosphorus ions under a controlled reaction temperature with a pH greater than 9. A controlled pH is needed for a stable and stoichiometric apatitic structure. Wet-chemical is a suitable technique to synthesize HA when purity is needed since there is no foreign elements involve except water as the by product (Yoruc & Koca, 2009). The most common calcium precursor is calcium hydroxide, calcium nitrate 4-hydrate, calcium chloride and calcium sulphate dehydrate while phosphate precursor is phosphoric acid, diammonium hydrogen phosphate, natrium phosphate and potassium phosphate. Natrium hydroxide or ammonium aqueous is used for pH adjustment. Normally, a well-crystallized, stoichiometric and apatitic structure is obtained by sintering the precipitated powder at a high temperature (Liu, Troczynski & Tseng, 2001).

Generally, in wet precipitation HA can be prepared from Ca and P precursors by dissolving them with distilled or deionized water separately to make homogeneous solution. P solution is then added slowly to Ca solution and stirred vigorously. The pH is adjusted to pH 10-11 by adding the alkaline aqueous and aged for 24 hrs at room temperature and the precipitate formed is dried overnight at temperature of 80-100 °C. Normally, the precipitate is calcined to get a well-crystallined HA powder. The process of the precipitation can be seen as in Figure 2.3 below:

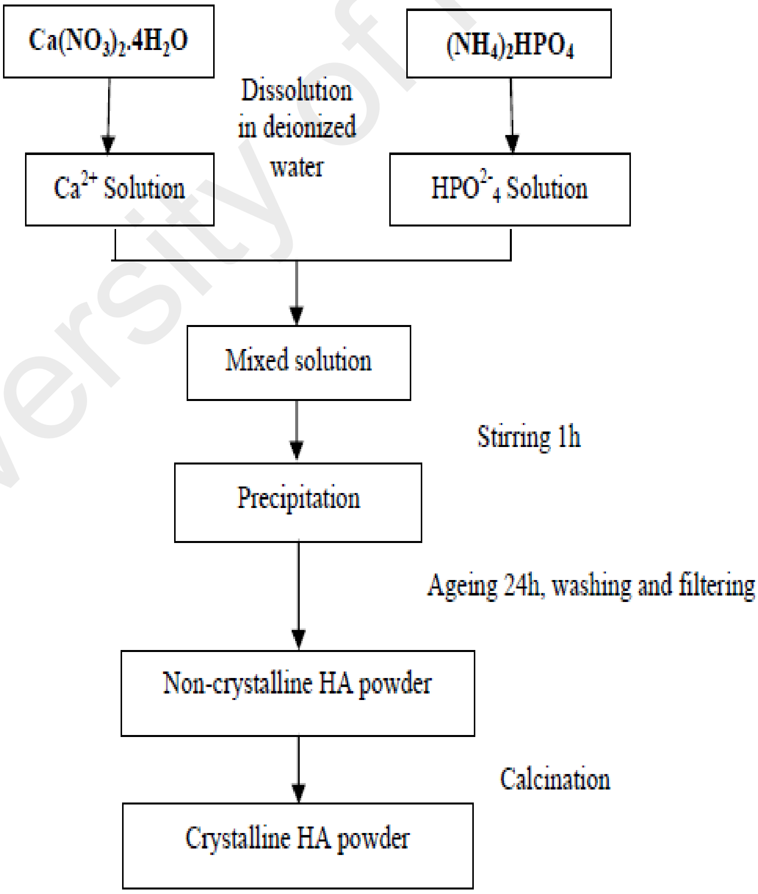

Figure 2.3: Modified chemical precipitation route for HA powder preparation (Sung et al., 2004)

Precipitation route has been extensively used owing to being simple, low cost, and suitable for bulk preparation which provides easy operation in industrial production (Cengiz, Gokce, Yildiz, Aktas & Calimli, 2008; Prabakaran et al., 2005). It also provides low working temperature and resulted in pure homogeneous product (Yoruc & Koca, 2009). Despite of being simple process, many has described it as a complicated process as it is dependent on many parameters such as concentrations of starting materials, pH, rate of addition, ionic strength temperature, stirring technique and its speed, etc (Meejoo, Maneeprakorn & Winotai, 2006). However, this method makes it possible to meet different demands by controlling its reaction parameters. The particles synthesized from wet precipitation also tend to agglomerate with a large particle size and wide particle size distribution (Cengiz et al., 2008). The resultant HA also suffer from calcium deficiency and has low thermal stability tending to decompose HA into α- or β-TCP phase which is highly resorbable (Sung et al., 2004). Sintering process improves the HA thermal stability and crystallinity. However, sintering at high temperature (> 1200 ^{o}C) will lead to β-TCP phase and other phases. The decomposition of HA is not suitable for bone replacement as it results in serious degradation in bone formation.

Sung et al. (2004) have prepared HA nanopowder of 50-100 nm size with different Ca/P ratio (1.67, 1.70 and 1.75) where the powder with a Ca/P ratio of 1.70 showed the lowest β-TCP content while HA with a Ca/P ratio of 1.75 showed a minor phase of CaO. However, the as-dried synthesized HA powder using this route resulted in low crystallinity particles. It was found that sintering the powder at higher temperature (1000 ^{o}C) for an hour improved its crystallinity as shown in the diffraction peak in the Figure 2.4 below.

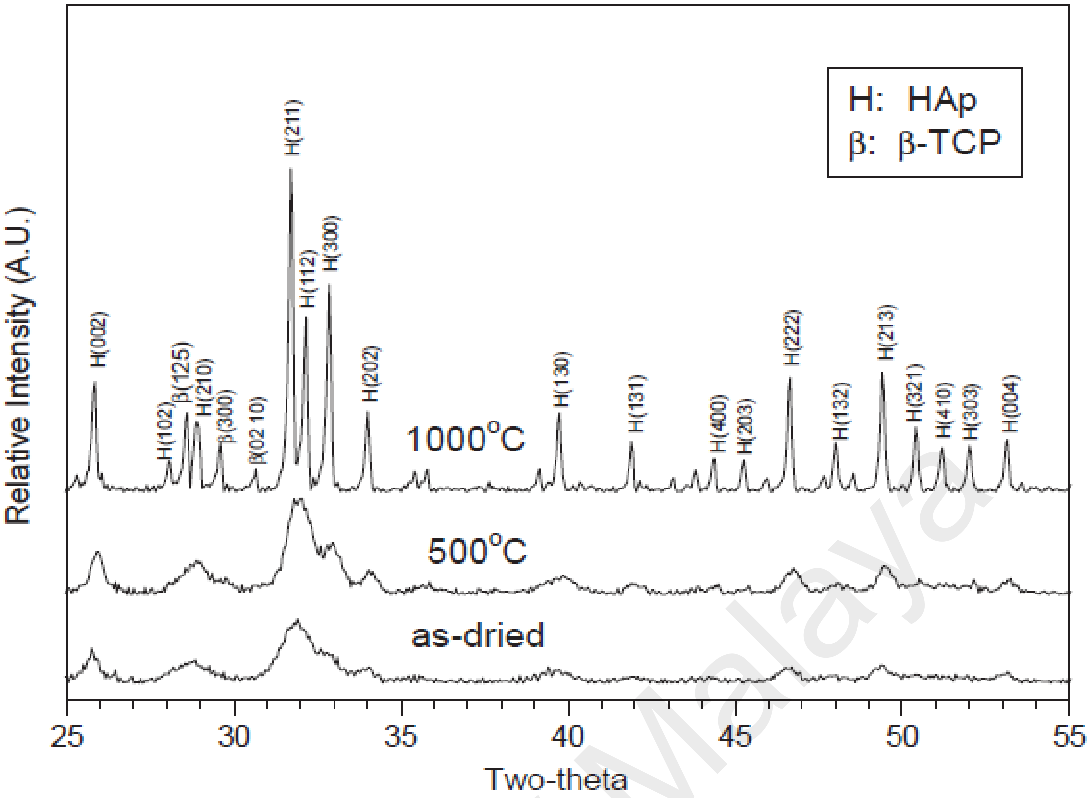

Figure 2.4: XRD patterns of HA powder dried and calcined (Sung et al., 2004)

Monmaturapoj (2008) has synthesized nHA powders with different concentration of starting materials from low, medium to high concentration to observe the amount of as-dried HA powders formed under reflux process and excess reaction time up to 48hrs. It was found that all the particles of as-dried powder agglomerate with the low concentration has the highest density followed by medium and high concentration. At 1200 °C of calcination for 1hr, it appeared that TCP was the dominant phase in all samples except for low concentration under reflux with minor phase of TCP.

According to Ramli, Adnan, Bakar & Masudi (2011), a chitosan template helped in the formation of nanosize pores of HA with calcination process. The resulting composite HA- chitosan (HA-CS) without calcination can be seen in a scaffold structure with an average pore size of 26.7 ± 11.7 µm. It was found that the calcined HA-CS composite had a higher pore size and pore volume compared to the nonporous calcined HA. From the XRD and FTIR analysis, it can be seen that no impurities were found in calcined HA-chitosan while carbonate apatite occurred in calcined HA and uncalcined HA showed low crystallinity.

Cao, Zhang & Huang (2005) have used carbamide as a source of precipitator to enhance the formation of HA nanoparticles via precipitation technique with the aid of ultrasonic irradiation. Ultrasonic technique showed that the HA particles to be needle-like structure and TEM result revealed that the particles size to be 20 nm. Cao et al. also reported that the HA content was increased with the increase of the temperature and reaction time.

It is reported by Tahriri, Solati-Hashjin and Eslami (2008) that hydroxyapatite was formed in this sample and traces of other $CaPO_4$ impurities were not detected by this technique. Secondary phase calcium oxide was observed.

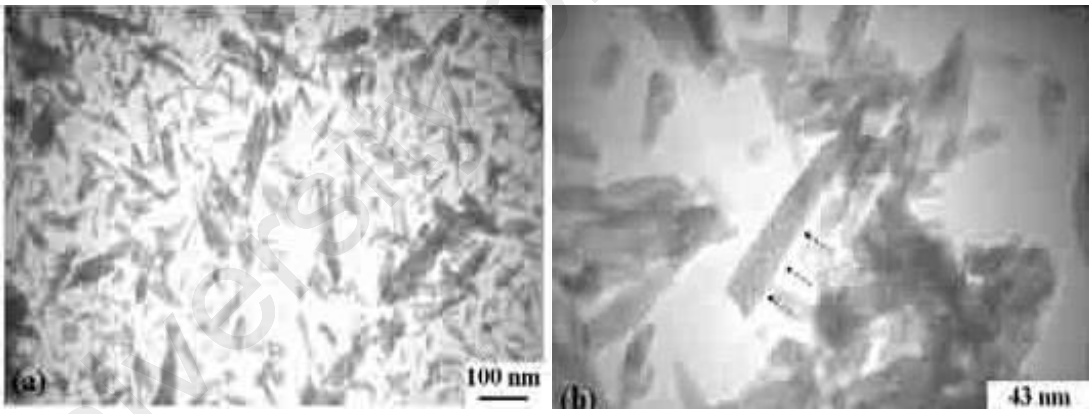

Figure 2.5: TEM micrographs of hydroxyapatite powder at (a) low magnification, and (b) high magnification Tahriri et al., 2008

The microstructure of HA crystal obtained was almost like a needle. As indicated by arrow-head (Figure 2.5), the nanoparticles contained some fine holes in their intrastructures due to alkaline environment upon synthesis of HA. Thus, there is some high corrosive hydroxyl groups in the synthesis reactor which they cause the defects in the structure.

Over the past few years, studied on using biowaste materials as calcium source with various synthesis techniques has been progressively advanced in HA production. The materials including chicken eggshells, mussels, seashells, animal bone and etc. These materials are chosen as alternative to fabricate HA due to their advantage to reduce the production cost and control the waste management (Laonapakul, 2015). In addition, it is biocompatible with human bone and less likely to be rejected when it is inserted inside the body (Ibrahim et al., 2015).

Nayar and Guha (2009) used biowaste eggshells as Ca source to substitute the chemical solution in their work. They used hydrochloric acid, HCl to dissolve the eggshells and reacted it with diammonium hydrogen phosphate, $(NH_4)_2$HPO4. 25% liquer ammonia, NH_3 was used to maintain the mixture pH. It took one week to age the mixture to allow the HA formation. However, the HA formed was non-stoichiometric HA. In this study, the method was adapted because it used biowaste product that abundantly available from food processing industry. However, instead of aging we use microwave irradiation technique to accelerate the production of HA as microwave heating is well-known to provide rapid heating. The advantages of microwave irradiation is discussed in Section 2.3.4.

2.3.2 Hydrothermal Method

Hydrothermal is another method to synthesis ceramic powders due to low temperature processing, possibility of particle morphology control and production of sintered powders. The hydrothermal reaction involves a single or compound phase reactions in aqueous solution from room temperature to crystallize anhydrous ceramic materials by controlling the thermodynamic variables such as temperature, pressure and composition (Riman, Suchanek & Lencka, 2002). This process offers high crystallinity and uniformity of the shape and particle size of the materials by employing a low temperature (Xing &

Vecchioa, 2007). This method also provides high energy, accelerated process and better equilibrium (Jiménez, Gasga & Lugo, 2003).

According to Wang et al. (2006), the thermal temperature is a major factor in controlling the crystal morphology and size rather than the reaction time. Even though, HA was obtained below 120 °C, the powder did not well crystallized. Whilst, the XRD pattern of HA powder shows a regular pattern with sharp peaks when subjected to temperature of 120 °C at various reaction time (12 hrs, 16 hrs, 20 hrs and 24 hrs) as seen in Figure 2.6.

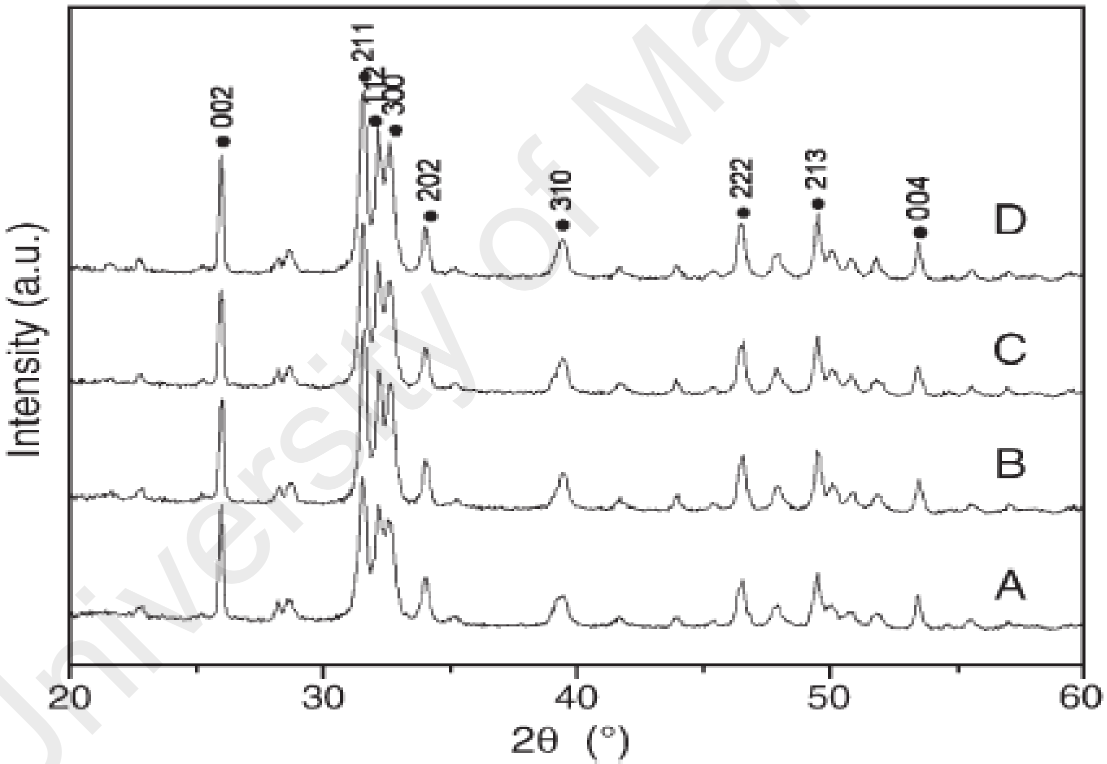

Figure 2.6: The XRD patterns of the HA powders obtained at 120 °C for 12 hours (A), 16 hours (B), 20 hours (C) and 24 hours (D) (Wang et al., 2006)

Pure HA has been synthesized using calcium chloride and dipotassium hydrogen phosphate as precursors with cetyltrimethylammonium bromide, CTAB as a template which suppresses the crystal growth even the reaction time was elongated. Earl, Wood, & Milne (2006) have synthesized nanorod HA powder along with secondary phase i.e monotite due to prolonging the reaction time. However, upon elongated time, the morphology and size of the powder did not affected as seen in Figure 2.7. The HA powder was synthesized using $Ca(NO_3)_2.4H_2O$ and $(NH_4)_2HPO_4$ at 200 ^oC with time ranging from 24 to 72 hours.

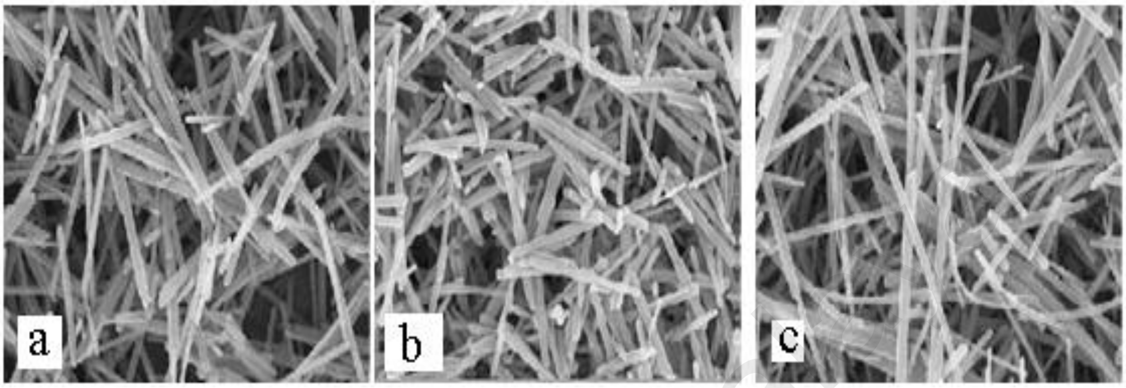

Figure 2.7: SEM micrographs of powders synthesized for different treatment times at 200 ^oC: (a) 24 hours,(b) 48 hours, (c) 72 hours (Earl et al., 2006)

It is reported from Zhang and Vecchio (2007) that the amount of calcite decreased with increasing reaction time and increase the crystallite size.

A modified hydrothermal process was developed by García et al. (2012) with employment of microemulsion system based on CTAB/toluene/n-butanol/water that can control the physical properties of the powder. The size of HA particles can be controlled by changing the microemulsion parameters such as the water to surfactant molar ratio (W_0) and cosurfactant to surfactant molar ratio (P_0). For instance, (a) when W_0=10 and P_0=5, the obtained HA particle was 60 nm, (b) when W_0=45 and P_0=5, the size of HA particle was close to 100 nm and (c) when W_0=30 and P_0=10, a hexagonal prism-like HA powder was obtained.

H. Liu (1997) synthesized a slightly calcium-deficient HA with Ca/P ratio of 1.640-l .643 via simplified hydrothermal process using the pressurized cook. $Ca(H_2P0_4)_2.H_20$ and $Ca(OH)_2$ were ball-milled and dried under infrared lamp. After heating and being pressured for 1-3 hours, the pressurized cook was heated by an electric oven at a constant power of 800 W. The HA powder obtained was needle-like with size of 13-170 nm in length and I5-25 nm in width and the XRD diffractogram indicated the absence of impurity phases. Although hydrothermal process able to control the morphology and size of the materials by varying the temperature and reaction time, its procedure are considered to be complicated since several heat-treatment steps are required which increase the cost of the HA synthesis (Avecedo-Davilla et al., 2007).

2.3.3 Sol-gel Technique

Sol gel technique can be used to synthesis many biomaterial such as ceramics powders, glasses, films and composites at low temperature and materials can be fabricated into many forms such as powders, organic and inorganic hybrids, fibers, coating, thin films, monolith and porous membranes (Vijayalakshmi & Rajeswari, 2006). Sol gel method is a process of formation of materials via a sol preparation, formation of gelation of the sol and solvent removal.

Normally, calcium alkoxides or salts and phosphorus compounds such as oxide, triethylphosphate and triethylphosphite are used as calcium and phosphate precursors respectively to synthesize HA in water or organic solvents phase (Beganskiene, Dudko, Sirutkaitis & Giraitis, 2003). Sol-gel process involves hydrolysis and condensation reactions to convert the calcium and phosphorus compound to amorphous gel to formation of ceramics when subjected to low temperature. The hydrolysis and condensation reactions take place at the same time. For example, metal alkoxide derivatives is synthesized via sol gel from glasses with high purity and crystalline oxidic ceramics material through hydrolysis and condensation reaction (Vijayalakshmi & Rajeswari, 2006). In HA sol-gel processes, calcium nitrate is frequently used as Ca precursor as well as oxidizing agent which helps in decomposition of organics easily and resulted in relatively lower temperature processing (Beganskiene et al, 2003).

Several studies on synthesis of HA have been conducted using sol-gel technique because of homogeneity of molecular mixing and high purity of product at low temperature synthesis compared to conventional methods (Fathi & Hanifi, 2007). Besides, it provides a simple control of chemical composition and operation process (Vijayalakshmi & Rajeswari, 2006). It also has the ability to generate sized particles, bulk amorphous monolithic solids and thin films (Padmanabhan et al., 2009). The sol-gel processing of HA, however, has some limitations such as high cost of raw materials and non-homogeneous of final products (Sopyan, Singh & Hamdi, 2008). Vijayalakshmi & Rajeswari (2006) have reported that they have produced HA powder along with calcium carbonate presence after heat treatment at 900 ˚C and have to carry out acid treatment to remove the carbonate group from HA powder.

Moreover, sol-gel technique require a long period of aging time to produce desirable product i.e 24 hours or longer as reported in the literature due to slow reaction between Ca and P precursors in the sol phase (Beganskiene et al., 2003). Sanosh et al. (2009) have successfully synthesized nano-rod HA having similarity properties of human teeth using $Ca(NO_3)_2.4H_2O$ and KH_2PO_4 as calcium and phosphorus precursors respectively under aging time of 24 hours. In the research performed by Padmanabhan et al. (2009), they have fabricated a rod-like stoichiometric HA using sol-gel method. However, this process which used $Ca(NO_3)_2.4H_2O$ and KH_2PO as starting materials has to be aged for 48 hours. This showed that sol-gel process is a time-consuming procedure to synthesize HA.

In addition, Beganskiene et al. (2003) have investigated the effect of aging time using different phosphate precursors i.e. trimethyl phosphate and diethyl phosphite via sol-gel technique. When aged at 24 hours, the XRD pattern showed that HA along with secondary phases such as $Ca(OH)_2$ and CaO phase were detected using the trimethyl phosphate precursor. At aging time of 72 hours, the Ca $(OH)_2$ was eliminated and CaO was diminished. By using diethyl phosphate, at same aging time, only a weak CaO phase was detected. This shows that phosphate precursor also plays an important role to fabricate HA powder although it is non-stoichiometric product and the long aging time can be reduced.

Several factors influence the synthesis of HA via sol-gel method such as (Liu, Troczynski and Tseng, 2001) (a) catalysts such as acids or bases influence the sol gel kinetics (b) chain-like or branched networks can be built depending on the pH value (c) in developing an apatitic phase, aging of the precursor solution is important. Under proper thermal heating, appropriate aging time is required to form apatite phase under complete reaction between Ca and P precursors

2.3.4 The Citric Acid Solution Combustion (Sol–Gel Combustion) Technique (SCS)

The citric acid solution combustion (sol–gel combustion) technique is a non-alkoxide sol–gel method. It is efficiently used for synthesis of nanocrystalline inorganic powders (Han, Li, Wang & Chen, 2004). This process involves a self-sustained reaction in homogeneous solution of different oxidizers (e.g., metal nitrates) and fuels (e.g., urea, glycine, hydrazides) (Aruna & Mukasyan, 2008). The SCS may occur as either volume or layer-by-layer propagating combustion modes which depends on the type of the precursors and on conditions used for the process organization (Aruna & Mukasyan, 2008). To prepare oxides by SCS, the important component required is fuel. Most commonly fuels are urea and glycine which produce highly uniform, complex oxide ceramic powders with precisely controlled stoichiometry. Various organic compounds such as alanine, asparagine, serine, methyl cellulose, ammonium acetate, ammonium citrate and ammonium tartarate have been explored as fuels.

In order to obtain organic free pure nanocrystalline powders, further calcinations are needed even though the complex fuels favor the formation of nanosize particles (El-Maghraby & Refat, 2014). Most common starting precursors are calcium nitrate, $(NH_4)_2HPO_4$, citric acid monohydrate and nitrate acid. While maintaining the reaction mixture of both precursor, it is heated on a hot plate where it undergoes dehydration reaction and transforms into a transparent viscous gel. A further heating burnt to form black ash. Calcinations of black ash will produce phase pure HA powder. Dehydration reaction occurs followed by gelation upon heating the mixture on hot plate. Citric acid is a strong complex forming agent which forms stable complex compound with many metal ions mainly under acidic condition (Pratihar et al., 2005). The cross-linking reaction of calcium citrate with the linkage of hydrogen appears to be responsible for the gelation as it is very stable and does not consist of the active groups for condensation polymerization (Czernuszka, 2001).

Gel is formed when viscosity of mix solution increases. The citric acid used acts as a fuel and is a strong reducing agent while the nitrate is a strong oxidant where reaction between them forms the oxidation-reduction reaction. The HA formation is shown in Table 2.2. The black ash remains amorphous up to $450^{o}C$ and crystallizes phase pure HA powder at $550^{o}C$.

Table 2.2: Summary of processes involve in Synthesis of HA using SCS

Process	Chemical reaction	Remarks
The oxidation-reduction reaction	$9Ca(NO_3)_2 + 5C_6H_8O_7 = 30CO_2 + 9N_2 + 20H_2O + 9CaO$	This reaction leads to combustion which forms the black ash.
Formation of HA	$10CaO + 6(NH_4)_2HPO_4 = Ca_{10}(PO_4)_6(OH)_2 + 12NH_3 + 8H_2O$	The heat from oxidation-reduction reaction helps in the reaction of amorphous calcium oxide with $(NH_4)_2HPO_4$ to form HA.

(Han et al., 2004)

Factors influencing SCS are as followed (Pratihar et al., 2005):

- Incomplete burning of the gel during combustion forming amorphous powder in nature.
- The size of crystallite increases with increasing temperature. At low temperature range (550-750 ^{o}C), the increase in crystallite size is slow while at the high temperature ranges 750-950 ^{o}C, it increases rapidly.

2.3.5 Microwave Radiation Technique

Microwave assisted synthesis has enabled the reaction that take long hours or days to be synthesized in shorter time. Hence, this method has rapidly gain attention in synthesizing biomaterials and organic materials. Microwave irradiation at 2.45 GHz frequency is considered as a new method to process HA ceramics. It is said to produce finer microstructures widening its application in the development of transparent and translucent ceramics for many applications. A microwave is a form of electromagnetic energy and falls between infra-red radiation and radio-waves in electromagnetic spectrum (Surati, Jauhari & Desai, 2012; Ravichandran & Karthikeyan, 2011). Microwave energy is different from other radiations as it is non-ionizing and provided only thermal activation. Hence, there is no changes of molecular structure of the materials being heated (Ravichandran & Karthikeyan, 2011).

During microwave heating, the sample itself becomes the source of heat resulting in a rapid rise of temperature and homogeneous of products. This is due to the heat is generated internally within the material instead of originating from external heating and subsequent radiative transfer (Kalita & Verma, 2010; Meejoo et al., 2006). In contrast, conventional heating uses external heat source which slowly activates the reaction of samples as it needs to pass through the walls of vessel then only reach the samples (Ravichandran & Karthikeyan, 2011). Microwave heating also provides a rapid and shorter synthesis time as its high depths penetration enables the entire substance to be subjected to uniform and rapid heating (Dávila, Cuevas, Gutiérrez, Angeles & Nonell, 2007; J. Liu, 2004). This causing the thermal gradients to minimize and reduce the time for particle diffusion; thus the product can be formed in a shorter time.

Microwave heating offers several advantages including fast reaction, easy reproducibility, narrow particle distribution, high yield, high purity, efficient energy transformation and throughout volume heating (Kalita & Verma, 2010). With the aid of soft template of CTAB, Arami et al. (2009) has successfully synthesized nanostrips HA by microwave synthesis technique. The use of CTAB helps in epitaxial growth of nanostructures and controls the size and morphology of the HA. The size of HA obtained was 10 and 55 nm in width and length respectively with a very short time of microwave heating (2.45 GHz, 900 W) of 5 minutes. No secondary phases were found.

In other study, Meejoo et al. (2009) have performed a simple microwave-assisted wet precipitation of HA by immediately subjected the mixture solution of the starting materials to microwave heating (850 W) for 20 mins. This work did not require a pH control as reported by others. This is because the $Ca(OH)_2$ precursor used is a strong base. Even though the HA obtained was calcium deficient HA, it was completely removed after annealing it at 800 ^{o}C. A needle-shaped particles with nano size of 50 nm in diameter and 200 nm in length has been achieved using this method.

2.4 Waste Materials as Source of Calcium Carbonate

There are several ways to synthesized HA either by chemical substance or raw natural sources. Coral, bovine bone, cuttlefish bone as well as extraction of potato peel and papaya leaf are the example of natural materials that are used as alternative to synthesize HA due to their high contents of Ca source. Lee, Lee and Yoon (2007) have successfully synthesized non-stoichiometric HA as well as β-TCP by simply varied the ratio of cuttlefish bone to phosphorus precursor by a wet, ball-milling method. However, HA was fully crystallized above 900 ^oC. Zamani, Mobasherpour, and Salahi, (2012) reported synthesis of HA by hydrothermal method using coral at 200 ^oC for 6 hours. By using the Scherrer formula, the HA crystallites was found to be 26.2 nm and 21.0 nm at plane (211) and (300) respectively while from the SEM analysis, the HA particle size was 200-300 nm. Irregular shape of obtained HA can be observed.

Natural sources are said to be safer in terms of reaction and more immunologic compared to synthetic HA. However, they are being extinct if continuously used and some of their availability are limited especially the corals since they are under preservation in many countries and have a slow growth rate. Hence, biowaste can serve as an alternative to fabricate HA. Egg shells have the richest source of Ca content which is constituted by the palisades (outer layer of the eggshells) and cuticle layer (the outermost surface) that consist of number of protein (Rivera et al., 1999; Tangboriboon, 2011). On the other hand, a matrix constituted by protein fibers bounded to calcite crystal can be found between the outer and palisade membranes (Sasikumar & Vijayaraghavan, 2006). During the eggshells formation, the palisades consisting of polysaccharide influences the calcification process and the morphology of the calcium carbonate crystals (Dávila et al., 2007). It is found that the composition of duck eggshells and chicken eggshells are similar. The eggshells represent 11% of the total weight of the hen eggs. They comprise about 94% of calcite, 1% of magnesium carbonate, 1% of $CaPO_4$ and other 4% is organic matter and other minerals (Dávila et al., 2007; Tangboriboon, 2011).

In marine, Anadara granosa is a class of bivalve cockles. This cockle or known as "kerang" in Malaysia can be found mudflats along the western coast of Peninsular Malaysia. Similar to eggshells, calcium carbonate from cockle shells also can be used as calcium precursor to fabricate HA. It is found that cockle shells has almost identical mineral composition to the coral. Coral minerals consist of more than 97% of Ca, about 0.05% to 0.2 % Mg, less than 1% of Na and less than 0.05% of P (Mohammad, Zahid, Awang, Zakaria & Abdullah, 2010).

Waste products are used because these products are available in huge amount in food processing industry. The recycle of these materials will be helpful in waste disposal problems facing by the industry since tones of chicken eggshells, duck eggshells as well as edible cockle shells are consumed daily. The recycle of this waste materials into highly value product also can minimize the environmental pollution as they favour the microbial activity. When the concentration of waste in the environment is in excess, it may affect the population of human, animals and plants. According to Department of Fisheries Malaysia, statistic in 2011 shows that 57,544.40 tonnes of cockle were produced along the west coast of Peninsular Malaysia including Johor and Pahang (Othman, Abu Bakar, Don & Johari, 2013). While it is estimated 642,600.00 tonnes of chicken eggs was produced in Malaysia in the year (Rohim, Ahmad, Ibrahim, Hamidin & Abidin, 2014). Since 11% of the total weight of egg represents the shell, about 70686 tonnes of waste generated per year. This indicates more waste are generated as well. Since these wastes will be discarded and left untreated, they may lead to unpleasant odour and create a disturbing scenery to the surrounding. The HA derived from waste materials provide a cost-effective production compared to other commercial available HA which uses high purity of reagents (Adak & Purohit, 2011).

It has been proven that waste materials used to fabricate HA shows a similar composition and biocompatibility properties to the natural bone. Apart from that, a pure, high quality and better morphology of HA powder can be produced. A latest study by Azis, Jamarun, Arief and Nur (2015) showed that HA was successfully synthesized using cockle shells by hydrothermal route. They found that the best condition where a homogeneous in crystal sizes and high purity of HA was obtained at temperature of 140 ^{o}C (16 hours) based on the XRD and SEM analysis.

CHAPTER 3: METHODOLOGY

3.1 Preparation of Raw Materials

Duck eggshells and chicken eggshells used are free-range products. They were obtained from various households in Melaka who consumed the duck eggs and chicken eggs almost daily. The eggshells were ensured to be raw by not undergo any cooking process. While cockle shells were collected along the shore of beach in Tanjong Keling, Melaka. Since the cockle shells were deposited along tide marks in the sand, they were found to be white in colour and clean. All the raw materials were cleaned using brush to remove the dirt on their surfaces and repetitively washed with distilled water. The membranes of the eggshells were peeled off as it contains protein. All the cleaned materials were further boiled in water for 15 mins to remove dirt and organic residue. They were dried in a drying oven at 50 ^{o}C for 30 mins. The dried materials were then ground to fine powder using agate mortar and pestle and was used as a calcium carbonate ($CaCO_3$) source in this study.

3.2 Preparation of Stock Solution

3.2.1 Dilution of 6M Hydrochloric Acid (HCl) to 1M HCl

The concentration of provided HCl was 6M and it was diluted with distilled water to get 1M HCl. Hence, 167 ml 6M HCl was put in 1L volumetric flask and then distilled water was added until it reached the 1L mark. The flask was swirled slowly to allow the solution to mix homogenously. The dilution was prepared by using the calculation below:

Formula: $M_1V_1 = M_2V_2$

Where, M_1 = initial molarity of HCl

V_1 = initial volume of HCl

M_2 = final molarity of HCl

V_2 = final volume of HCl

Hence, $V_1 = M_2 V_2 / M_1$

$= (1\text{M})\,(1\text{L})/(6\text{M})$

$= 0.167\ \text{L HCl}$

3.2.2 Weight of Diammonium Phosphate, $(NH_4)_2HPO_4$ powder required for dilution

$(NH_4)_2HPO_4$ powder was weighted to 20.6 g and dissolved in 800 ml 0f distilled water in 1000 ml beaker and stirred for a few minutes. Then, the distilled water was added to 1L and stirred until the solution was complete dissolved to give 0.156M ($(NH_4)_2HPO_4$) aqueous solution. The amount of ($(NH_4)_2HPO_4$) powder required to make 1L of 0.156M ($(NH_4)_2HPO_4$) aqueous solution was calculated using the below calculation:

$$m = MV$$

Where, m = number of moles of $(NH_4)_2HPO_4$

M = molarity of $(NH_4)_2HPO_4$

V = volume of distilled water

Hence, $m = (0.156\ \text{M})(1\text{L})$

$= 0.156\ moles\ of\ (NH_4)_2HPO_4$

Then, the mass of $(NH_4)_2HPO_4$ required was:

$$mass = mW$$

Where, w = molecular weight of $(NH_4)_2HPO_4$

Hence, $m = (0.156\ \text{moles})(132.05\ \text{gmol}^{-1})$

$= 20.6\ \text{g}\ (NH_4)_2HPO_4)$

3.3 Synthesis of Hydroxyapatite

Precipitation method of the precursors in producing the HA was adapted from Nayar and Guha (2009). Waste materials such as chicken eggshells, duck eggshells and cockle shells were used as Ca source instead of using chemical solution (refer to Section 2.3.1). Slight modification was done in this study. Instead of long aging process, microwave irradiation technique was used to accelerate the formation of HA.

Mostly, the power used ranging from 250-980 W with time ranging from1-20 min (Cao et al., 2005; Han, Song, Saito & Lee, 2006; Kundu, Waghode, Bahadur & Datta, 1998; Sarig & Kahana, 2002; Vaidhyanathan & Rao, 1996; Yang, Jiang, Wang, Ma & Li, 2004). Considering the volume of reactant used in this study, it is decided the reaction time of microwave heating is 15 mins to ensure the synthesis reaction is complete. The experimental procedure will be discussed as below. 25g of chicken eggshells (CES) powder was dissolved in 100 ml HCl: 300 ml H_2O. The mixture was stirred rigorously for 30 minutes with the help of magnetic stirrer. It was then filtered to eliminate the residue of eggshells. 1850 ml $(NH_4)_2HPO_4$ solution was added to the eggshells solution and stirred thoroughly. The mixture pH was maintained 10-11 by adding drop wise of 1:1 of 25% liquor ammonia and distilled water. The mixture was immediately subjected to microwave heating in a domestic oven operating at 2.45GHz (550W, 700W and 900W) for 15 min. The precipitate formed was centrifuged at the rotation speed of 3000 rpm several times with distilled water to eliminate the remaining ammonia. It was then dried overnight at 100 ˚C in drying oven. As-dried precipitate was ground to fine powder. The experiment was repeated exactly using duck eggshells (DES) and cockle shells (CS). This procedure was repeated for several times to obtain identical phase of the HA powder. The microwave power (550W, 700W and 900W) were varied to study their effect on the HA particles morphology. Table 3.1 shows the synthesis condition and sample ID.

Table 3.1: Synthesis condition and ID sample of hydroxyapatite powder

$CaCO_3$ Source	Sample ID	Product ID	Microwave power (W)
Chicken eggshells	CES	CHA550	550
		CHA700	700
		CHA900	900
Duck eggshells	DES	DHA550	550
		DHA700	700
		DHA900	900
Cockle shells	CS	SHA550	550
		SHA700	700
		SHA900	900

3.4 Compaction of Powder for Compression Test

Approximately, 0.4 g of as-synthesized HA powder was uniaxial compacted at 2.5 MPa into cylindrical form (5mm diameter and 10 mm height) using a steel die set as in Figure 3.1. The HA powder used was dry and without any binder or composite content. To avoid the compacted HA being lodged in the die, zinc oxalate powder was used to smoothly eject the compacted powder out of the die. A thin layer of the powder was dispersed inside the die steel before HA powder was incorporated in it.

Figure 3.1: Steel die set for compaction of HA powder (From left; plunger (back), stopper (front), die base plate, die steel body and large base plate).

The schematic diagram of the hydraulic press is shown in Figure 3.2.

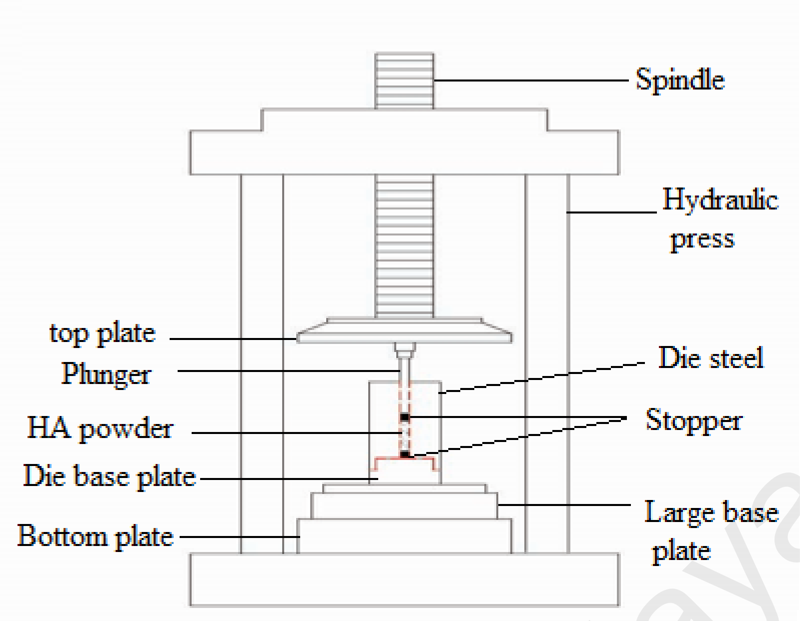

Figure 3.2: Schematic diagram of hydraulic press with the die steel set.

The HA powder was filled in the die with the small base plate attached to the die. It was then placed on top of the large base plate for support during the compaction. The plunger was vertically aligned with die/small base plate and large base plate to compact the powder at desired pressure using the lever. The pressure value was observed on the gauge. Once the desired pressure (2.5 MPa) was achieved, the force was allowed to hold for five minutes and removed slowly by unlocking the screw. The small base plate was separated from the die and the large base plate was put on the bottom of die to eject the compacted powder by slowly pulling the lever until the plunger ejected it from the die.

Five cylindrical HA for each samples were made and tested for compression test. The compacted HA powder can be seen as in Figure 3.3. It is important to clean the die with alcohol and deionized water to prevent contamination.

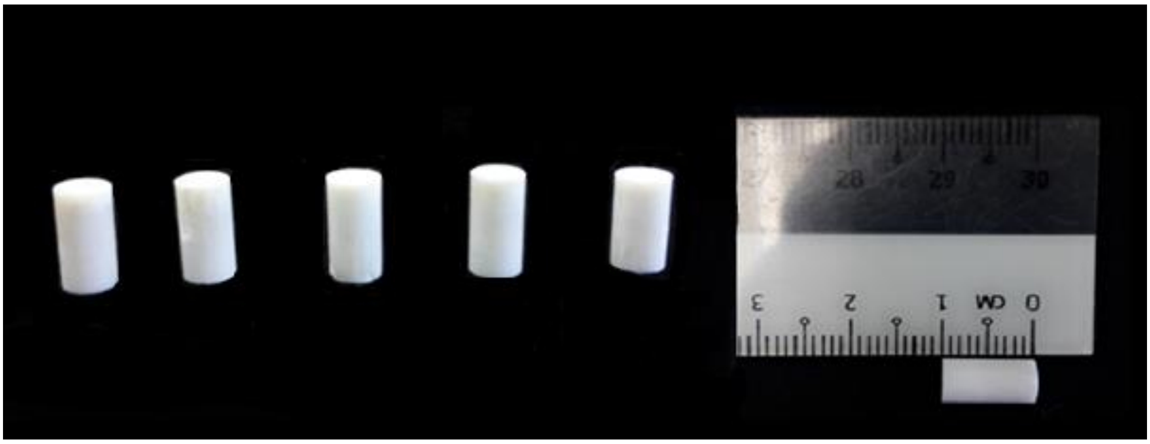

Figure 3.3: Product of HA powder after compaction using hydraulic press.

3.5 Characterization of Hydroxyapatite Powder

3.5.1 X-ray Diffraction (XRD)

XRD is a technique for identifying a crystalline material as well as the unit cell dimensions (Dutrow & Clark, 2009). When exposed to monochromatic x-radiation, each powder particle will be properly oriented as it contains of many fine and randomly oriented particles which in turns providing every set of crystallographic planes for diffraction (Callister & Rethwisch, 2007). XRD also provides information of crystal structure such as arrangement of atoms in the crystalline state, the angle and distance of the interatomic (Whittingham, 1997). It is also used to measure sample purity as well as the composition of impurities present (Dutrow & Clark, 2009). The crystallography of materials can be determined using both diffraction graphs and Bragg's Law. The powder samples were analyzed using XRD (Panalytical) of Cu-Kα radiation (1.540600 Å) with voltage and current settings at 45kV and 40mA respectively. The XRD patterns were recorded in step size (°2Th.) 0.03° and step time 1s in the range of $20^o – 60^o$. A thin layer of the powder was adhered to a glass slide before placing it in the XRD machine chamber.

3.5.2 Fourier Transform Infra-red (FTIR)

FTIR uses spectroscopy method which depends on the absorption of infrared photon. The applications of FTIR include chemical bonds identification of molecule, identification of molecular structure, identification of unknown material, quality or consistency determination and amount of components in a mixture determination. FTIR (Nicolet iS10) was used to determine the functional groups of the sample powders. The FTIR spectra was recorded in transmittance mode with region of 400-4000 cm^{-1} using the KBr pellet technique. Approximately, 2 mg of HA powder and 300 mg of KBr powder were grind with agate pestle until they were well dispersed. The powder mixture was then pressed into disk with appropriate die using hydraulic press. The disk was then mounted at the holder in the spectrometer.

3.5.3 Field Electron Scanning Electron Microscope (FESEM)

FESEM is an analytical technique used widely in materials science. The images of the samples surface are scanned with a high- energy beam of electrons in raster scan pattern to provide information about the sample such as its surface features, size and shape of the features (Alyamani & Lemine, 2012). The morphology of sample powders were obtained with a Hitachi model S-3500N scanning electron microscope, operated at 20 kV with magnification of 100 000 x. Small amount of powder was coated with gold palladium using a sputter coater. Then it was held at the sample holder to observe the images.

3.5.4 Energy-Dispersive X-ray Spectroscopy (EDX)

EDX is an analytical technique which is usually integrated with SEM or FESEM. It is used to analyze the element or chemical composition of a sample. Jeol JSM 7600-F coupled with EDX operated at 25 kV accelerating voltage and 10 mm working distance was used to analyze elemental composition of HA.

3.5.5 Universal Testing Machine (UTM)

Universal testing machine is also known as materials testing machine. It is used to measure tensile stress, compressive strength as well as flexural strength depending on the set up. Both ultimate strength and yield strength of a sample can be measured. Throughout the entire test, it records the load and deformation values which forms stress-strain curve for each sample. This graph can be used for further analysis. The elastic region below the stress-strain graph in compression test determines the young’s modulus. The compression test was performed on UTM (Shimadzu) using 5 kN load. The cross-head speed was set at 0.5mm/min. The maximum extension of the compressive head was set at 6 cm.

CHAPTER 4: RESULTS AND DISCUSSION

4.1 Introduction

One of the important parameters that affects the complete reaction of HA is alkaline pH around 9-10. After the mixing of chicken eggshells, duck eggshells and cockle shells solution with $(NH_4)_2HPO_4$, the preliminary pH of the mixture was around 7-8. The pH was adjusted to 10-11 by using 25% liquor ammonia (NH_3). It is found that above pH 10, pure crystalline HA phases with narrow size distribution and uniform morphology was formed as obtained by Jadalannagari, More, Kowshik and Ramanan (2011) in their previous study. Upon increasing the microwave power, it was found that there were only slightly changes in the final temperature of the solution i.e. 56 ^{o}C, 58 ^{o}C and 59 ^{o}C for microwave power at 550W, 700W and 900W respectively.

4.2 Hydroxyapatite Powder Characterization

4.2.1 X-ray diffraction (XRD) analysis

The XRD patterns for products from sample CES, DES and CS powders are shown in Figure 4.1-4.3. The phase identification was verified according to standard JCPDS file-00-024-0033. Phase analysis revealed that all major peaks of HA were presented in all powders except for plane (300) in CHA550 and DHA550 samples. However, this plane was observed in CHA and DHA irradiated at power 700 W and 900 W respectively. Similarly, (300) hkl plane was observed by Krishna, Siddharthan, Seshadri and Kumar, (2007) when they irradiated HA-derived chicken eggshells at 800 W power. Therefore, the absence of (300) plane in both CHA550 and DHA550 samples might be due to low microwave power used which was insufficient to induce the formation of this peak. Since microwave radiation provides a rapid heating rate and uniform heating throughout the entire volume of the substance, the energy was sufficient to produce the major peaks of HA at planes of (002), (211), (112), (300), (202), (130), (222), (213) and (004).

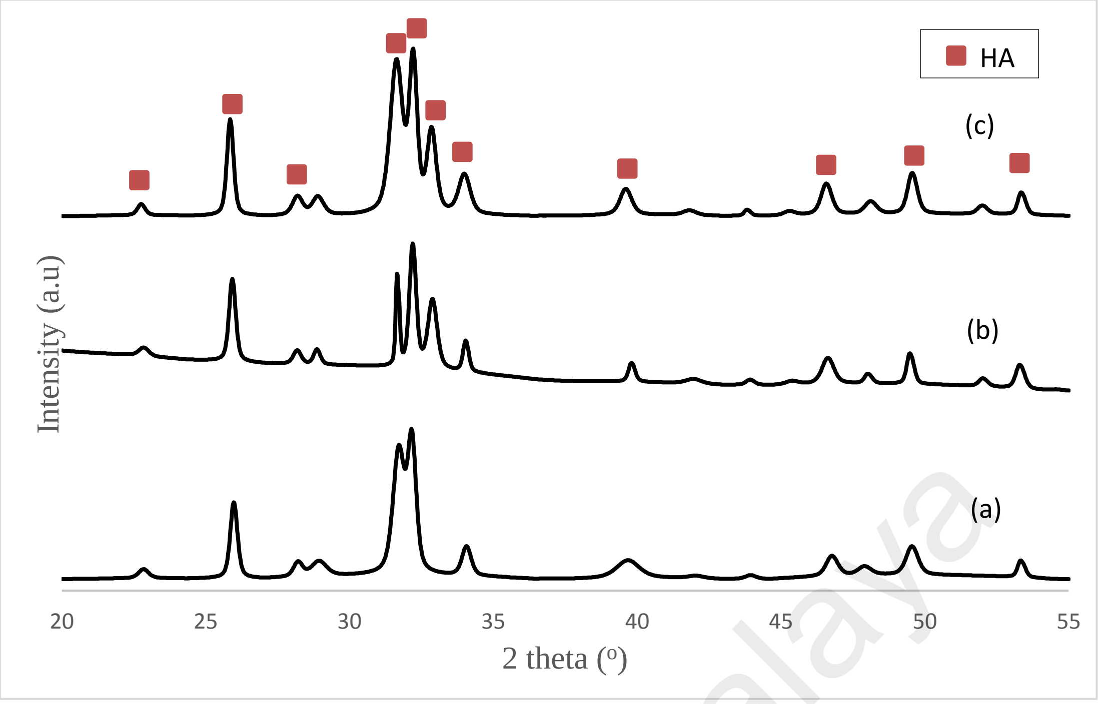

Figure 4.1: X-ray diffraction patterns with corresponding peaks of HA for CHA samples at microwave power of (a) 550W (b) 700W and (c) 900W

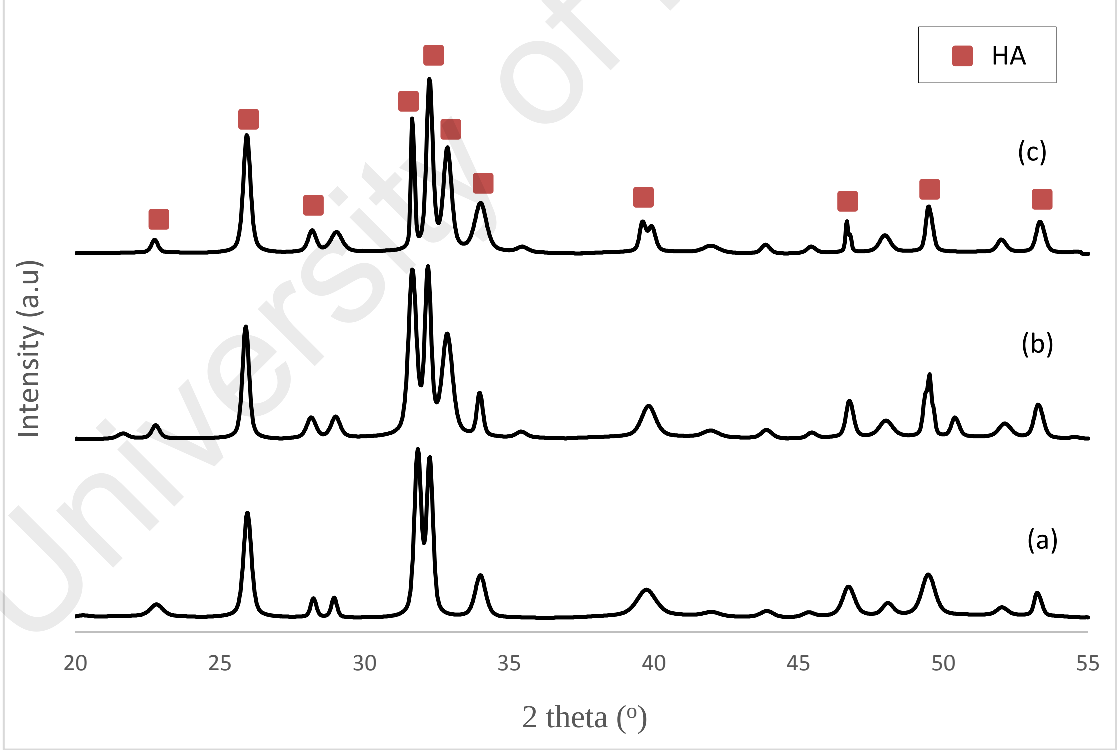

Figure 4.2: X-ray diffraction patterns with corresponding peaks of HA for DHA samples at microwave power of (a) 550W (b) 700W and (c) 900W

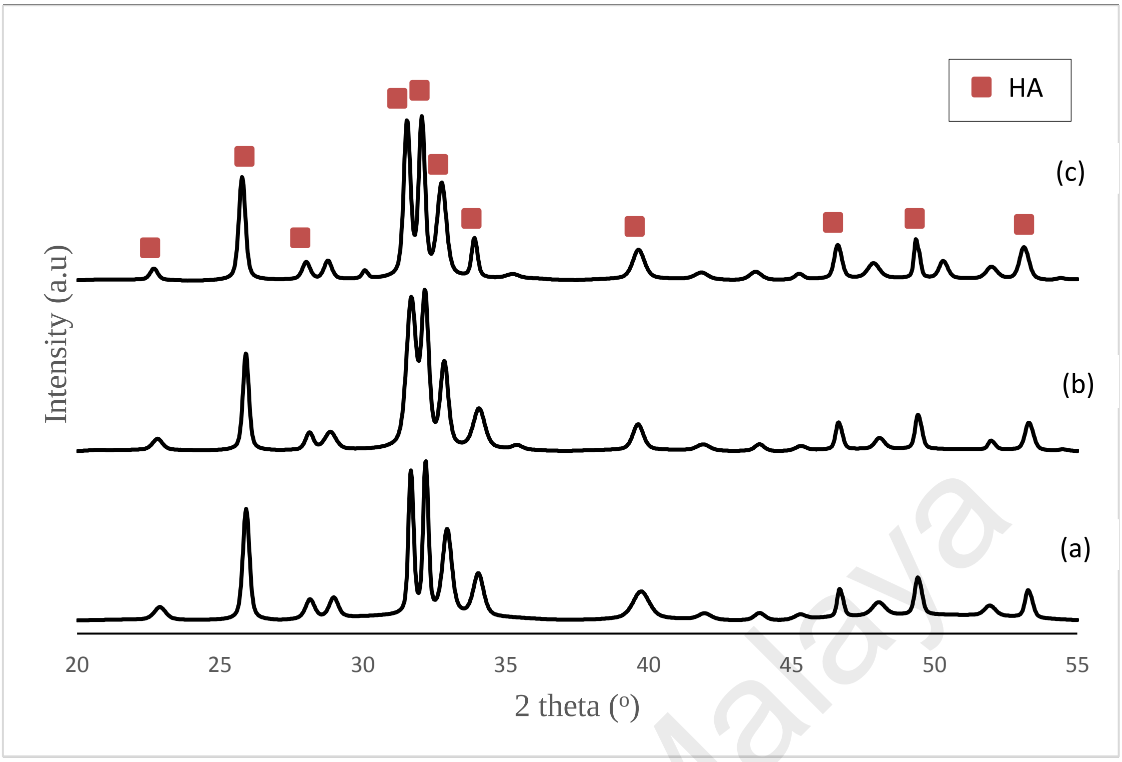

Figure 4.3: X-ray diffraction patterns with corresponding peaks of HA for SHA samples at microwave power of (a) 550W (b) 700W and (c) 900W

The absence of other peaks corresponding to impurities such as β-TCP, α-TCP or calcium carbonate indicates a pure phase of HA has been synthesized as seen in Figure 4.1-4.3. There is no indication of other secondary phases in all samples upon increasing the microwave power from 550W to 900W from the XRD diffractograms. However, there was a slight increment in intensity in all samples as the microwave power level increased. All peaks corresponding to HA characteristics were well presented. The sharp and high intensity peaks of the XRD patterns indicated that HA powder were well crystallized.

The peaks were in a good agreement with standard data for HA which confirmed the formation of HA during microwave heating. The summary is shown in Table 4.1.

Table 4.1: Comparison between standard HA 2Theta and CHA, DHA and SHA samples with plane where the major HA peak characteristic occurred.

Plane (h, k, l) Samples (2θ)	002	211	112	300	202	130	222	213	004
Standard HA	25.88	31.74	32.19	32.87	34.05	39.77	46.66	49.46	53.21
CHA550	25.96	31.69	32.14	-	34.04	39.65	46.74	49.52	53.31
CHA700	25.90	31.65	32.17	32.86	34.02	39.78	46.60	49.46	53.28
CHA900	25.83	31.61	32.19	32.83	33.97	39.57	46.54	49.53	53.33
DHA550	25.93	31.82	32.23	-	33.97	39.71	46.69	49.45	53.39
DHA700	25.87	31.63	32.17	32.83	33.96	39.78	46.73	49.54	53.25
DHA900	25.91	31.64	32.22	32.84	33.98	39.90	46.67	49.48	53.32
SHA550	25.9	31.66	32.18	32.92	34.02	39.70	46.67	49.40	53.26
SHA700	25.87	31.72	32.24	32.77	34.07	39.80	46.62	49.48	53.27
SHA900	25.76	31.52	32.04	32.74	33.89	39.62	46.59	49.35	53.10

Figure 4.4-4.6 show the comparison of XRD pattern at microwave power of 550W, 700W and 900W between the CHA, DHA and SHA samples, respectively. At microwave power 550W, the SHA550 has well resolved and sharp prominent peaks in comparison to CHA550 and DHA550. At microwave power of 700W, DHA was observed to have most sharp and high intensity of peaks in comparison to CHA700 and SHA700. Whilst at microwave power 900 W, all samples have high intensity of peaks. However, the peak of CHA900 was not fully resolved.

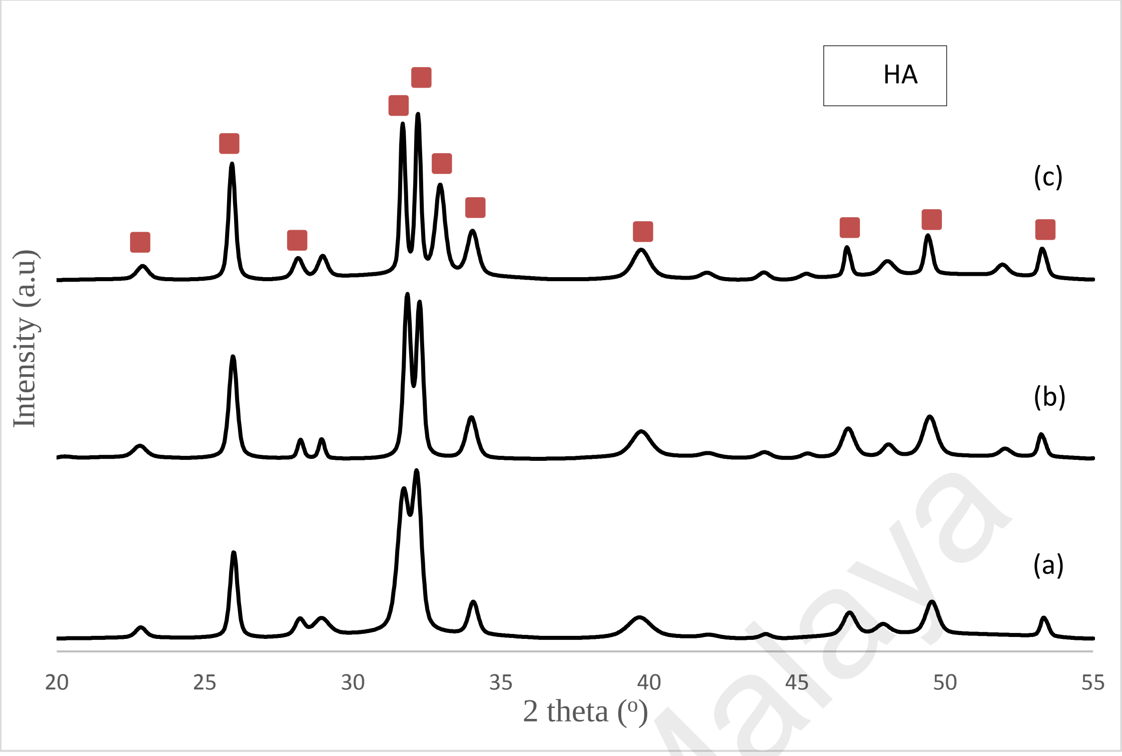

Figure 4.4: X-ray diffraction patterns of HA samples at microwave power of 550W with corresponding peaks of HA (a) CHA550 (b) DHA550 and (c) SHA550

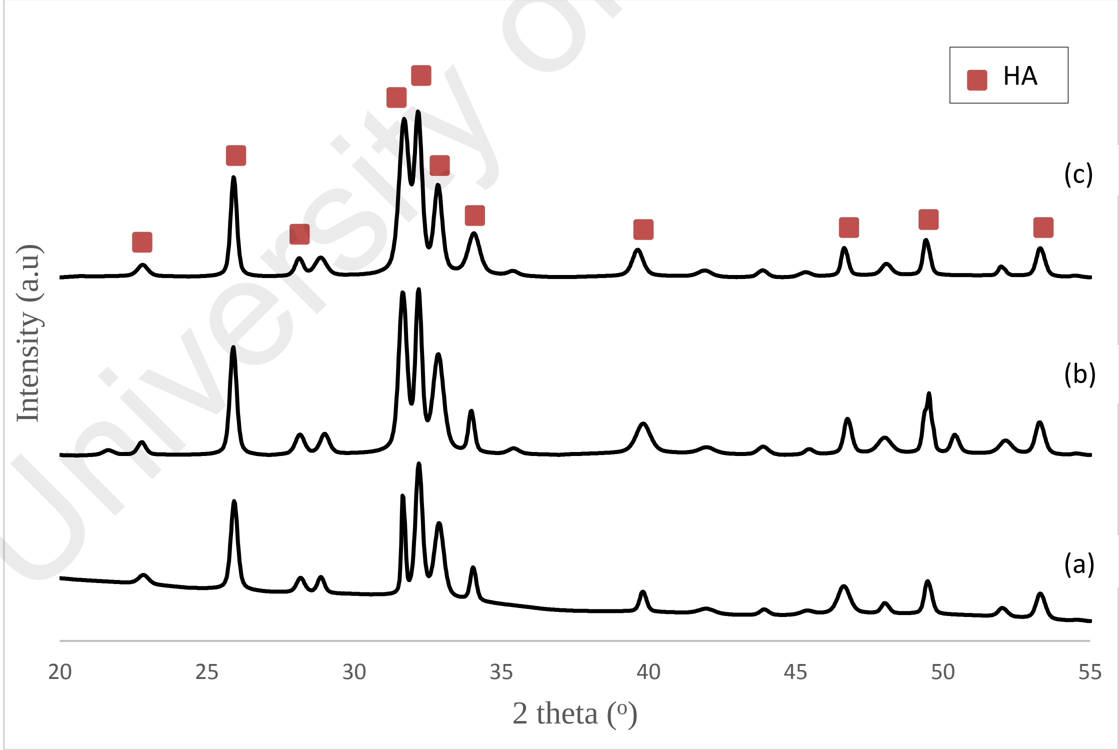

Figure 4.5: X-ray diffraction patterns of HA samples at microwave power of 700W with corresponding peaks of HA (a) CHA700 (b) DHA700 and (c) SHA700

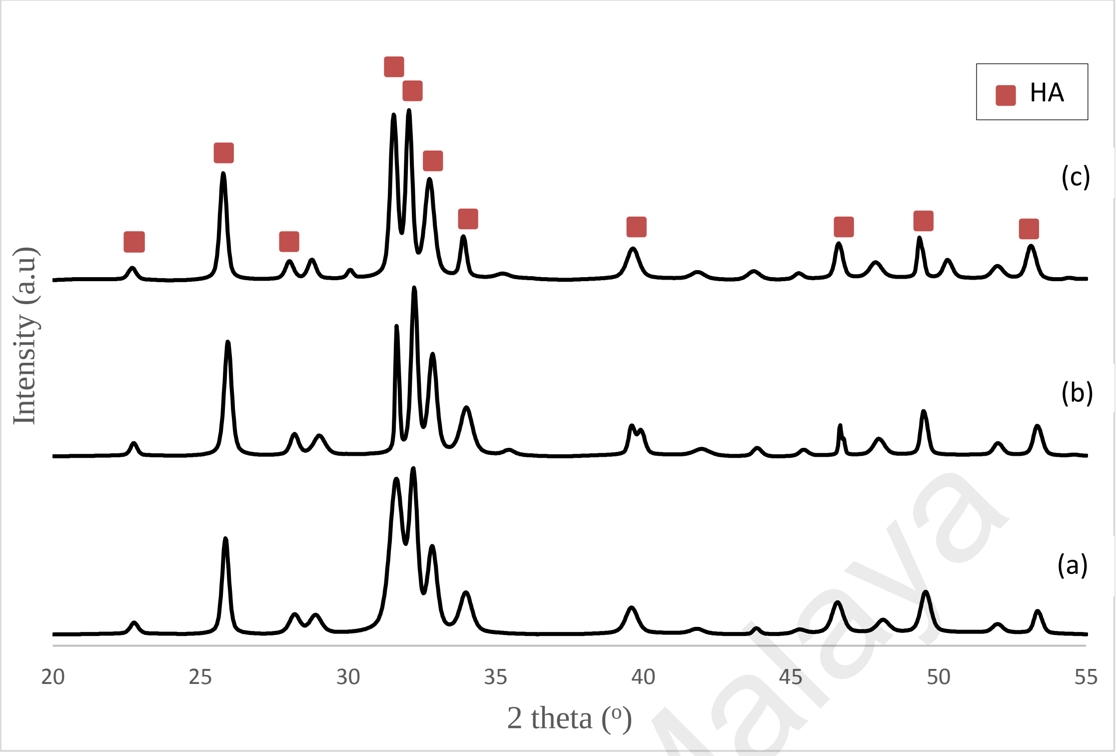

Figure 4.6: X-ray diffraction patterns of HA samples at microwave power of 900W with corresponding peaks of HA (a) CHA900 (b) DHA900 and (c) SHA900

The efficient transformation of energy and heating of microwave synthesis caused a well crystallized HA powder to be synthesize. Unlike conventional heating, microwave heating is rapid as the heat is transferred directly to the molecules instead of external heating source (Agrawal, 1998). Transfer of microwave irradiation energy to molecules occurs within 10^{-9} second resulting in non-equlibrium condition and rapid temperature rise enhancing the degree of crystallinity and increase the crystallite size as the molecules rapidly move and collide with each other with high energy (Akram et al., 2015; Hayes, 2002).

In addition, the solution during microwave heating experienced superheating where the solution temperature can be above its boiling points (Das, Bhowmik & Chaudhuri, 2012). This higher temperature area may occur due to the uneven distribution of the electromagnetic field strength causing the dielectric properties to alter (Zhang, Hayward & Mingos, 2003) and instant rise in temperature causing the molecules to move faster and decrease the diffusion barrier. Consequently, atoms are transported to the lattice site enhancing the degree of crystallinity of final product (Farzadi, Solati-Hashjin, Bakhshi & Aminian, 2011).

In microwave heating, highly polar solvent such as water will directly couple with the molecules in the reactant mixture thus provides high ability to absorb microwave radiation (Hayes, 2002). This enhances the efficiency transfer of heat energy during microwave heating which contributes to high degree of crystallinity of materials (Akram et al., 2015).

> According to theory of nucleation, an increase in the supersaturation reduces the nucleation activation energy which enhances the nucleation rate but suppresses the particle growth. Due to the direct transfer of heat to the reacting species during microwave heating, rate of supersaturation becomes high, which ultimately reduces the nucleation activation energy and thus crystallinity and phase purity of HA are positively influenced under the effect of microwave environment (Kashchiev & Van Rosmalen, 2003, p. 557).

Akram et al. (2015) found that in synthesis mesoporous HA, as the microwave power increased from 450 to 800 W, the XRD pattern of HA showed a considerable increased of intensity and sharpness of the (211), (300) and (202) diffraction planes which confirmed the increase in the degree of crystallinity and particle size compared to synthesized HA without exposure of microwave heating containing low intensity broad peaks. However, no secondary phases were observed in the XRD pattern in both synthesis of HA.

4.2.2 Fourier Transform Infra-red (FTIR) analysis

The FTIR spectrum of the as-synthesized CHA, DHA and SHA are shown in the Figure 4.7-4.9.

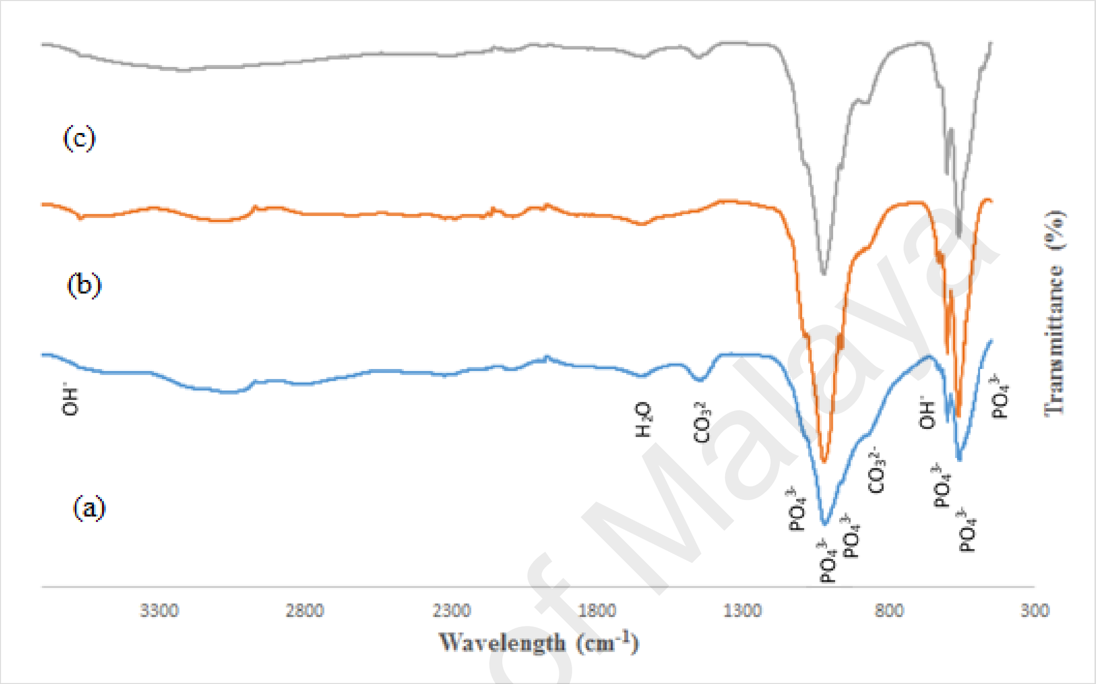

Figure 4.7: FTIR spectra of (a) CHA550 (b) CHA700 and (c) CHA900 show a match wavelength of functional groups for standard HA

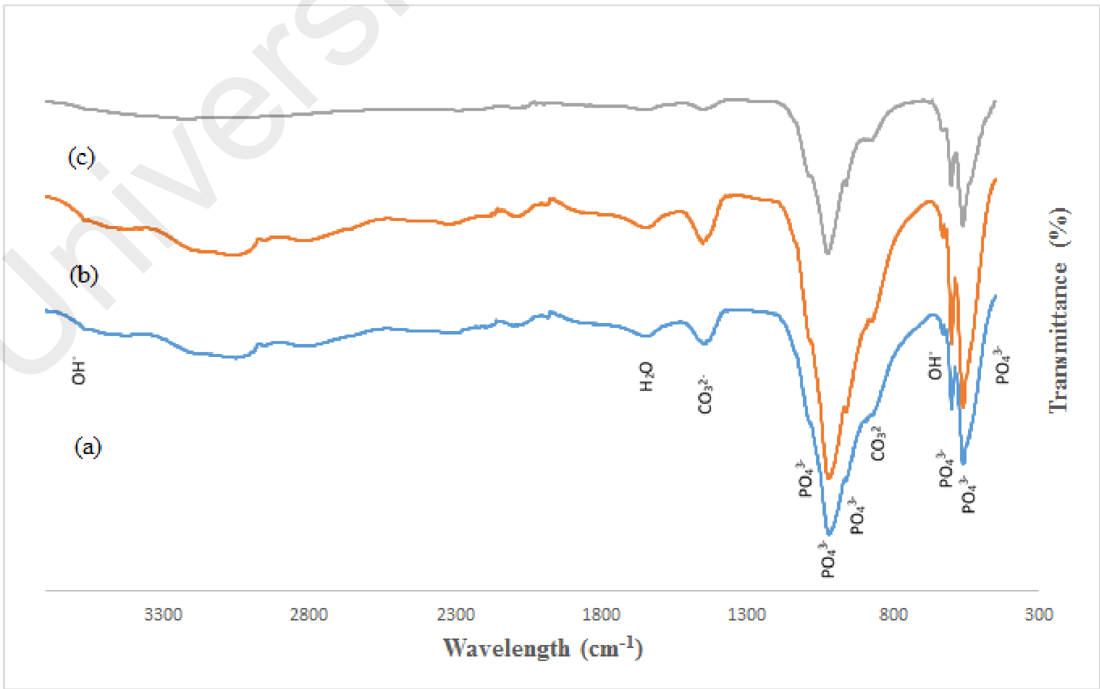

Figure 4.8: FTIR spectra of (a) DHA550 (b) DHA700 and (c) DHA900 show a match wavelength of functional groups for standard HA

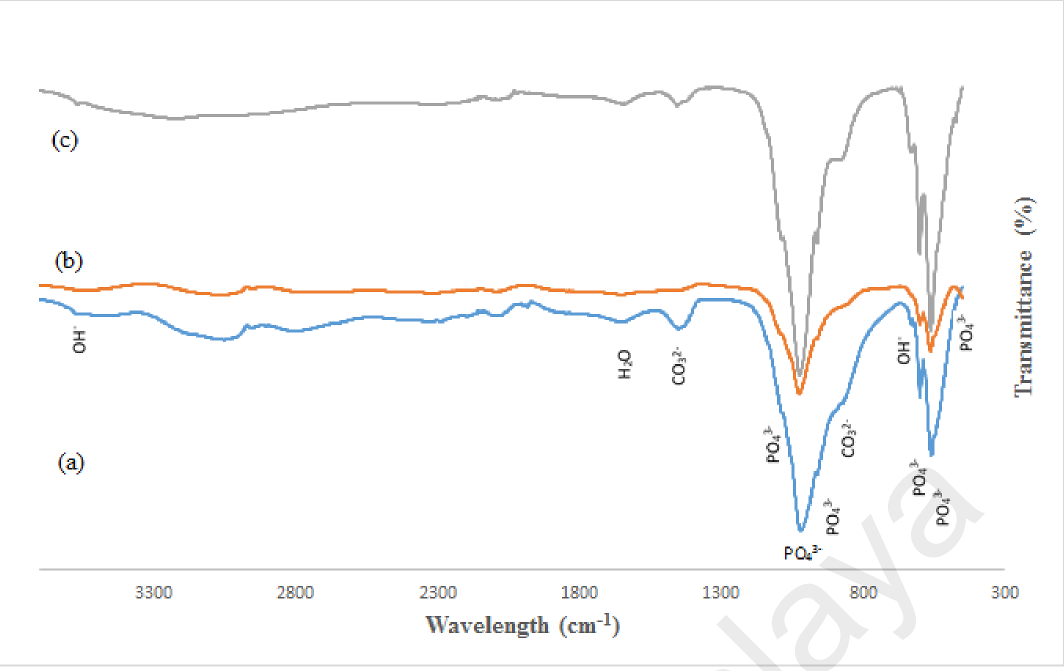

Figure 4.9: FTIR spectra of (a) SHA550 (b) SHA700 and (c) SHA900 showed a match wavelength of functional groups for standard HA

All the characteristic of PO_4^{3-} and OH^- groups appeared at the frequencies quite similar to standard HA spectrum (Ahmed & Ahsan, 2008; Kumar, Thamizhavel & Girija, 2012; Singh, 2012; Zou, Lin, Chen & Chang, 2012). In CHA and SHA samples, as microwave power increased, the intensity of peaks also increasing while DHA samples showed a decreasing trend of intensity as microwave power increased. However, the peaks of OH^- groups (~3542 cm^{-1} and 631 cm^{-1}) and adsorbed H_20 (~1646 cm^{-1}) appeared to be very weak when the microwave power increased in all samples. PO_4^{3-} group can be seen at ~472 cm^{-1} (ν3, asymmetric stretching), ~564 cm^{-1} and ~605 cm^{-1} (ν4, bending), ~961 cm^{-1} (ν1, symmetric stretching) and ~1032 cm^{-1} and ~1090 cm^{-1} (ν2, bending) in CHA, DHA and SHA samples. The weak presence of CO_3^{2-} group in CHA, DHA and SHA samples at frequencies of ~874 cm^{-1} and ~1454 cm^{-1} might be adsorbed from atmosphere during the synthesis process (Zou et al., 2012). It is common for biological apatite to allow other non-apatite ions substitution such as carbonate, fluoride and chloride substitutions which substitutes either OH^- or PO_4^{3-} groups (Kalita & Verma, 2010; Meejoo et al., 2006)

All the FTIR spectrum characteristics of HA for sample CHA, DHA and SHA can be seen in Table 4.2.

Table 4.2: Hydroxyapatite and the FTIR absorption bands of their chemical groups of CHA, DHA and SHA

Corresponding assignments	Observed Vibrational Frequencies (cm^{-1})									
	Standard HA	CHA550	CHA700	CHA900	DHA550	DHA700	DHA900	SHA550	SHA700	SHA900
$PO_4{}^{3-}$ bend V_2	472	474	474	475	475	475	475	475	475	474
$PO_4{}^{3-}$ bend V_4	574	564	560	560	560	560	561	561	561	561
$PO_4{}^{3-}$ bend V_4	601	602	601	601	601	601	601	601	601	601
Structural OH^{-}	631	630	631	631	630	631	629	631	631	631
$CO^{3\ 2-}$	873	874	874	877	877	877	879	875	872	877
$PO_4{}^{3-}$ stretch V_1	962	961	962	962	961	962	962	961	960	962
$PO_4{}^{3-}$ bend V_3	1040	1024	1024	1023	1024	1023	1024	1023	1021	1023
$PO4^{3-}$ bend V_3	1090	1080	1080	1090	1080	1088	1090	1088	1085	1090
$CO_3{}^{2-}$ V_3	1450	1454	1455	1453	1454	1417	1454	1417	1417	1456
H_2O adsorbed V_2	1630	1646	1646	1645	1650	1648	1647	1648	1640	1647
Structural OH^{-}	3572	3542	3542	3542	3542	3570	3567	3542	3550	3544

The spectrum between CHA, DHA and SHA at 550W, 700W and 900W are shown in Figure 4.10-4.12. At microwave power of 550W, DHA550 has the highest intensity peak compared to CHA550 and SHA550. At microwave power of 700W, DHA700 showed a broad peak and lowest intensity compared to CHA700 and SHA700. At microwave power of 900W, DHA900 has the lowest intensity followed by CHA900 and DHA900.

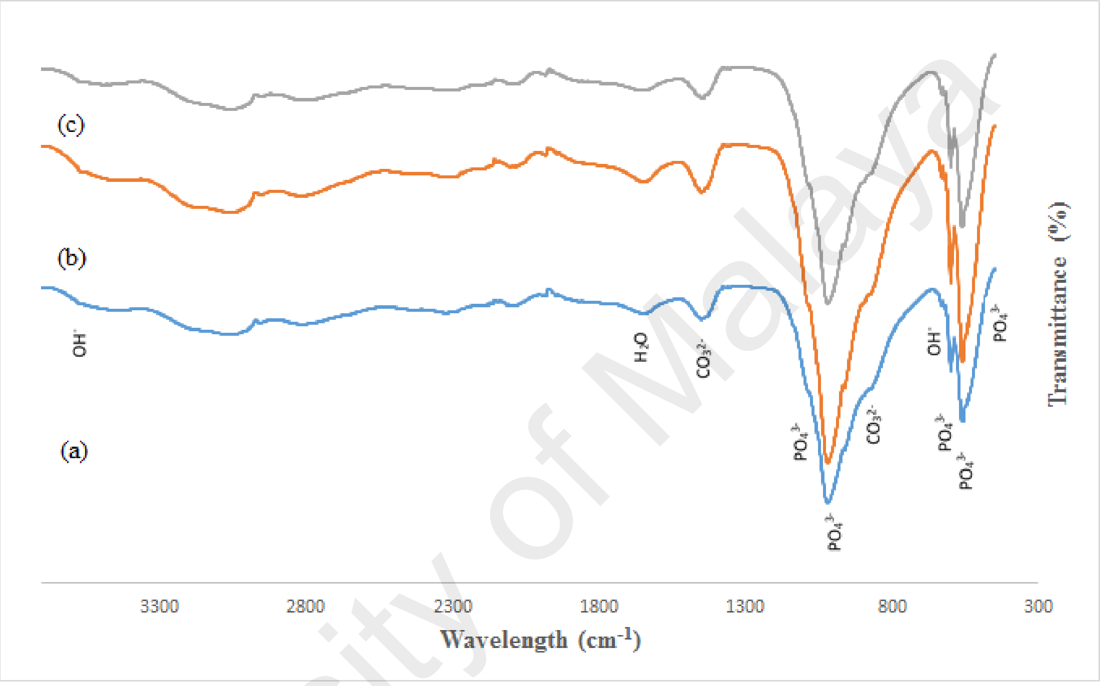

Figure 4.10: FTIR spectra at microwave power of 550W (a) CHA550 (b) DHA550 and (c) SHA550

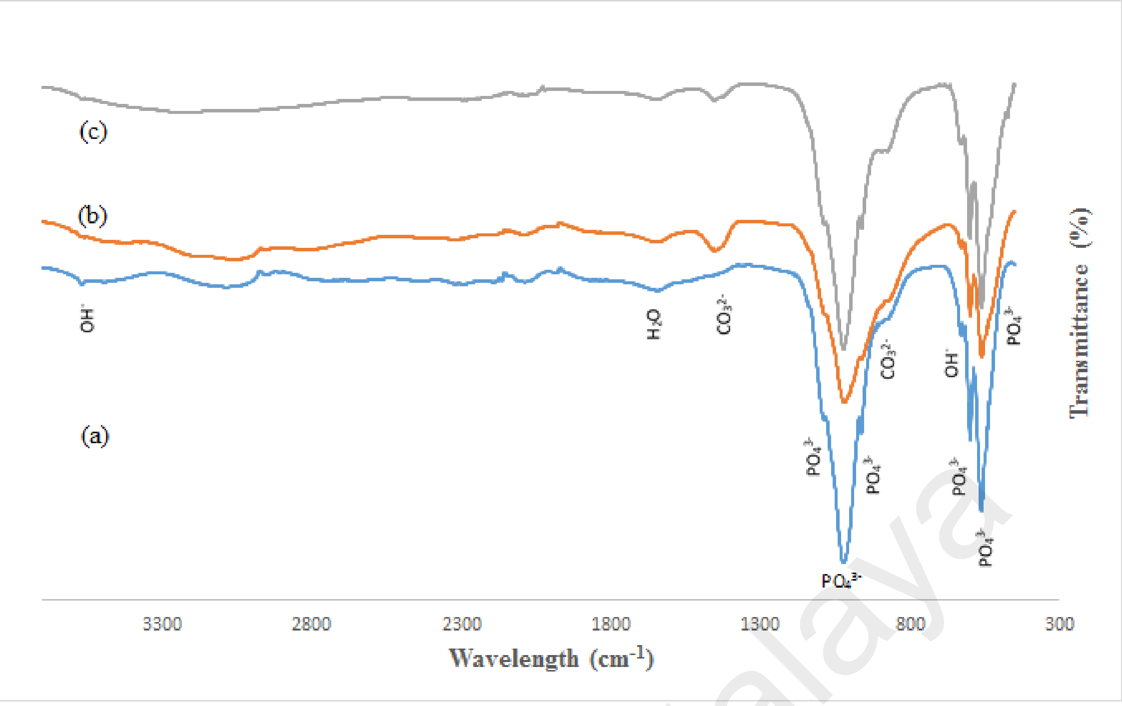

Figure 4.11: FTIR spectra at microwave power of 700W (a) CHA700 (b) DHA700 and (c) SHA700

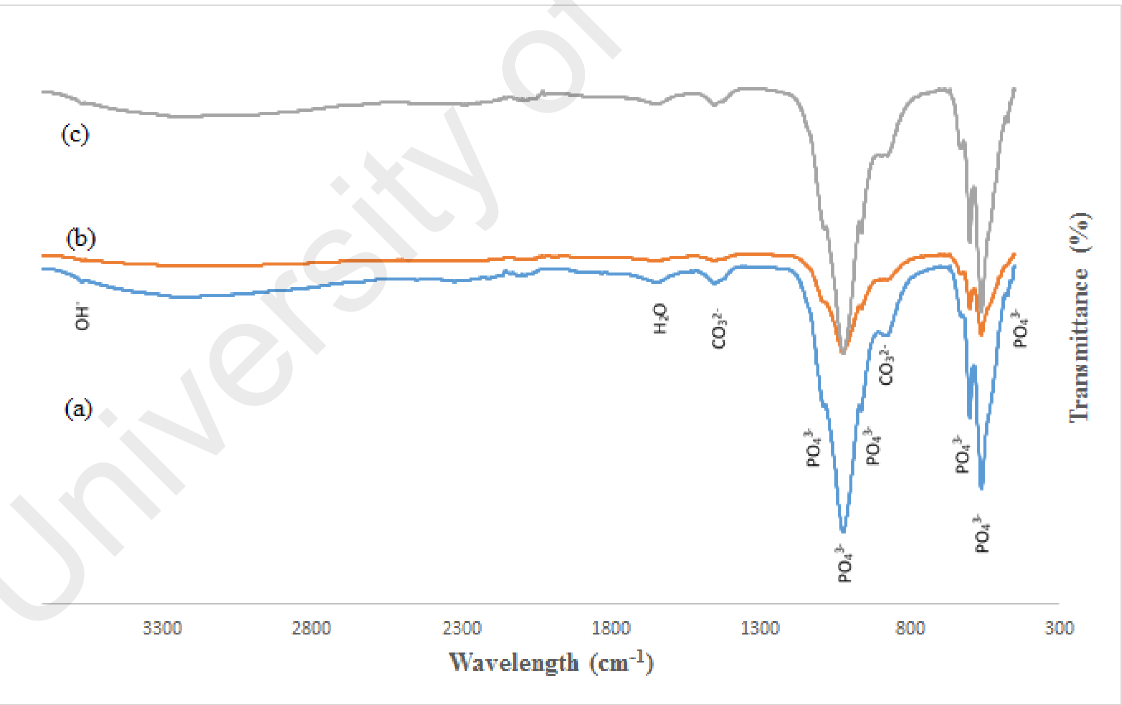

Figure 4.12: FTIR spectra at microwave power of 900W (a) CHA900 (b) DHA900 and (c) SHA900

4.2.3 Field Emission Scanning Electron Microscope (FESEM) analysis

FESEM observations of the synthesized-HA powders can be seen in Figure 4.13-4-16. High magnification images were taken to locate the particles down to nanometer large surface area. At microwave power of 550W, the particles shape for all the samples were needle-like as observed in Figure 4.13.

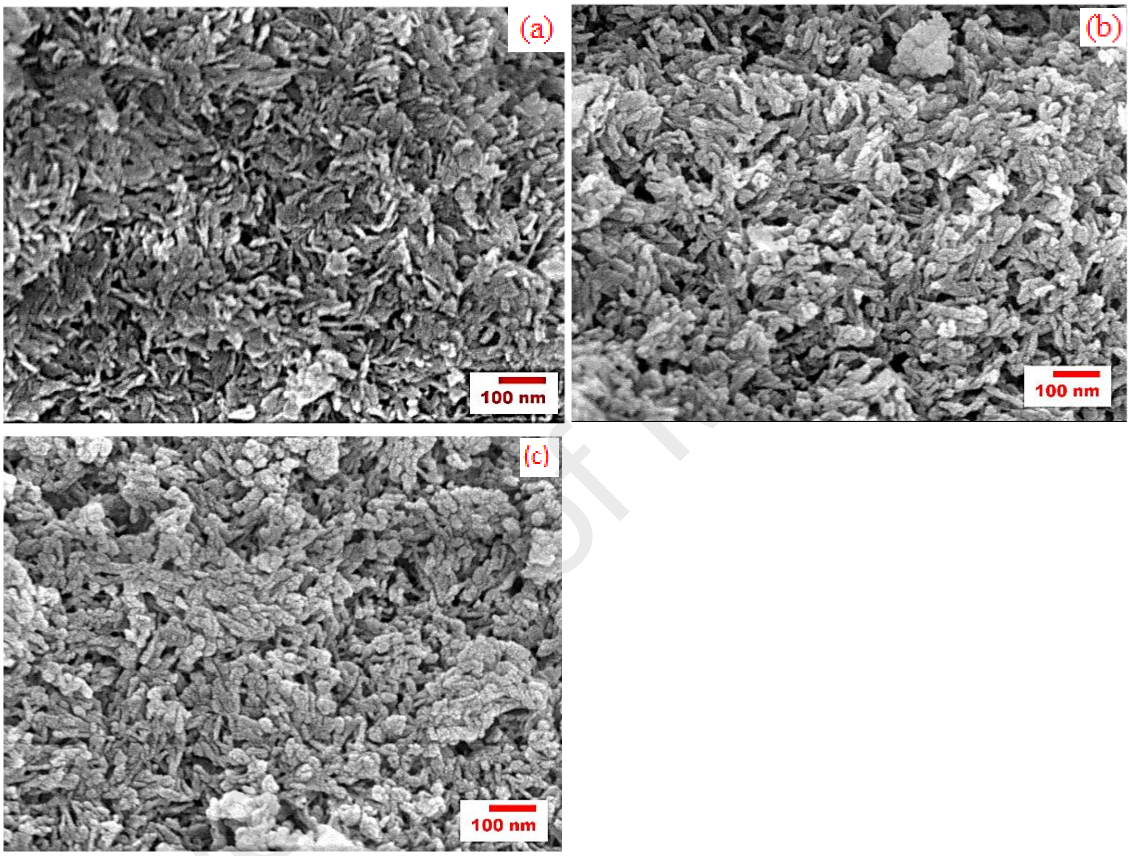

Figure 4.13: The field emission scanning electron micrograph of (a) CHA550 (b) DHA550 and (C) SHA550 at magnification of 100000X

At microwave power 700W, HA with mixture particles of needle-like and spherical shapes was evident as in Figure 4.14.

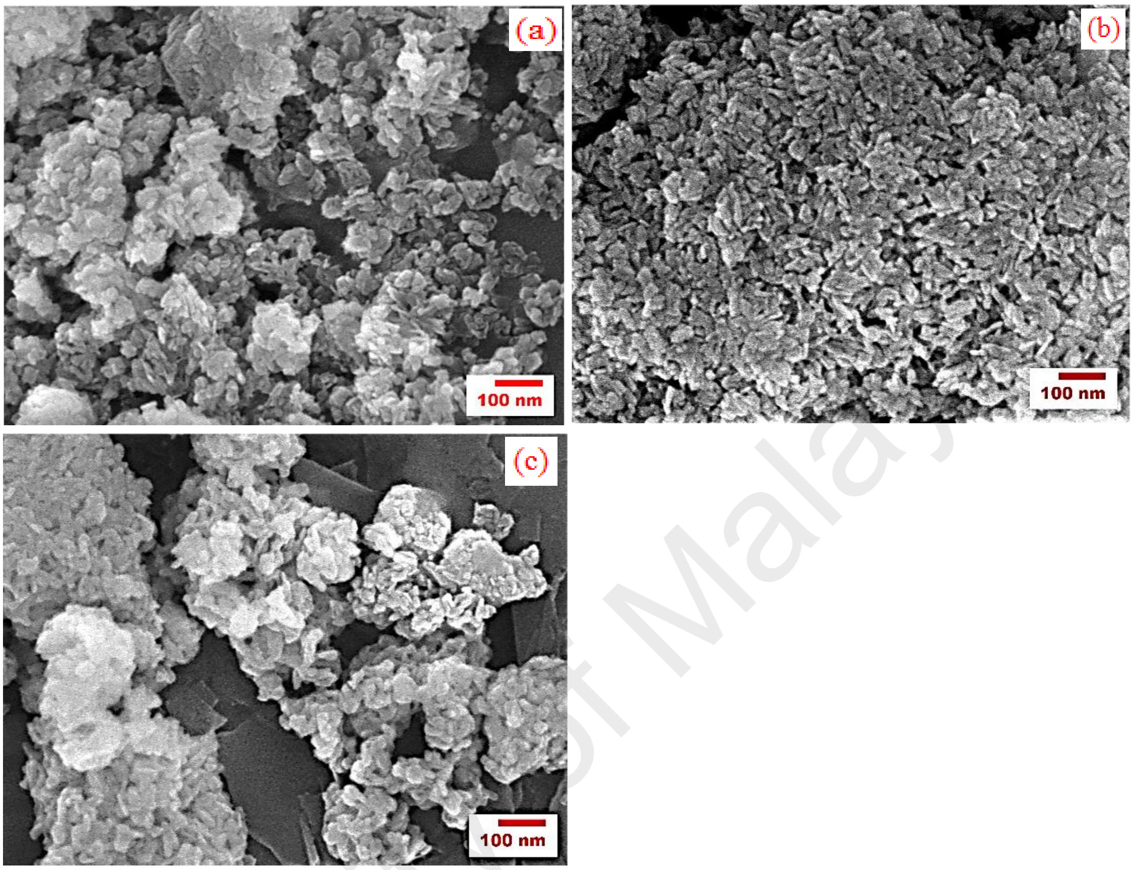

Figure 4.14: The field emission scanning electron micrograph of (a) CHA700 (b) DHA700 and (C) SHA700 at magnification of 100000X

However, the HA formed at microwave power of 900W only has spherical shape as seen in Figure 4.15.

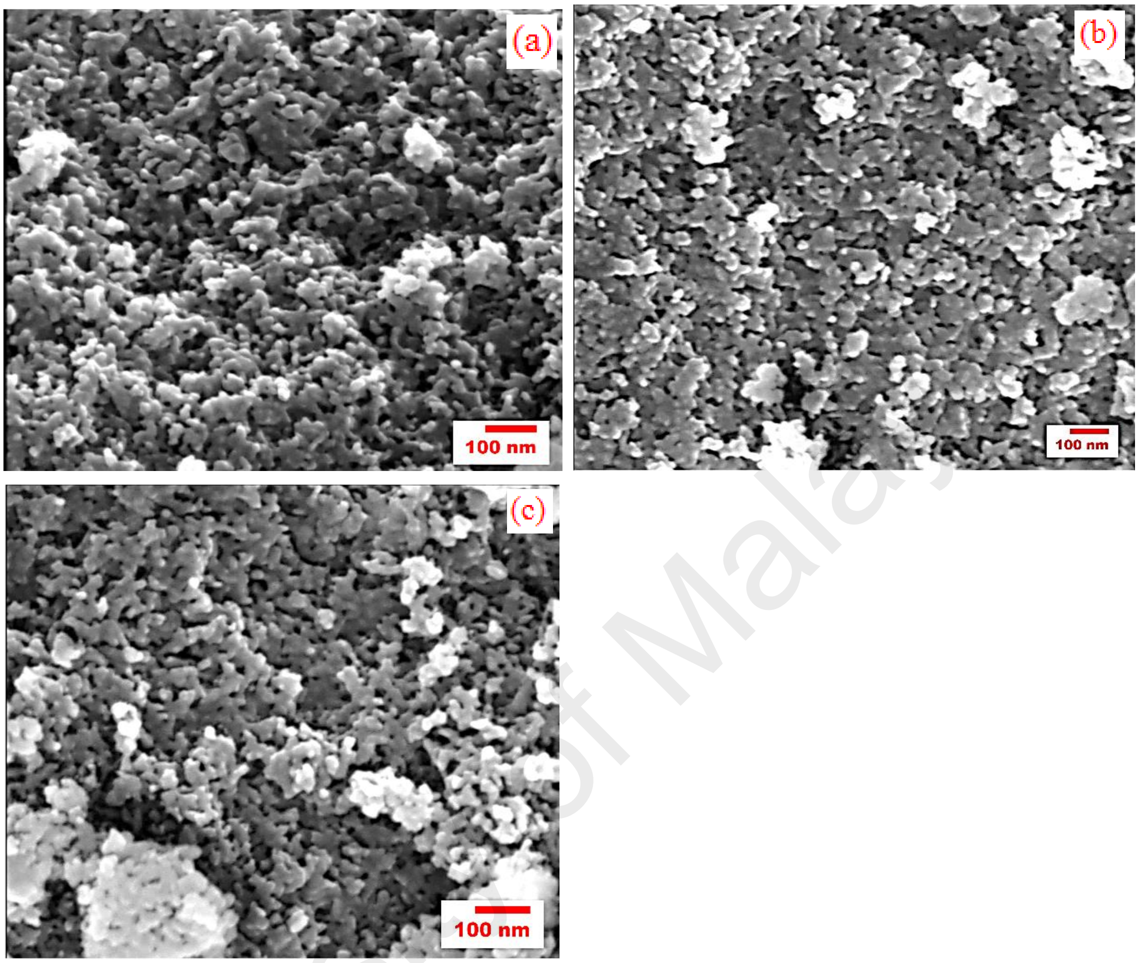

Figure 4.15: The field emission scanning electron micrograph of (a) CHA900 (b) DHA900 and (C) SHA900 at magnification of 100000X

Particles size was calculated using ImageJ software. The whole area of FESEM images were used to calculate the particle size of each samples randomly, for example Figure 4.16 was used to calculate the particle size for sample CHA550. The ImageJ software will automatically measure the average particle size according to the scale of the image.

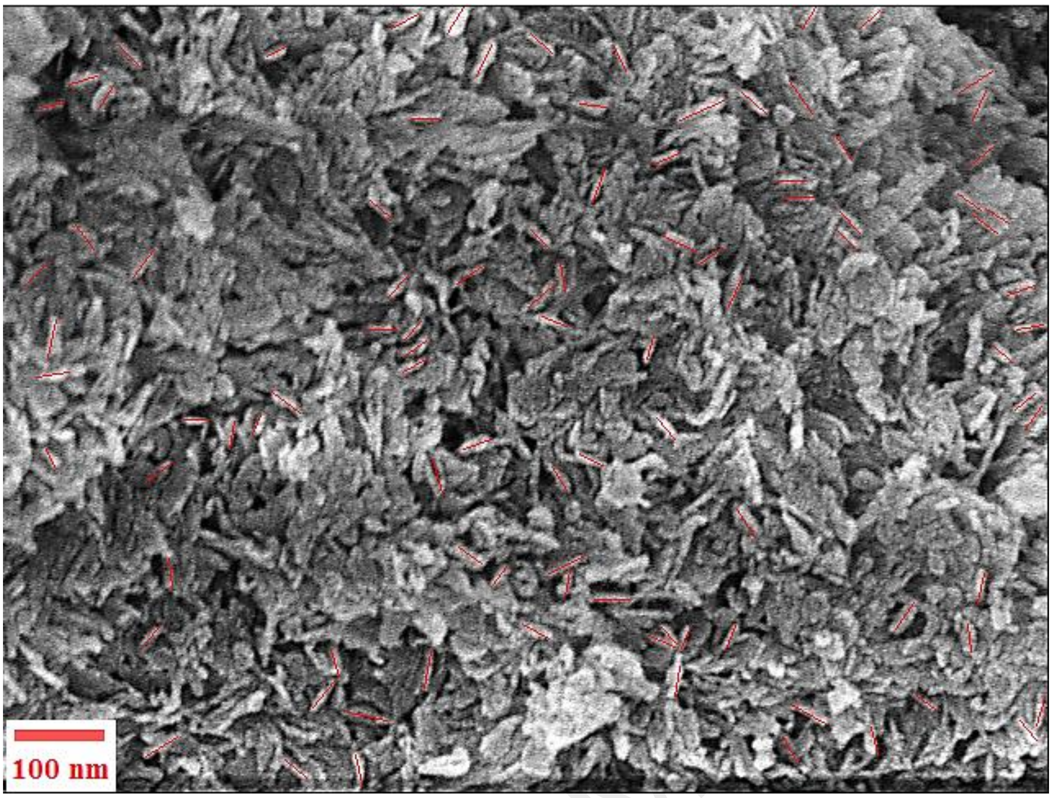

Figure 4.16: Area of particle size measurement for CHA550

Average particle size for the samples (n = 100) can be seen in Table 4.3.

Table 4.3: Particle size and shape for sample CHA, DHA and SHA

Sample	Particle shape	Particle size (nm)
CHA550	needle-like	31.91 (length), 12.63 (width)
CHA700	needle-like + spherical	31.93 (length), 12.76 (width) ; 23.87
CHA900	spherical	45
DHA550	needle-like	35.03 (length), 12.79 (width)
DHA700	needle-like + spherical	34.04 (length), 12.01 (width) ; 22.04
DHA900	spherical	49.07
SHA550	needle-like	30.6(length), 11.52 (width) ;
SHA700	needle-like + spherical	34.93 (length), 12.76 (width) ; 22.78
SHA900	spherical	42.85

Properties and performance of HA depend on the powder particle size and shape, their distribution, and agglomerates (Kalita & Verma, 2010). It is important to achieve nanosized (less than 100 nm) particle as it will affect the surface area available to react with cells and biological fluid. Nanostructured-HA is said to enhance biocompatibility, bioactivity, and flexibility which provides homogeneous resorption (Nathanael, Hong, Mangalaraj & Chen, 2011). Many have reported the works on nHA; for example, H. Liu (1997) synthesized a needle-like HA with size of 13–170 nm in length and 15–25 nm in width using hydrothermal process.

By using wet precipitation technique, Monmaturapoj (2008) has successfully synthesized irregular nanosized HA of 25 nm by varying the concentration of the precursors. However, there was difference of HA particles shape, size, and agglomeration with increase of microwave power. Upon increasing the microwave power, the particles size for all samples were increased except for needle-like DHA. Increased microwave power shows a significant change in HA particles morphology i.e. the particles structure changed from needle-like to a mix structure of needle-like and spherical to spherical shape at 550W, 700W and 900W respectively. Although the particles from all samples seemed to be agglomerated and closely packed as the microwave power increased, the particles were uniformly distributed. FESEM analysis confirmed that the agglomeration of particles in all samples which might due to Van der Waals interaction (Rodrigues et al., 2012).

In conventional synthesis, increasing the reaction temperature results in shape changes. By utilizing the eggshells biowaste, Kumar et al. (2012) reported a fabrication of flower-like HA nanostructure by using microwave heating at 600 W for 10 min. This was done with the aid of ethylenediaminetetraacetic acid (EDTA) which enhanced the crystalline growth. The flower-like nHA consisted of leaf-like flakes with dimension of 100–200 nm width and 0.5–1 nm length. However, magnesium from the eggshells was found along with HA produced. Siddharthan et al. (2006) found that the crystallite size showed an oscillating trend with increasing microwave power. The nHA was synthesized using calcium nitrate and orthophosphoric acid. The shape of HA particles were changed from needle-like to acicular to platelet structure at 175 W, 525 W and 660 W respectively.

4.2.4 Energy-Dispersive X-ray Spectroscopy (EDX) analysis

Figure 4.17 shows there is a decreasing pattern in Ca/P ratio of CHA samples as the microwave power increasing. All CHA samples were non-stoichiometric with CHA550, CHA700 and CHA900 Ca/P ratio were 1.76, 1.75 and 1.71 respectively. Increasing the microwave power higher than 900 W might decreased the Ca/P ratio of CHA sample.

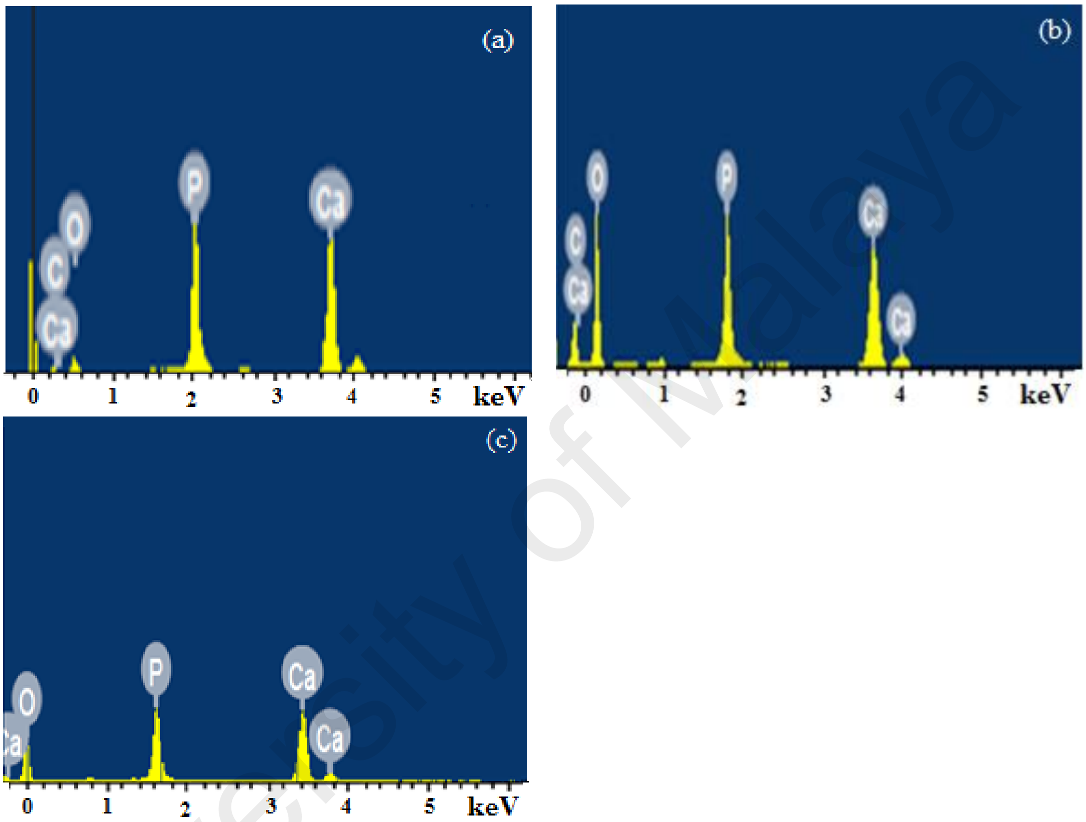

Figure 4.17: EDX spectrum of CHA powder (a) CHA550 (b) CHA700 and (C) CHA900

As the microwave power increased, the Ca/P ratio of DHA decreasing with DHA550, DHA700 and DHA900 were 1.76, 1.70 and 1.60 respectively which is closer to stoichiometric HA Ca/P ratio as seen in Figure 4.18.

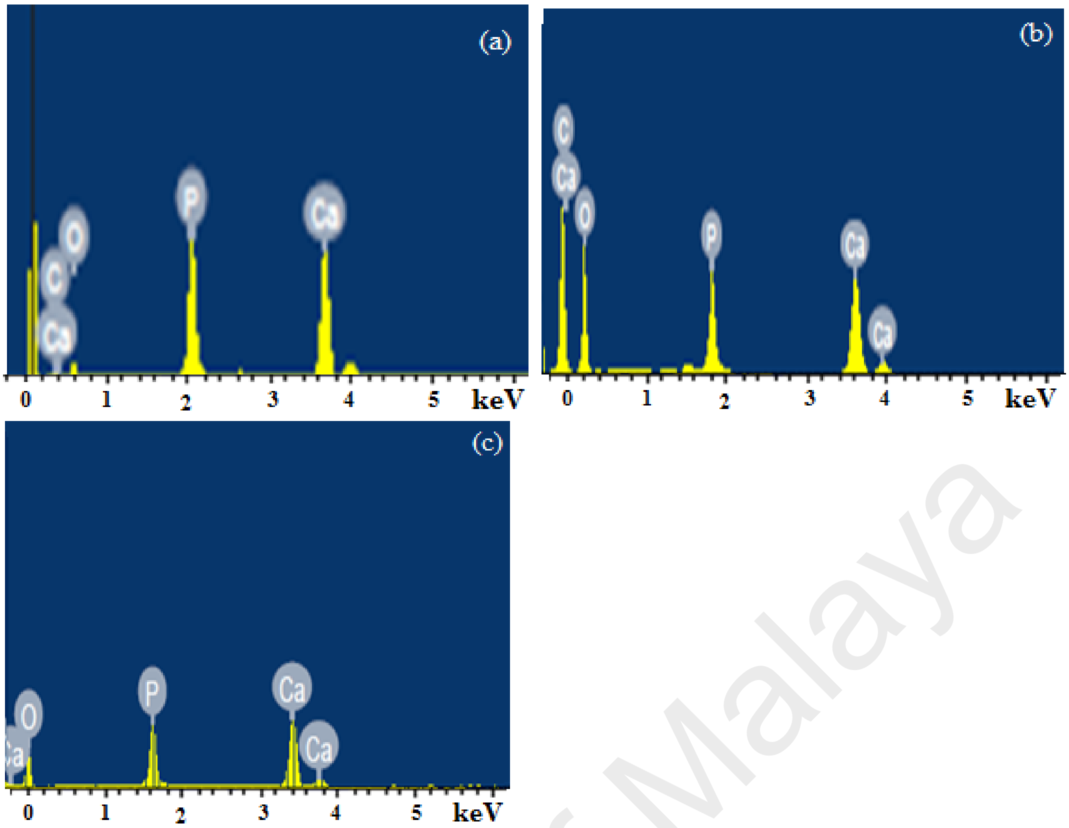

Figure 4.18: EDX spectrum of DHA powder (a) DHA550W (b) DHA700W and (C) DHA900W

Figure 4.19 shows increasing the microwave power increased the Ca/P ratio of SHA to values close to stoichiometric HA indicating the higher microwave power was required to produce stoichiometric HA. It was found that SHA900 has the closest Ca/P ratio to stoichiometric natural HA which was 1.66.

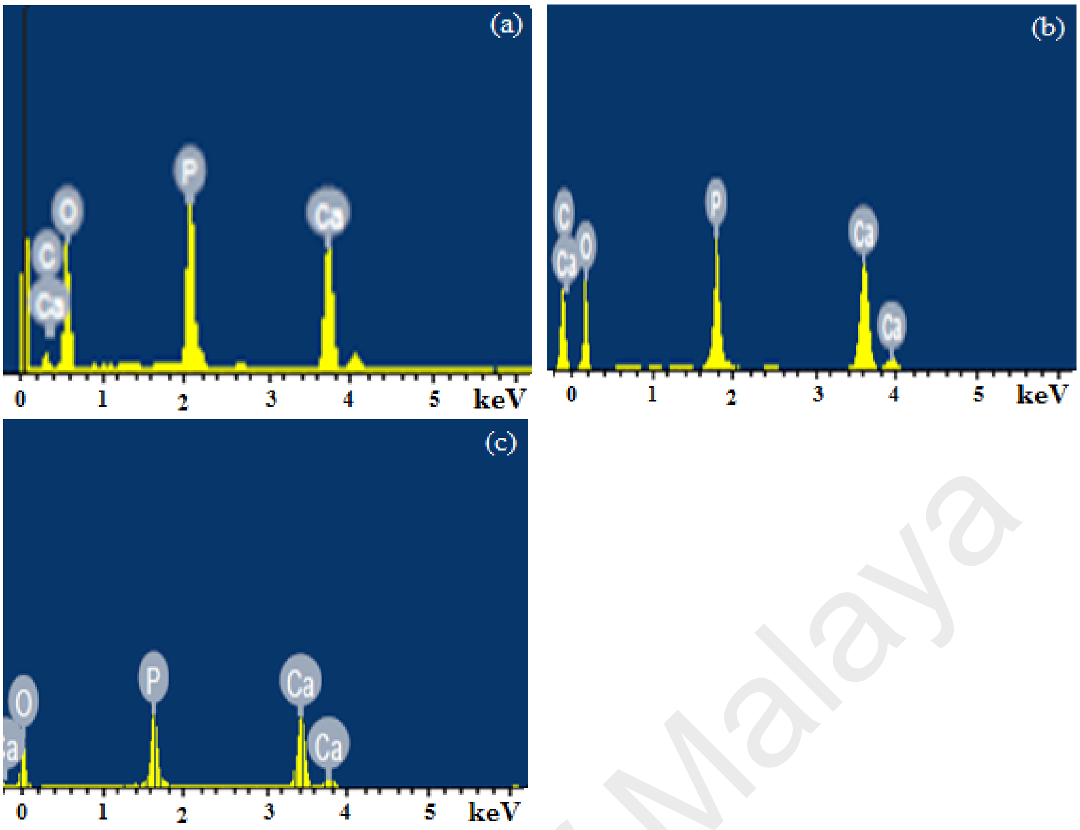

Figure 4.19: EDX spectrum of SHA powder (a) SHA550 (b) SHA700 and (C) SHA900

Table 4.4 Elemental composition and Ca/P ratio of HA powder derived from chicken eggshells (CHA), duck eggshells (DHA) and cockle shells (SHA) as a calcium source.

Sample	Element	Weight (%)	Atomic (%)	Ca/P ratio
CHA550	C	12.24	25.07	1.76
	O	17.83	27.42	
	P	25.34	20.13	
	Ca	44.6	27.38	
	Total (%)	100		
CHA700	C	8.89	15.20	1.75
	O	46.24	59.35	
	P	16.34	10.84	
	Ca	28.53	14.62	
	Total (%)	100		
CHA900	O	44.42	64.28	1.71
	P	21.28	15.91	
	Ca	34.3	19.82	
	Total (%)	100		
DHA550	C	12.24	25.07	1.76
	O	17.83	27.42	
	P	25.34	20.13	
	Ca	44.6	27.38	
	Total (%)	100		
DHA700	C	40.14	52.68	1.70
	O	38.63	38.06	
	P	7.87	4.01	
	Ca	13.35	5.25	
	Total (%)	100		
DHA900	O	48.87	68.27	1.60
	P	19.67	14.19	
	Ca	31.46	17.54	
	Total (%)	100		
SHA550	C	8.44	14.09	1.40
	O	49.88	62.51	
	P	17.36	11.23	
	Ca	24.33	12.17	
	Total (%)	100		
SHA700	C	31.76	45.52	1.48
	O	36.46	39.22	
	P	12.8	7.11	
	Ca	18.98	8.15	
	Total (%)	100		
SHA900	O	45.87	65.65	1.66
	P	20.37	15.06	
	Ca	33.77	19.29	
	Total (%)	100		

At microwave power of 550 W, the Ca/P ratio is 1.76 for CHA and DHA550 while SHA550 has 1.40 of Ca/P ratio. At microwave power of 700 W, the Ca/P ratio is 1.75, 1.70 and 1.48 for CHA700, DHA700 and SHA700 respectively. The Ca/P ratio of CHA900, DHA900 and SHA900 have Ca/P ratio closer to stoichiometric HA with value of 1.71, 1.60 and 1.66 respectively. In other HA synthesis study conducted using $Ca(NO_3)_2{\cdot}4H_2O$ and $(NH_4)_2HPO_4$ by microwave irradiation, the Ca/P ratio was found to increase as the microwave power increasing. The Ca/P ratios were found to be 1.55, 1.59 and 1.64 at microwave power of 450W, 600W and 800W respectively (Akram et al., 2015). Kumar et al. (2017) has successfully synthesized HA from mussel shells as calcium source using microwave irradiation technique at microwave power of 700 W for 15 mins. Even though they maintained the Ca/P ratio at 1.67 in the early experiment, the final product turned out to be non-stoichiometric HA with Ca/P of 1.79. Figure 4.17-4.19 show the EDX spectrum with elemental composition contained in the CHA, DHA and SHA powder.

By using microwave irradiation method, Santhosh and Balasivanandha Prabu (2012) reported fabrication of HA at 800 W for 10 mins using seashell as calcium source. The HA formed was non-stoichiometric despite of maintaining Ca/P ratio at the beginning of experiment. Azis et al. (2015) found that even the Ca/P ratio was maintained at 1.67, the final product of HA derived from cockle shells was 1.78.

All the element composition of HA were presented i.e. calcium, phosphorus and oxygen. It showed that no impurities were found except of carbon. Despite of having Ca/P ratio near 1.50, bone mineral has a similarity in structural and chemical to the stoichiometric HA with Ca/P ratio of 1.67. At high temperature, a non-stoichiometric HA is found to be thermally unstable and increased in solubility. This is due to the number of crystalline structure defects caused by increasing calcium ions vacancies (Smoleń et al., 2012). Below the stoichiometric HA (< 1.67), the β-TCP or α-TCP is said to be presented at high temperature (Fanovich et al., 2001). TCP has high biodegradable characteristic making it uses as a composite with HA in implantation to control the biodegradation rate (Ghosh, Datta & Roy, 2004). By using precipitation technique, Neelakandeswari, Sangami and Dharmaraj (2011) had synthesized non-stoichiometric HA from inner membrane of eggshell with Ca/P ratio of 1.43 at pH 10.

4.3 Compressive Strength Analysis

It is well-known that HA is brittle in nature. It is important to investigate the compressive strength of HA as main property in characterizing mechanical behaviour of bone substitutes is their compressive strength (Hannink & Arts, 2011). In addition, there are many fracture or compressive injuries happen in the body such as patellar pain, fractures in vertebrae and femoral neck fractures (Bankoff, 2012). Figure 4.20 shows decreasing trends of compressive strength for all types of samples as the microwave power increased. It can be seen from Table 4.5 that different types of HA samples with highest compressive strength (CHA550, DHA550 and SHA550) have smaller crystallite size (refer to Table 4.3, Section 4.2.3). This is in agreement with the theory that smaller particles size and high crystallinity tend to give high compressive strength (Krishna et al, 2007).

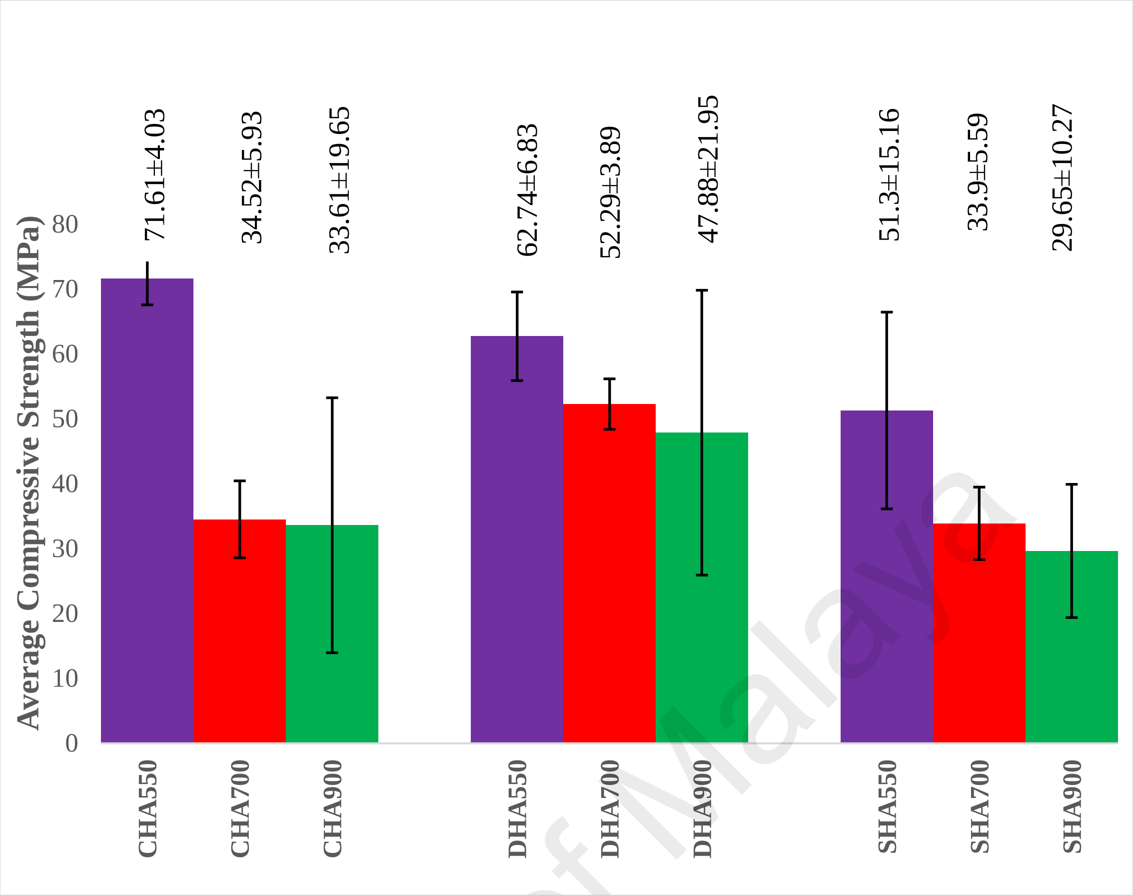

Figure 4.20: Average compressive strength of CHA, DHA and SHA with standard deviation showed a decreasing trend of strength with increased microwave power

Table 4.5: Average compressive strength of CHA, DHA and SHA samples.

Sample	Compressive strength (MPa)
CHA550	71.61±4.03
CHA700	34.52±5.93
CHA900	33.61±19.96
DHA550	62.74±6.83
DHA700	52.29±3.89
DHA900	47.88±21.95
SHA550	51.30±15.16
SHA700	33.90±5.59
SHA900	29.65±10.27

The different particle and morphology of HA might contribute to decreasing compressive strength as the microwave power increased. For needle-like HA particles, it is expected that the crystal growth is in longitudinal direction causing the gap between the particles is increasingly bridged and the density to increase (Liang et al., 2012). Thus, increased the compressive strength. In addition, needle-like particle has high surface area compared to spherical particles which resulted in good bonding between the HA particles (Prakasam et al, 2015). Compared to micro-particle, nano-particle is said to have better mechanical properties. This is due to nano-particle provides larger surface area resulting in larger contact area between particles (Ginebra et al. 2007). Even though the compressive strength of all the samples were not as high as human cortical bone (~170 MPa), they were better than compressive strength of cancellous bone (4-12 MPa) that would enable its application in low load-bearing field such as orbital floor, bone filler, coating for metal implants and in drug delivery (Ginebra et al. 2007). In total hip implant, it is crucial to prepare bone cement that yield high strength values of compressive strength because the main direction of load on bone cement is compression loading (Serbetci, Korkusuz & Hasirci, 2004). Woodard et al. (2007) had synthesized HA as scaffold with compressive strength range from 27-34 MPa and decreased to 23-24 MPa when implanted in human. Demirkol et al. (2012) fabricated HA from calcinated sheep bones. They found that increasing the sintering temperature (1000-1300 ^{o}C) resulted in increased of compressive strength (31-69 MPa). However, the maximum strength that can be achieved was up to temperature of 1300 ^{o}C.

To optimize its mechanical properties, HA is normally undergo sintering process or used as additives to metallic materials, ceramic oxides, whiskers or fibers (Demirkol, Meydanoglu, Gökçe, Oktar & Kayali, 2012). Batin, Popa, Brandusan and Vida-Simiti (2011) reported that the compressive strength of Ti/HA produced from powder metallurgy route ranged between 132 MPa and 528 MPa have been successfully sintered at 400 MPa in vacuum (0.01 Pa) at 1160 ºC for two hours. They found that incorporation of HA to titanium increased the mechanical strength of the composite where the addition of 10% of HA exhibited the maximum compressive strength (528 MPa). However, the strength decreased with increasing HA amount. Using co-precipitation method, Li, Huang, Wang, Ma and Xie (2011) have successfully prepared phosphorylated chitosan/chitosan/hydroxyapatite (PCS/CS/HA) composites with different weight ratio. PCS/CS/HA composites with weight ratio of 30/30/ 40 showed highest compressive strength (70.25 MPa) and has a rough surface morphology and relatively tight structure. When soaking for 20 days in SBF solution, it kept its compressive strength up to 64% from original strength.

CHAPTER 5: CONCLUSION AND RECOMMENDATION

5.1 Conclusion

HA bioceramics were successfully synthesized in this study from various waste materials i.e. chicken eggshells, duck eggshells and cockle shells. The particle morphology, size and shape of synthesized HA can be controlled by varying the microwave powder used in irradiating the precursors mixture (Ca and P source). These HA characteristics play an important role in the compressive strength especially for its application in biomedical field. The results and findings are as follow:

i. The possibility of producing HA with different morphology from waste materials have been proven to be low cost, efficient and faster technique. The whole process only took about 5 hours from preparation of raw materials and precursors, mixing of chemical solution and microwave heating to formation of precipitate.

ii. All the characteristics of XRD pattern occurred in the prominent peaks at 2θ = ~25.88θ, ~31.74θ, ~32.19θ, ~32.87θ, ~34.05θ, ~39.77θ, ~46.66θ, ~49.46θ and ~53.21θ which complemented the standard HA characteristics according to JCPDS file- 00-024-0033 for HA. As microwave power increased, no traces of other secondary phases were detected showing a pure HA were produced and the intensities of peaks were slightly increased in all samples. However, peak at plane (300) for CHA550 and DHA550 were missing.

iii. FTIR spectrum in HA characteristic of PO_4^{3-} (~472 cm^{-1}, ~574 cm^{-1}, ~601 cm^{-1}, ~962 cm^{-1}, ~1040 cm^{-1} and ~1090 cm^{-1}) and OH^- (~631 cm^{-1} and ~3572 cm^{-1}) groups appeared at the frequencies quite similar to standard HA spectrum. A weak spectra of $CO^{3\ 2-}$ ion group was detected at ~873 cm^{-1} and ~1450 cm^{-1} and adsorbed H_2O at 1630 cm^{-1}. As the microwave power increased, CHA and SHA samples showed an increasing trend of peak intensity while DHA showed a decreasing trend of peak intensity.

iv. The influence of microwave power on the shape and size of the HA particle for all samples can be clearly seen. As the microwave power increased, the shape of the HA particle change from needle-like to the mix of needle-like and spherical to spherical particles. The size also increased as the microwave power increased. On the other hand, there were no changes in HA phase composition.

v. CHA and DHA samples showed a non-stoichiometric HA with abundant of Ca. As the microwave power increased, the Ca/P ratio of CHA and DHA samples were decreasing and DHA samples have Ca/P ratio value close to stoichiometric HA which were 1.70 (DHA700) and 1.60 (DHA900). Conversely, SHA samples have an increasing trend of Ca/P ratio as the microwave power increased with Ca deficiency HA. Increasing the microwave power in SHA proved to form HA with the Ca/P ratio close to stoichiometric HA (1.66).

vi. HA from chicken eggshells showed a higher compressive strength compared to duck eggshells and cockle shells. Even though the compressive strength (29.65 MPa-71.61 MPa) of all the samples were not as high as the sintering HA product, its value is much higher than cancellous bone (4-12 MPa) and useful in non-load bearing application such as orbital floor, bone filler, coating for metal implants and in drug delivery.

5.2 Recommendation

During the study, there were several observation and ideas that required further investigation to enhance the mechanical properties of HA. It is widely known that HA is brittle in nature. Hence, it is worth trying to come up with suggestions which can improve its properties and limitation. The recommendation are as follow:

i. In order to improve hydroxyapatite mechanical properties, sintering process should be done. Many has reported that sintering process has enhance the HA properties. However, at temperature above 1200 ^{o}C, secondary phases such as α- and β-TCP will occur. The optimum temperature to sinter HA are between 1000-1200 ^{o}C.

ii. An addition of other materials such as titanium, PMMA, carbon nanotubes,etc also is proven to increase HA mechanical properties and provide good biological properties to the materials where HA is reinforced.

iii. A study on porosity should be conducted as porous HA shows strong bonding to the bone and its interlock characteristics provides a firm fixation to the material. Porous HA increases the strength of implant as bone tissues grows well in to the pores. However, it is limited to non-load bearing applications because larger pores will decrease the implant strength.

iv. Varying other parameters such as pH, irradiation time, volume of precursor, etc. may result in many useful finding. In addition, more natural or waste materials could be used to synthesize HA using the same technique such as bovine bone, coral, snail shells, cuttlefish bone and many more.

REFERENCE

Abidi, S. S. A., & Murtaza, Q. (2014). Synthesis and characterization of nano hydroxyapatite powder using wet chemical precipitation reaction. *Journal of Materials Science & Technology, 30*(4): 307-310.

Abulikemu, M. (2008). *Energy dispersive X-ray analysis principle and application.* Retrieved 4th august 2009

Adak, M. D., & Purohit, K. M. (2011). Synthesis of Nano-crystalline Hydroxyapatite from Dead Snail Shells for Biological Implantation. *Trends in Biomaterials and Artificial Organs*, 25(3), 101-106.

Adak, M., Chattopadhyay, A., & Purohit, K. (2011). Study on calcination of Nano-Crystalline Hydroxy-Apatite synthesised from Kitchen Waste (used Egg shells). *Journal Of Pharmacy Research, 4*(3): 912-914.

Agrawal, D. K. (1998). Microwave processing of ceramics. *Current Opinion in Solid State and Materials Science*, *3*(5), 480-485

Ahmed, S., & Ahsan, M. (2008). Synthesis of Ca-hydroxyapatite bioceramic from egg shell and its characterization. *Bangladesh Journal of Scientific and Industrial Research, 43*(4): 501-512.

Akram, M., Alshemary, A. Z., Goh, Y. F., Ibrahim, W. A. W., Lintang, H. O., & Hussain, R. (2015). Continuous microwave flow synthesis of mesoporous hydroxyapatite. *Materials Science and Engineering: C*, *56*, 356-362.

Allwood, T. (2013). *Template based nanomanufacturing.* Worcester Polytechnic Institute.

Alyamani, A. & Lemine, O. (2012). *FE-SEM Characterization of Some Nanomaterial*: INTECH Open Access Publisher.

Al-Sanabani, J. S., Madfa, A. A., & Al-Sanabani, F. A. (2013). Application of calcium phosphate materials in dentistry. *International journal of biomaterials*, *2013*.

Angelescu, N., Ungureanu, D. N., & Anghelina, F. V. (2011). Synthesis and characterization of hydroxyapatite obtained in different experimental conditions. *Sci Bull Valahia Univ Mater Mech*, *6*(9), 15-18.

Arami, H., Mohajerani, M., Mazloumi, M., Khalifehzadeh, R., Lak, A., & Sadrnezhaad, S. (2009). Rapid formation of hydroxyapatite nanostrips via microwave irradiation. *Journal of Alloys and Compounds, 469*(1): 391-394.

Aruna, S. T. & Mukasyan, A. S. (2008). Combustion synthesis and nanomaterials. *Current Opinion in Solid State and Materials Science, 12*(3): 44-50.

Avecedo-Davilla, J. L., Lopez-Cueves, J., Gutierrez, G.V., Rendon-Angeles, J.C. & Mendez-Nonell, J. (2007). Chemical synthesis of bone-like carbonate hydroxyapatite from hen eggshells and its characterization. *Bol. Soc. Esp. Ceram., 46*: 225-231.

Azis Y., Jamarun N., Arief S. & Nur H. (2015). Facile Synthesis of Hydroxyapatite from Cockle Shells (Anadaragranosa) by Hydrothermal Method. *Oriental Journal of Chemistry*, 31(2), 1099-1105

Bakan, F., Laçin, O. & Sarac, H. (2013). A novel low temperature sol–gel synthesis process for thermally stable nano crystalline hydroxyapatite. *Powder Technology, 233*: 295-302.

Balázsi, C., Wéber, F., Kövér, Z., Horváth, E. & Németh, C. (2007). Preparation of calcium–phosphate bioceramics from natural resources. *Journal of the European Ceramic Society*, *27*(2), 1601-1606.

Balázsi, K., Sim, H. Y., Choi, J. Y., Kim, S. G., Chae, C. H. & Balázsi, C. (2013). Biogenic nanosized hydroxyapatite for tissue engineering applications. In *International Symposium on Biomedical Engineering and Medical Physics, 10-12 October, 2012, Riga, Latvia* (pp. 190-193). Springer Berlin Heidelberg.

Batin, G., Popa, C., Brandusan, L. & Vida-Simiti, I. (2011). Mechanical properties of Ti/HA functionally graded materials for hard tissue replacement. *Powder Metallurgy Progress, 11*(3-4): 206-209.

Bankoff, A. D. P. (2012). Biomechanical characteristics of the bone. In*Human Musculoskeletal Biomechanics*. InTech.

Beganskiene, A., Dudko, O., Sirutkaitis, R. & Giraitis, R. (2003). Water based sol-gel synthesis of hydroxyapatite. *Materials Science*, *9*(4): 383-386.

Ben-Arfa, B. A., Salvado, I. M. M., Ferreira, J. M. & Pullar, R. C. (2017). Novel route for rapid sol-gel synthesis of hydroxyapatite, avoiding ageing and using fast drying with a 50-fold to 200-fold reduction in process time. *Materials Science and Engineering: C, 70*, 796-804.

Ben-Nissan, B. (Ed.). (2014). Advances in Calcium Phosphate Biomaterials. Retrieved from http://download.e-bookshelf.de/download/0002/6788/95/L-G-0002678895-0013251436.pdf

Bilton, M., Brown, A. & Milne, S. (2010). Sol-gel synthesis and characterisation of nano-scale hydroxyapatite. *Paper presented at the Journal of Physics: Conference Series.*

Callister, W. D. & Rethwisch, D. G. (2007). *Materials science and engineering: an introduction* (Vol. 7): Wiley New York.

Cao, L., Zhang, C. & Huang, J. (2005). Synthesis of hydroxyapatite nanoparticles in ultrasonic precipitation. *Ceramics International*, *31*(8): 1041-1044.

Cengiz, B., Gokce, Y., Yildiz, N., Aktas, Z. & Calimli, A. (2008). Synthesis and characterization of hydroxyapatite nanoparticles. *Colloids and Surfaces A: Physicochemical and Engineering Aspects*, *322*(1): 29-33.

Chandrasekar, A., Sagadevan, S. & Dakshnamoorthy, A. (2013). Synthesis and characterization of nano-hydroxyapatite (n-HAP) using the wet chemical technique. *International Journal of Physical Sciences*, *8*(32): 1639-1645.

Connolly, J. (2007). Introduction to X-ray Powder Diffraction. Retrieved 4 August 2012, from www.unm.edu/xrd/xrdclass/01-XRD-Intro.pdf

Czernuszka, J. (2001). Biomaterials- An overview. Retrieved 4 August 2009, from http://www.azom.com/details.asp?ArticleID=108

Das, B. C., Bhowmik, D. & Chaudhuri, S. (2012). Microwave System. *The Pharma Innovation*, *1*(6).

Dasgupta, P., Singh, A., Adak, S.A. & Purohit, K.M. (2004). Synthesis and characterization of hydroxyapatite produced from eggshell. *Paper presented at the International Symposium of Research Students on Materials Science and Engineering*, Cennai, India.

Dávila, J. A., Cuevas, J. L., Gutiérrez, G. V., Angeles, J. R. & Nonell, J. M. (2007). Chemical synthesis of bone-like carbonate hydroxyapatite from hen eggshells and its characterization. *Boletín de la Sociedad Española de Cerámica y Vidrio, 46*(5): 225-231.

Denry, I. & Kelly, J. R. (2008). State of the art of zirconia for dental applications. *Dental materials, 24*(3): 299-307.

Demirkol, N., Meydanoglu, O., Gökçe, H., Oktar, F. N. & Kayali, E. S. (2012). Comparison of mechanical properties of sheep hydroxyapatite (SHA) and commercial synthetic hydroxyapatite (CSHA)-MgO composites. In *Key Engineering Materials* (Vol. 493, pp. 588-593). Trans Tech Publications.

Dong, X. N. & Guo, X. E. (2004). The dependence of transversely isotropic elasticity of human femoral cortical bone on porosity. *Journal of biomechanics*, *37*(8), 1281-1287.

Dorozhkin, S. V. (2013). Calcium orthophosphate-based bioceramics. *Materials, 6*(9): 3840-3942.

Dorozhkin, S. V. (2010). Calcium Orthophosphates as Bioceramics: State of the Art. *J. Funct. Biomater., 1*(1): 22-107.

Dutrow, B. & Clark, C. (2009). X-ray Powder Diffraction (XRD). Retrieved 4 August 2012 http://serc.carleton.edu/research_education/geochemsheets/techniques/XRD.html

Earl, J., Wood, D. & Milne, S. (2006). Hydrothermal synthesis of hydroxyapatite. *Paper presented at the Journal of Physics: Conference Series.*

El-Maghraby, A. & Refat, M. S. (2014). Preparation of ceramics pigment as nano-powder using organic fuels in approach for the solution combustion synthesis. *Nature & Science, 12*(4).

Eliaz, N. & Metoki, N. (2017). Calcium Phosphate Bioceramics: A Review of Their History, Structure, Properties, Coating Technologies and Biomedical Applications. *Materials*, *10*(4), 334.

Fanovich, M. A., Castro, M. S. & Lopez, J. P. (2001). Structural analysis of modified hydroxyapatite powders. *Materials research bulletin*, *36*(3), 487-496

Farzadi, A., Solati-Hashjin, M., Bakhshi, F. & Aminian, A. (2011). Synthesis and characterization of hydroxyapatite/β-tricalcium phosphate nanocomposites using microwave irradiation. *Ceramics International*, *37*(1), 65-71.

Fathi, M. H. & Hanifi, A. (2007). Evaluation and characterization of nanostructure hydroxyapatite powder prepared by simple sol–gel method. *Materials letters*, *61*(18), 3978-3983.

Ferraz, M., Monteiro, F. & Manuel, C. (2004). Hydroxyapatite nanoparticles: a review of preparation methodologies. *Journal of Applied Biomaterials and Biomechanics, 2*(2): 74-80.

Franco, A. A. (2013). Polymer Electrolyte Fuel Cells: Science, Applications, and Challenges: CRC Press.

Furlong, R. J. & Osborn, J. F. (1991). Fixation of hip prostheses by hydroxyapatite ceramic coatings. Bone & Joint Journal, 73(5), 741-745.

García, C., García, C. & Paucar, C. (2012). Controlling morphology of hydroxyapatite nanoparticles through hydrothermal microemulsion chemical synthesis. Inorganic Chemistry Communications, 20: 90-92.

Ghosh, S. K., Datta, S. & Roy, S. K. (2004). Solution combustion synthesis of calcium hydroxyapatite nanoparticles. *Transactions of the Indian Ceramic Society, 63*(1): 27-32.

Ginebra, M. P., Delgado, J. A., Harr, I., Almirall, A., Del Valle, S. & Planell, J. A. (2007). Factors affecting the structure and properties of an injectable self-setting calcium phosphate foam. *Journal of Biomedical Materials Research Part A, 80*(2): 351-361.

Gross, K. (2002). Bioceramics- An overview including calcium phosphates, hydroxyapatite, alumina, zirconia and pyrolytic carbon. Retrieved 4 August 2009, from http://www.azom.com/details.asp?ArticleID=1743

Han, Y., Li, S., Wang, X. & Chen, X. (2004). Synthesis and sintering of nanocrystalline hydroxyapatite powders by citric acid sol–gel combustion method. *Materials Research Bulletin*, *39*(1), 25-32.

Han, J. K., Song, H. Y., Saito, F. & Lee, B. T. (2006). Synthesis of high purity nano-sized hydroxyapatite powder by microwave-hydrothermal method. *Materials chemistry and physics*, *99*(2), 235-239.

Hannink, G. & Arts, J. C. (2011). Bioresorbability, porosity and mechanical strength of bone substitutes: what is optimal for bone regeneration?. *Injury*,*42*, S22-S25.

Hench, L. (1991). Bioceramics: from concept to clinic. *Journal of the American Ceramic Society*, *74*(7): 1487-1510.

Heness, G. & Ben-Nissan, B. (2004). Biocomposites- bone cement, hydroxyapatite and biomimetic composites for bone repair. Retrieved 4 August 2009, 4 August 2009, from http://www.azom.com/details.asp?ArticleID=2639

Hayes, B. L. (2002). *Microwave synthesis: chemistry at the speed of light*. Cem Corporation

Huang, S., Gao, S. & Yu, H. (2009). Effect of nano-hydroxyapatite concentration on remineralization of initial enamel lesion in vitro. *Biomedical Materials, 4*(3), 034-104.

Huggett, J. & Shaw, H. (1997). Field emission scanning electron microscopy; a high-resolution technique for the study of clay minerals in sediments. *Clay Minerals, 32*(2): 197-203.

Hui, K., Balamurugan, A. & Rajeswari, S. (2005). Development of calcium phosphate based apatite from hen’s eggshell. *Bulletin of Materials Science, 28*(2): 115-119

Hui, P., Meena, S.L., Singh, G., Agarawal, R.D. & Prakash, S. (2010). Synthesis of Hydroxyapatite Bio-Ceramic Powder by Hydrothermal Method. *Journal of Minerals & Materials Characterization & Engineering, 9*(8): 683-692.

Ibrahim, A. R., Li, X., Zhou, Y., Huang, Y., Chen, W., Wang, H., & Li, J. (2015). Synthesis of Spongy-Like Mesoporous Hydroxyapatite from Raw Waste Eggshells for Enhanced Dissolution of Ibuprofen Loaded via Supercritical CO2. *International journal of molecular sciences*, *16*(4), 7960-7975.

Jadalannagari, S., More, S., Kowshik, M. & Ramanan, S. R. (2011). Low temperature synthesis of hydroxyapatite nano-rods by a modified sol–gel technique. *Materials Science and Engineering: C, 31*(7): 1534-1538.

Jaffe, W. L. & Scott, D.F. (1996). Current Concepts Review Total Hip Arthroplasty with Hydroxyapatite-Coated Prostheses. *J Bone Joint Surg Am*, *78*: 1918-1934.

Jiménez, M. J. A., Gasga, J.R. & Lugo, V.R. (2003). Electron Microscopy Characterization of Hydroxyapatite Obtained by Hydrothermal Synthesis. *Microsc Microanal, 9*(2): 1298-1299.

Jingbing, L., Kunwei, L., Hao, W., Mankang, Z. & Hui, Y. (2004). Rapid formation of hydroxyapatite nanostructures by microwave irradiation. *Chemical Physics Letters 396:* 429–432.

Kalia, P., Vizcay-Barrena, G., Fan, J. P., Warley, A., Di Silvio, L. & Huang, J. (2014). Nanohydroxyapatite shape and its potential role in bone formation: an analytical study. *Journal of the Royal Society Interface*, *11*(93).

Kalita, S. J. & Verma, S. (2010). Nanocrystalline hydroxyapatite bioceramic using microwave radiation: Synthesis and characterization. *Materials Science and Engineering: C, 30*(2): 295-303.

Kashchiev, D. & Van Rosmalen, G. M. (2003). Nucleation in solutions revisited. *Crystal Research and Technology*, *38*(7-8), 555-574.

Kaur, G. (Ed.). (2017). Clinical Applications of Biomaterials: State-of-the-Art Progress, Trends, and Novel Approaches. Springer.

Kothapalli, C., Wei, M., Vasiliev, A. & Shaw, M. T. (2004). Influence of temperature and concentration on the sintering behavior and mechanical properties of hydroxyapatite. *Acta Materialia*, *52*(19), 5655-5663.

Kramer, K. E. (2005). Improving the robustness of multivariate calibration models for the determination of glucose by near-infrared spectroscopy. *Theses and Dissertations*, 99.

Kumar, G. S., Girija, E. K., Venkatesh, M., Karunakaran, G., Kolesnikov, E. & Kuznetsov, D. (2017). One step method to synthesize flower-like hydroxyapatite architecture using mussel shell bio-waste as a calcium source. *Ceramics International*, *43*(3), 3457-3461.

Kumar, G. S., Thamizhavel, A. & Girija, E. (2012). Microwave conversion of eggshells into flower-like hydroxyapatite nanostructure for biomedical applications. *Materials Letters*, *76*: 198-200.

Kundu, P. K., Waghode, T. S., Bahadur, D. & Datta, D. (1998). Cell culture approach to biocompatibility evaluation of unconventionally prepared hydroxyapatite. *Medical and Biological Engineering and Computing*, *36*(5), 654-658.

Laonapakul, T. (2015). Synthesis of hydroxyapatite from biogenic wastes. *KKU Engineering Journal*, *42*(3), 269-275.

Lee, S., Lee, Y. & Yoon, Y. (2007). Characteristics of calcium phosphate powders synthesized from cuttlefish bone and phosphoric acid. *Journal of Ceramic Processing Research, 8*(6): 427.

Lewis, K., Choi, A., Chou, J. & Ben-Nissan, B. (2007). Bioceramics–The Changing Role of Ceramics and Nanoceramics in Medical Applications. *Materials Australia Magazine, 40*(3): 32-34.

Li, B., Huang, L., Wang, X., Ma, J. & Xie, F. (2011). Biodegradation and compressive strength of phosphorylated chitosan/chitosan/hydroxyapatite bio-composites. *Materials & Design*, *32*(8): 4543-4547.

Liang, W., Niu, Y., Ge, S., Song, S., Su, J. & Luo, Z. (2012). Effects of hydrothermal treatment on the properties of nanoapatite crystals.*International journal of nanomedicine, 7,* 5151.

Lin, K., Wu, C. & Chang, J. (2014). Advances in synthesis of calcium phosphate crystals with controlled size and shape. *Acta biomaterialia, 10*(10): 4071-4102.

Liu, D.-M., Troczynski, T. & Tseng, W. J. (2001). Water-based sol–gel synthesis of hydroxyapatite: process development. *Biomaterials*, *22*(13): 1721-1730.

Liu, H., Chin, T., Lai, L., Chiu, S., Chung, K., Chang, C. & Lui, M. (1997). Hydroxyapatite synthesized by a simplified hydrothermal method. *Ceramics International*, *23*(1): 19-25.

Liu, J., Li, K., Wang, H., Zhu, M. & Yan, H. (2004). Rapid formation of hydroxyapatite nanostructures by microwave irradiation. *Chemical physics letters*, *396*(4): 429-432.

Liu, X., Chu, P. K. & Ding, C. (2004). Surface modification of titanium, titanium alloys, and related materials for biomedical applications. *Materials Science and Engineering: R: Reports*, *47*(3): 49-121.

Martinetti, R., Dolcini, L., and Mangano, C. (2005). Physical and chemical aspects of a new porous hydroxyapatite. *Analytical and bioanalytical chemistry, 381*(3): 634-638.

Meejoo, S., Maneeprakorn, W. & Winotai, P. (2006). Phase and thermal stability of nanocrystalline hydroxyapatite prepared via microwave heating. *Thermochimica Acta, 447*(1): 115-120.

Middleton, J. C. & Tipton, A. J. (2000). Synthetic biodegradable polymers as orthopedic devices. *Biomaterials, 21*(23): 2335-2346.

Mishra, V. K., Rai, S. B., Asthana, B. P., Parkash, O. & Kumar, D. (2014). Effect of annealing on nanoparticles of hydroxyapatite synthesized via microwave irradiation: Structural and spectroscopic studies. *Ceramics International, 40*(7): 11319-11328.

Mohammad, N. F., Zahid, M. A., Awang, S. A., Zakaria, Z. & Abdullah, A. A (2010, October 3-5). *Synthesis and Characterization of Bioceramic from Malaysian Cockle Shell.* Paper presented at the 2010 IEEE Symposium on Industrial Electronics and Applications (ISIEA 2010), Penang, Malaysia (pp: 413-416): IEEE.

Monmaturapoj, N. (2008). Nano-size hydroxyapatite powders preparation by wet-chemical precipitation route. *Journal of Metals, Materials and Minerals, 18*(1): 15-20.

Nasab, M. B. & Hassan, M. R. (2010). Metallic biomaterials of knee and hip-A review. *Trends in Biomaterials and Artificial Organs, 24*(1): 69-82.

Nathanael, A. J., Hong, S. I., Mangalaraj, D. & Chen, P. C. (2011). Large scale synthesis of hydroxyapatite nanospheres by high gravity method. *Chemical Engineering Journal, 173*(3): 846-854.

Navarro, M., Michiardi, A., Castano, O. & Planell, J. (2008). Biomaterials in orthopaedics. *Journal of the Royal Society Interface, 5*(27): 1137-1158.

Nayar, S. & Guha, A. (2009). Waste utilization for the controlled synthesis of nanosized hydroxyapatite. *Materials Science and Engineering: C, 29*(4): 1326-1329.

Neelakandeswari, N., Sangami, G. & Dharmaraj, N. (2011). Preparation and characterization of nanostructured hydroxyapatite using a biomaterial. *Synthesis and Reactivity in Inorganic, Metal-Organic, and Nano-Metal Chemistry, 41*(5): 513-516.

Nejati, E., Mirzadeh, H. & Zandi, M. (2008). Synthesis and characterization of nano-hydroxyapatite rods/poly(L-lactide acid) composite scaffolds for bone tissue engineering. *Composites: Part A, 39*: 1589–1596.

Orlovskii, V., Komlev, V. & Barinov, S. (2002). Hydroxyapatite and hydroxyapatite-based ceramics. *Inorganic Materials, 38*(10): 973-984.

Othman, N. A., Abu Bakar, B. H., Don, M. M. & Johari, M. A. M. (2013). Cockle Shell Ash Replacement for Cement and Filler in Concrete. *Malaysian Journal of Civil Engineering, Penang*: University Sains Malaysia.

Padmanabhan, S. K., Balakrishnan, A., Chu, M.-C., Lee, Y. J., Kim, T. N. & Cho, S.-J. (2009). Sol–gel synthesis and characterization of hydroxyapatite nanorods. *Particuology, 7*(6): 466-470.

Park, J. B. & Bronzino, J. D. (2002). *Biomaterials: principles and applications*: CRC Press.

Prakasam, M., Locs, J., Salma-Ancane, K., Loca, D., Largeteau, A. & Berzina-Cimdina, L. (2015). Fabrication, properties and applications of dense hydroxyapatite: a review. *Journal of functional biomaterials*, *6*(4), 1099-1140.

Petit, R. (1999). The use of hydroxyapatite in orthopaedic surgery: a ten-year review. *Eur J Orthop Surg Traumatol (1999), 9*: 71-74.

Pratihar, S. K., Garg, M., Mehra, S. & Bhattacharyya, S. (2005). Phase Evolution and Sintering Kinetics of Hydroxyapatite Synthesized by Solution Combustion Technique. *Journal of Materials Science: Materials in Medicine, 12*: 1-24.

Raizada, A., Bandari, A. & Kumar, B. (2010). Polymers in drug delivery: a review. *International Journal of Pharmaceutical Research and Development, 2*: 9-20.

Ramakrishna, S. (2000). *Biomedical applications of polymer composite materials.* Paper presented at the Proc. of the second Asian-Australasian Conference on Composite Materials (ACCM-2000), Korea. Advanced Institute of Science and Technology: Korea.

Ramli, R. A., Adnan, R., Bakar, M. A. & Masudi, S. A. M. (2011). Synthesis and characterisation of pure nanoporous hydroxyapatite. *J. Phys. Sci, 22*(1): 20-37.

Ravichandran, S. & Karthikeyan, E. (2011). Microwave Synthesis-A Potential Tool for Green Chemistry. *Int J Chem Tech Res, 3*, 466-470.

Rey, C., Combes, C.,Drouet, C. & Glimcher, M. J. (2009). Bone mineral: update on chemical composition and structure. *Osteoporos Int, 20*: 1013-1021.

Rice, R. W. (1996). Grain size and porosity dependence of ceramic fracture energy and toughness at 22 C. *Journal of materials science*, *31*(8), 1969-1983.

Riman, R. E., Suchanek, W. L. & Lencka, M. M. (2002). *Hydrothermal crystallization of ceramics.* Paper presented at the Annales de Chimie Science des Materiaux.

Rivera, E. M., Araiza, M., Brostow, W., Castano, V. M., Dıaz-Estrada, J., Hernandez, R. & Rodrıguez, J. R. (1999). Synthesis of hydroxyapatite from eggshells. *Materials Letters, 41*(3): 128-134.

Rivera-Muñoz, E. M. (2011). Hydroxyapatite-Based Materials: Synthesis and Characterization. In R. Fazel-Rezai (Ed.), *Biomedical Engineering – Frontiers and Challenges* (pp. 75-95): InTech.

Rodríguez-González, F. Á. (2009). *Biomaterials in Orthopaedic Surgery*: ASM International.

Rodrigues, L. R., Davila, M. A., Monteiro, F. J. M. & Zavaglia, C. A. D. C. (2012). Synthesis and characterization of nanocrystalline hydroxyapatite gel and its application as scaffold aggregation. *Materials Research*, *15*(6), 974-980.

Rohim, R., Ahmad, R., Ibrahim, N., Hamidin, N. & Abidin, C.Z.A. (2014). Characterization of Calcium Oxide Catalyst from Eggshell Waste. *Advance Environmental Biology*, 8(22): 35-38

Sadat-Shojai, M., Khorasani, M.-T., Dinpanah-Khoshdargi, E. & Jamshidi, A. (2013). Synthesis methods for nanosized hydroxyapatite with diverse structures. *Acta biomaterialia, 9*(8): 7591-7621.

Sanosh, K., Chu, M.-C., Balakrishnan, A., Lee, Y.-J., Kim, T. & Cho, S.-J. (2009). Synthesis of nano hydroxyapatite powder that simulate teeth particle morphology and composition. *Current Applied Physics*, *9*(6): 1459-1462.

Santhosh, S. & Balasivanandha Prabu, S. (2012). Characterization of Hydroxyapatite synthesized from Sea shells and Electrospin Coating of Hydroxyapatite for Biomedical Applications. In *Advanced Materials Research*(Vol. 584, pp. 435-439). Trans Tech Publications.

Sarig, S. & Kahana, F. (2002). Rapid formation of nanocrystalline apatite.*Journal of crystal growth*, *237*, 55-59.

Sasikumar, S. & Vijayaraghavan, R. (2006). Low temperature synthesis of nanocrystalline hydroxyapatite from egg shells by combustion method. *Trends Biomater. Artif. Organs, 19*(2): 70-73.

Serbetci, K., Korkusuz, F. & Hasirci, N. (2004). Thermal and mechanical properties of hydroxyapatite impregnated acrylic bone cements. *Polymer Testing*, *23*(2), 145-155.

Shavandi, A., Bekhit, A. E. D. A., Ali, A. & Sun, Z. (2015). Synthesis of nano-hydroxyapatite (nHA) from waste mussel shells using a rapid microwave method. *Materials Chemistry and Physics, 149*, 607-616.

Siddharthan, A., Seshadri, S. & Kumar, T. S. (2006). Influence of microwave power on nanosized hydroxyapatite particles. *Scripta materialia, 55*(2): 175-178.

Singh, A. (2012). Hydroxyapatite, a biomaterial: Its chemical synthesis, characterization and study of biocompatibility prepared from shell of garden snail, Helix aspersa. *Bulletin of Materials Science, 35*(6): 1031-1038.

Smoleń, D., Chudoba, T., Gierlotka, S., Kedzierska, A., Łojkowski, W., Sobczak, K., . . . Kurzydłowski, K. J. (2012). Hydroxyapatite nanopowder synthesis with a programmed resorption rate. *Journal of Nanomaterials*, 7.

Sopyan, I., Singh, R. & Hamdi, M. (2008). Synthesis of nano sired hydroxyapatite powder using sol-gel technique and its conversion to dense and porous bodies. *Indian journal of chemistry. Section A, Inorganic, bio-inorganic, physical, theoretical & analytical chemistry, 47*(11): 1626.

Sung, Y.-M., Lee, J.-C. & Yang, J.-W. (2004). Crystallization and sintering characteristics of chemically precipitated hydroxyapatite nanopowder. *Journal of crystal growth, 262*(1): 467-472.

Surati, M. A., Jauhari, S. & Desai, K. R. (2012). A brief review: microwave assisted organic reaction. *Archives of Applied Science Research*, *4*(1), 645-661.

Tahriri, M., Solati-Hashjin, M., and Eslami, H. (2008). Synthesis and characterization of hydroxyapatite nanocrystals via chemical precipitation technique. *Iranian Journal of Pharmaceutical Sciences, 4*(2): 127-134.

Tangboriboon, N. (2011). *Synthesis of pure calcium compounds from duck eggshells.* Paper presented at the 49. Kasetsart University Annual Conference, Bangkok (Thailand), 1-4 Feb 2011.

Thamaraiselvi, T. V. & Rajeswari, S. (2004). Biological Evaluation of Bioceramic Materials - A Review. *Trends Biomater. Artif. Organs, 18*(1): 9-17.

Tian, H., Tang, Z., Zhuang, X., Chen, X. & Jing, X. (2012). Biodegradable synthetic polymers: preparation, functionalization and biomedical application. *Progress in Polymer Science, 37*(2): 237-280.

Vaidhyanathan, B. & & Rao, K. J. (1996). Rapid microwave assisted synthesis of hydroxyapatite. *Bulletin of Materials Science, 19*(6), 1163-1166.

Vasconcelos, C. (2012). New challenges in the sintering of HA/ZrO2 composites. In *Sintering of Ceramics-New Emerging Techniques*. InTech.

Vedantam, R. & Ruddlesdin, C. (1996). The fully hydroxyapatite-coated total hip implant: clinical and roentgenographic results. *The Journal of arthroplasty, 11*(5): 534-542.

Vijayalakshmi, U. & Rajeswari, S. (2006). Preparation and characterization of microcrystalline hydroxyapatite using sol gel method. *Trends Biomater. Artif. Organs, 19*(2): 57-62.

Wang, Y., Zhang, S., Wei, K., Zhao, N., Chen, J. & Wang, X. (2006). Hydrothermal synthesis of hydroxyapatite nanopowders using cationic surfactant as a template. *Materials Letters, 60*(12): 1484-1487.

Webster, T. J., Ergun, C., Doremus, R. H., Siegel, R. W. & Bizios, R. (2000). Enhanced functions of osteoblasts on nanophase ceramics. *Biomaterials, 21*(17): 1803-1810.

Whittingham, M. (1997). X-ray analysis of a solid. Retrieved 4 August 2012 http://materials.binghamton.edu/labs/xray/xray.html

Wojnar, R. (2010). Bone and cartilage–its structure and physical properties. *Biomechanics of Hard Tissues: Modeling, Testing, and Materials*: 1-75.

Woodard, J. R., Hilldore, A. J., Lan, S. K., Park, C., Morgan, A. W., Eurell, J. A. C., . . . Johnson, A. J. W. (2007). The mechanical properties and osteoconductivity of hydroxyapatite bone scaffolds with multi-scale porosity. *Biomaterials, 28*(1): 45-54.

Xing, Z. & Vecchioa, K.S. (2007). Hydrothermal synthesis of hydroxyapatite rods. *Journal of Crystal Growth, 308*: 133-140.

Yang, Z., Jiang, Y., Wang, Y., Ma, L. & Li, F. (2004). Preparation and thermal stability analysis of hydroxyapatite derived from the precipitation process and microwave irradiation method. *Materials Letters*, *58*(27), 3586-3590.

Yoruc, A. B. H. & Koca, Y. (2009). Double step stirring: A novel method for precipitation of nano-sized hydroxyapatite powder. *Digest J. Nanomater. Biostructures, 4*: 73-81.

Zamani, S., Mobasherpour, I. & Salahi, E. (2012, 12-14 March). *Synthesis of nano calcium hydroxyapatite from Persian Gulf coral.* Paper presented at the Proceedings of the 4th International Conference on Nanostructures, Kish Island, I.R. Iran.

Zhang, X., Hayward, D. O. & Mingos, D. M. P. (2003). Effects of microwave dielectric heating on heterogeneous catalysis. *Catalysis Letters*, *88*(1), 33-38

Zhang, X. & Vecchio, K. S. (2007). Hydrothermal synthesis of hydroxyapatite rods. *Journal of crystal growth*, *308*(1): 133-140.

Zhou, H. & Lee, J. (2011). Nanoscale hydroxyapatite particles for bone tissue engineering. *Acta Biomaterialia, 7*(7): 2769–2781.

Zhou, H., Yang, M., Zhang, M., Hou, S., Kong, S., Yang, L. & Deng, L. (2016). Preparation of Chinese mystery snail shells derived hydroxyapatite with different morphology using condensed phosphate sources. *Ceramics International*, *42*(15), 16671-16676.

Zou, Z., Lin, K., Chen, L. & Chang, J. (2012). Ultrafast synthesis and characterization of carbonated hydroxyapatite nanopowders via sonochemistry-assisted microwave process. *Ultrasonics sonochemistry, 19*(6): 1174-1179.

LIST OF PUBLICATIONS AND PAPERS PRESENTED

1. Sajahan, N. A., & Wan Ibrahim, W. M. A. (2014). Microwave Irradiation of Nanohydroxyapatite from Chicken Eggshells and Duck Eggshells. *The Scientific World Journal*, *2014*.
2. Sajahan, N. A., & Wan Ibrahim, W. M. A. (2012). Malaysian International Conference on Trends in Bioprocess Engineering, Meritus Pelangi Beach Resort and Spa, Langkawi Kedah, 3-5 July 2012. The School of Bioprocess Engineering of Universiti Malaysia Perlis (UniMAP).